이학박사 학위논문

Anti-biofilm mechanism of lipoteichoic acids from Lactobacilli and their therapeutic potential against periodontitis

유산균 유래 리포테이코익산의 바이오 필름 제어기전과 치주염 치료 효과

2023 년 2월

서울대학교 대학원

치의과학과 면역 및 분자미생물 전공

이 동 욱

Anti-biofilm mechanism of lipoteichoic acids from Lactobacilli and their therapeutic potential against periodontitis

by

Dongwook Lee

Under the supervision of

Professor Seung Hyun Han, Ph. D.

A Dissertation Submitted in Partial Fulfillment of the Requirements for the degree of

Doctor of Philosophy

February 2023

Program in Immunology and Molecular Microbiology
Department of Dental Science, School of Dentistry
The Graduate School, Seoul National University

Anti-biofilm mechanism of lipoteichoic acids from Lactobacilli and their therapeutic potential against periodontitis

지도교수 한 승 현

이 논문을 이학박사 학위논문으로 제출함

2023 년 01월

서울대학교 대학원

치의과학과 면역 및 분자미생물 전공

이 동 욱

이동욱의 박사학위논문을 인준함

2023 년 01월

위 원 장 박 주 홍 (인)

부위원장 한 승 현 (인)

위 원 윤 철 희 (인)

위 원 서 태 근 (인)

위 원 김 진 만 (인)

ABSTRACT

Anti-biofilm mechanism of lipoteichoic acids from Lactobacilli and their therapeutic potential against periodontitis

Dongwook Lee

Program in Immunology and Molecular Microbiology,

Department of Dental Science, School of Dentistry,

The Graduate School, Seoul National University

(Supervised by Professor Seung Hyun Han, Ph. D.)

Periodontitis, one of the most prevalent oral diseases, results in progressive periodontal destruction and alveolar bone resorption. *Porphyromonas gingivalis* is a Gram-negative keystone periodontopathogen that is frequently found in patients with chronic periodontitis. Moreover, since biofilm serves as a physical and chemical barrier against host immune responses and dental medicaments, alternative anti-biofilm strategies for effectively controlling *P. gingivalis* are needed. Since lipoteichoic acids (LTAs) are known to inhibit some oral bacterial pathogens including *Streptococcus mutans* and *Enterococcus faecalis*, here, LTAs from probiotic *Lactobacillus* species were purified and their anti-biofilm effect against *P. gingivalis* was examined. When compared to other *Lactobacillus* LTAs, such as *Lactobacillus acidophilus*, *Lactobacillus casei*, *Lactobacillus rhamnosus*, and *Lactobacillus plantarum*, *Lactobacillus reuteri* LTA (Lre.LTA) had a potent anti-biofilm activity against *P. gingivalis* without affecting its growth. Lre.LTA even dispersed pre-formed biofilm of *P.*

gingivalis. Interestingly, compared to intact Lre.LTA, the anti-biofilm activity of deacylated Lre.LTA was reduced, whereas dealanylated Lre.LTA was still effective against *P. gingivalis* biofilm, implying that acyl chain moieties are important for inhibiting the biofilm of *P. gingivalis*. Moreover, Lre.LTA effectively inhibited the biofilm of *P. gingivalis* clinical isolates and polymicrobial biofilm consisting of *P. gingivalis*, *Candida albicans*, and *Streptococcus gordonii*. Confocal microscopic analysis demonstrated that the dispersion of extracellular matrix by Lre.LTA is mediated through direct interaction with *P. gingivalis*. To elucidate anti-biofilm mechanism of Lre.LTA against *P. gingivalis*, Lre.LTA-binding proteins were obtained by precipitation with Lre.LTA conjugated with NHS-bead from *P. gingivalis* whole cell lysate. After precipitation, the Lre.LTA-binding proteins were subsequently identified by using LTQ Orbitrap hybrid-FT mass spectrometry. Among the total of 316 proteins identified, major fimbriae (FimA) and arginine gingipain (RgpA), which are known to be associated with *P. gingivalis* biofilm formation, were predominantly bound to Lre.LTA. *P. gingivalis* with *fimA* deletion, but not *kgp* or *kgp/rgpAB* deletion, abolished the anti-biofilm activity of Lre.LTA suggesting that Lre.LTA inhibits the biofilm of *P. gingivalis* via interaction with FimA. In addition, transcriptomic analysis showed that Lre.LTA affects metabolism-associated genes of *P. gingivalis* during its biofilm dispersion. Western blot and real-time PCR analysis showed that Lre.LTA inhibited the degradation of monocyte chemoattractant protein-induced protein 1 in oral squamous cell carcinoma cell line, an intracellular anti-inflammatory mediator for preventing excessive inflammation to alleviate periodontitis, by targeting the arginine gingipain (RgpA) of *P. gingivalis*. Furthermore, Lre.LTA attenuated the *P. gingivalis*-induced pro-inflammatory cytokines productions, such as IL-1β, IL-6, and IL-8. To examine whether Lre.LTA could alleviate periodontitis, Lre.LTA was given to the ligature-induced, *P. gingivalis*-exacerbated periodontitis mouse model and the maxillary molar of mice was then subjected to micro-computed tomography (micro-CT). Interestingly, the micro-CT analysis showed that distance from alveolar bone crest to the cemento-enamel junction was significantly decreased in the *P. gingivalis* plus Lre.LTA group

compared to the *P. gingivalis* infected group, implying that Lre.LTA could ameliorate *P. gingivalis*-exacerbated periodontitis. Collectively, these results suggest that controlling *P. gingivalis* biofilm and its pathogenesis by Lre.LTA could be a novel strategy for developing a therapeutic agent against periodontal diseases associated with *P. gingivalis*.

Keywords: *Lactobacillus*, Lipoteichoic acid, *Porphyromonas gingivalis*, periodontitis, anti-biofilm agent

Student number: 2017-32420

CONTENTS

List of figures

List of tables

Abbreviations

AI-2	Autoinducer-2
BHIHM	Brain Heart Infusion broth supplemented with 5 μg/ml hemin and 5 μg/ml menadione
CMC	Carboxymethylcellulose
CEJ-ABC	Cementum-enamel junction to alveolar bone crest
CFU	Colony forming units
DEGs	Differentially expressed genes
EPM	Extracellular protein matrix
EPS	Extracellular polymeric substance
FBS	Fetal bovine serum
FITC	Fluorescein isothiocyanate
GAPDH	Glyceraldehyde-3-phosphate dehydrogenase
La.LTA	*L. acidophilus* LTA
Lc.LTA	*L. casei* LTA
Lp.LTA	*L. plantarum* LTA
Lre.LTA	*L. reuteri* LTA
Lr.LTA	*L. rhamnosus* LTA
LPS	Lipopolysaccharide
LTA	Lipoteichoic acid
MCPIP-1	Monocyte chemoattractant protein-induced protein 1
MALT1	Mucosa-associated lymphoid tissue lymphoma translocation protein 1
MOI	Multiplicity of infection
NHS	N-hydroxysuccinimide
PBS	Phosphate buffered saline
Poly-Gro-P	poly-glycerol phosphate

SPR	Surface plasmon resonance
T9SS	Type 9 secretion system
TLR	Toll-like receptor
WT	Wild-type

Introduction

Bacteria forms biofilms in various anatomical locations of the human body, which are the aggregate of microorganisms attached to abiotic materials or living surfaces [1]. At the initial phase of biofilm formation, planktonic bacteria adhere to the surface and subsequently produce extracellular polymeric substances (EPS), such as extracellular DNAs, proteins, and polysaccharides, which cluster into immobile aggregates to form biofilm. The biofilm is progressively developed into multi-layered cell clusters thereby harnessing resistance against the host immune responses or antibiotics. Finally, these aggregates can disperse to other surfaces to form additional biofilms [2] (Figure 1). The regulation of bacterial biofilm involves the interaction of a number of positive and negative bacterial factors, such as quorum sensing systems, regulatory short RNAs, alternative sigma factors, two-component systems, and cyclic dinucleotides [3]. The oral cavity is the second most diverse biofilm-forming habitat followed by the gut, consisting over 700 different species of bacteria that belong to mainly *Actinobacteria*, *Bacteroidetes*, *Firmicutes*, *Fusobacteria*, and *Proteobacteria* phyla [4]. The oral microflora may gradually change into pathogenic communities as a result of sustained exposure to host and environmental stimuli, which can result in oral disorders as dental caries and periodontitis [5], [6], [7].

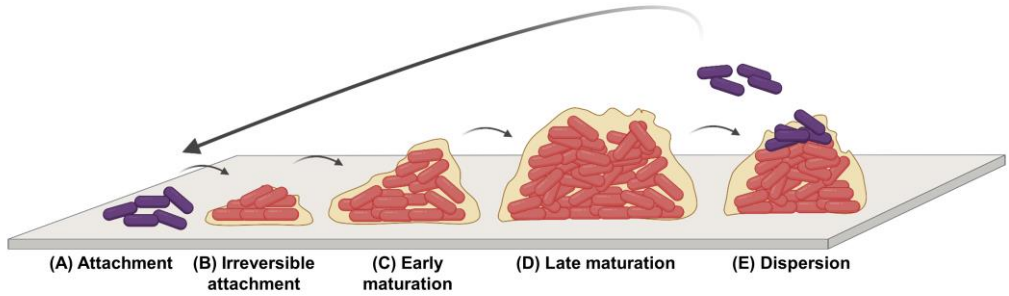

Figure 1. The five stages of biofilm development

(A) Initial planktonic bacterial adhesion to abiotic or biotic surfaces. (B) Irreversible attachment, growth of biofilm with EPS secretion. (C) Early development of multi-layered clusters that form biofilms. (D) Late maturation of biofilm serves as a physical and chemical barrier against the host immune response and antibiotics. (E) Cell detachment and dispersal of biofilm.

Periodontitis is a typical chronic inflammatory oral disorder that results in the resorption of alveolar bone and the destruction of tooth-supporting tissues [8]. Globally, periodontitis is the 11th most prevalent disease, and its prevalence was reported to range from 20 to 50 percent around the world [9]. Dental plaque production in periodontal pockets provides a suitable environment for the colonization of periodontopathogens, which causes periodontal diseases. These microbes are primarily asaccharolytic but are able to create potent proteases that facilitate the destruction of the periodontium [10]. Early colonization of bacteria in dental plaque is dominated by streptococcal species, such as *Streptococcus gordonii, Streptococcus mitis, Streptococcus oralis,* and *Actinomyces* species [11], [12]. These early colonizers can produce various substrates needed for attachment and development of bacterial communities [13]. According to the Socransky classification, bacteria in the red complex, such as *Porphyromonas gingivalis*, *Treponema denticola*, and *Tannerella forsythia* are late colonizers that contribute to the pathogenesis of the periodontal diseases by forming dysbiotic communities (Figure 2) [14]. Early colonizers, or the orange complex, can bridge the colonization of these keystone pathogens to help settle their dysbiotic microbiota. The dysbiosis of the periodontal microbiota creates unrestrained inflammatory conditions, which develop periodontal tissue destruction by forming a positive feedback loop (Figure 3) [15], [16].

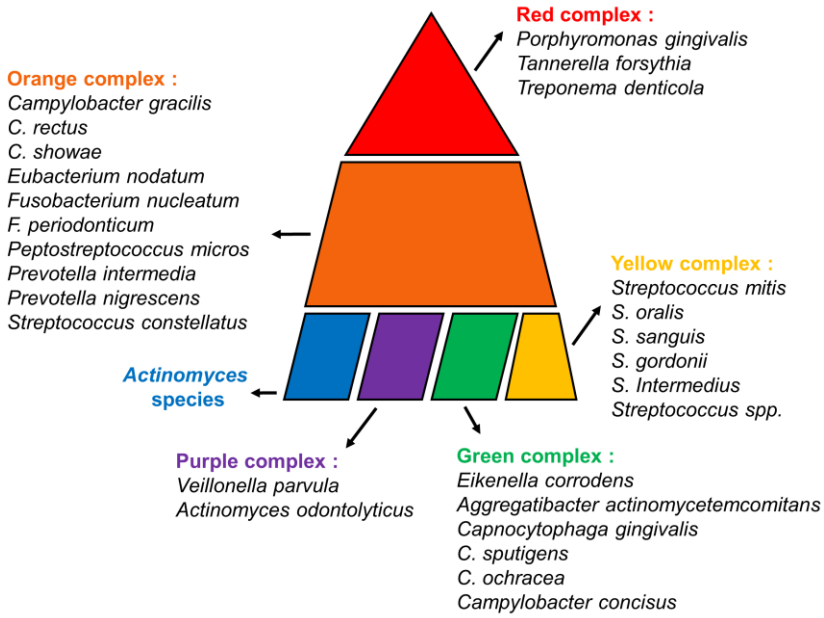

Figure 2. Socransky classification of microbial species differentially involved in the periodontitis

Approximately 13,321 dental plaque samples were examined for specific subgingival species using cluster analysis and community composition approaches [14]. The base of the pyramid is divided into six groups that are considered to inhabit the tooth plaque. *Actinomyces* species, yellow, purple, and green complex are known as early colonizers. Meanwhile, orange and red complexes are classified as late colonizers and recognized as major periodontopathogens.

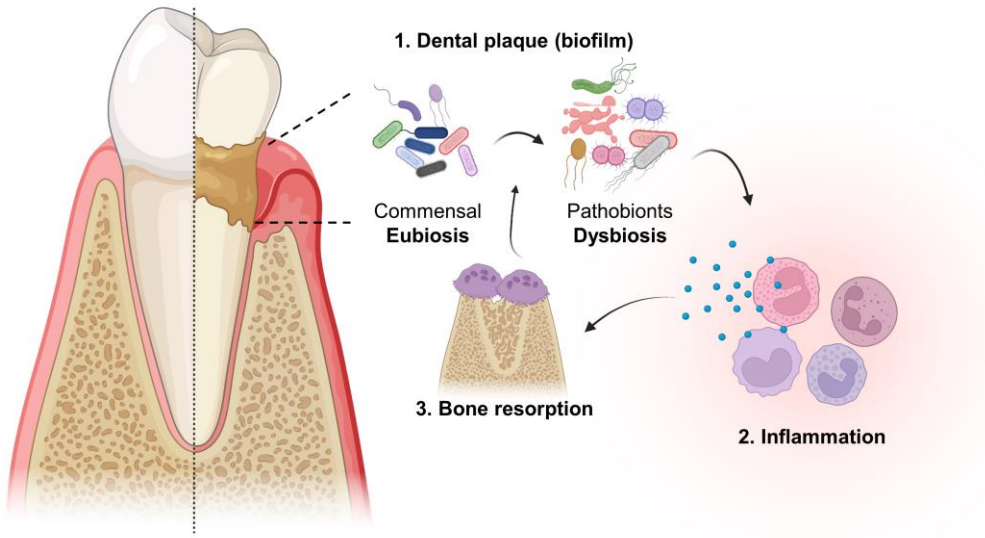

Figure 3. Schematic diagram for the development of periodontitis

Periodontal health is associated with host-microbe homeostasis in the periodontal pockets. Various genetic or environmental factors can shift the balance of host-microbe homeostasis to dysbiosis. Dysbiotic microbiota promotes local systemic inflammation in periodontal pockets, subsequently leading to tissue destruction and bone loss which are the hallmarks of periodontitis.

Porphyromonas gingivalis is a Gram-negative, anaerobic, and asaccharolytic bacterium that has been widely regarded as a keystone periodontopathogen that is frequently found in patients with chronic periodontitis [17], [18]. Moreover, *P. gingivalis* is also liked to the development of systemic diseases, such as atherosclerosis, Alzheimer's disease, rheumatoid arthritis, diabetes, and adverse pregnancy outcomes [17]. *P. gingivalis* induces periodontal destruction through expression of diverse virulence factors, such as fimbriae, lipopolysaccharide (LPS), and gingipain triggering an exaggerated pro-inflammatory response in the host (Figure 4). [19]. *P. gingivalis* can form biofilm using fimbriae, LPS, internalins, capsules, and gingipains. *P. gingivalis* biofilm also serves as a physical and chemical barrier against antibiotics and a favorable niche for its survival within the host by evading host immune responses [19], [20]. In addition, it has been reported that *P. gingivalis* interacts with various oral bacteria and yeast, such as *Fusobacterium nucleatum*, *Streptococcus gordonii*, and *Candida albicans*, to offer stability and persistence [13].

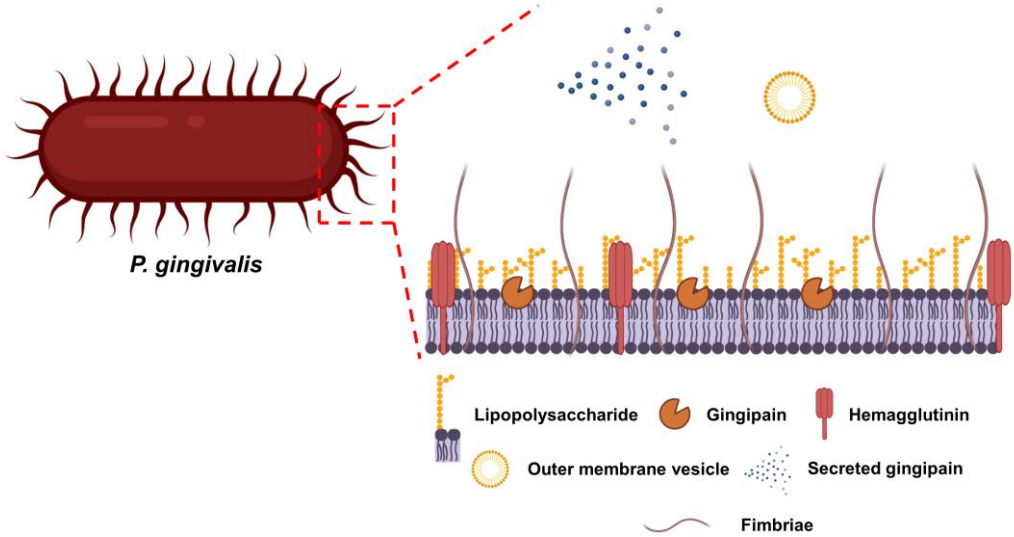

Figure 4. Representative virulence factors of *P. gingivalis*

The major virulence factors of *P. gingivalis* include LPS, fimbriae, hemagglutinin, membrane-bound gingipains, and secretory components, such as secreted gingipain and outer membrane vesicle.

Scaling and root planning are current treatment methods employed to detach biofilms physically. However, these physical therapies only cause transient removal of biofilms since biofilms from subgingival dental plaque are not completely eradicated [21], [22]. Moreover, accumulated studies showed the limitations of disinfectants as a periodontitis treatment, including taste alteration, soft-tissue lesions, and brown discoloration of the teeth [23]. In the case of antibiotics, antibiotic-resistance genes can be spread among oral bacterial biofilms using horizontal gene transfer, resulting in ineffective clearance [24]. Likewise, *P. gingivalis* biofilm is resistant to antibiotics and disinfectants such as chlorhexidine, minocycline, metronidazole, amoxicillin, and doxycycline, compared to planktonic state of *P. gingivalis* [25], [26], [27]. Moreover, previous studies have shown that clinical isolates of *P. gingivalis* from patients with periodontitis are resistant to amoxicillin, clindamycin, metronidazole, penicillin, erythromycin, azithromycin, and tetracycline, shedding a light on the research for new alternative therapies [28], [29].

Probiotics, especially *Lactobacillus*, have emerged as a promising alternative therapy for anti-biofilm agents which maintains a healthy community of the oral cavity, and prevents periodontal disease onset [30]. Previous studies have shown that cell-free supernatant of *Lactobacillus acidophilus*, *Lactobacillus rhamnosus*, and *Lactobacillus reuteri* reduces the homotypic or heterotypic biofilm of *P. gingivalis* by down-regulating virulence-associated factors [31]. In the animal periodontitis model, live *Lactobacillus gasseri* effectively prevents *P. gingivalis*-induced periodontitis by decreasing the secretion of TNF-α and IL-6 in gingival tissue [32]. In addition, *Lactobacillus* derivatives such as lipoteichoic acid (LTA), polysaccharides, biosurfactants, and bacteriocins can trigger anti-biofilm effects [33]. However, the use of intact whole cells

may lead to adverse effects such as dysregulated immune systems in individuals, resulting in exaggerated responses to vaccines or allergens [34]. Moreover, while the safety of *Lactobacillus* derivatives is under investigation to overcome the limitation of whole cells, the molecular mechanism behind their anti-biofilm activity is still poorly understood.

LTA is an amphipathic cell wall component of Gram-positive bacteria including *Lactobacillus*. Studies have shown that LTA is crucial for cell division in Gram-positive bacteria and acts as an osmoprotectant to preserve the integrity of the bacterial cell wall [35], [36]. Based on their structural difference, LTA can be classified into five distinct types as follows: type I LTA (1,3-poly-glycerolphosphate with glycolipid); type II LTA [α-Gal(1–6), α-Gal(1–3), poly-glycerolphosphate with glycolipid]; type III LTA [α-Gal(1–3), poly-glycerolphosphate, β-glucosamine(1–3) with glycolipid]; type IV LTA [2-acetamino-4-amino-2,4,6-trideoxygalactose, N-acetylgalactosamine, poly-ribitol phosphate with glycolipid]; type V LTA (α-D-N-acetylglucosamine repeating units with glycolipid) [37] (Figure 5). In general, type I LTA is the most generally found polymer in Gram-positive bacteria, and hydrophilic moiety of type I LTA is mainly composed of poly-glycerolphosphate (poly-Gro-P) backbone with D-alanine, glucose, or galactose residues, while hydrophobic moiety of type I LTA is either diacylated or triacylated glycolipids which are tethered to poly-Gro-P and anchored into the bacterial cell membrane [37]. In the previous study, since type I LTA from pathogens, such as *Streptococcus pneumoniae* and *Staphylococcus aureus*, elicit the inflammatory responses from macrophages, type I LTA is recognized as a major virulence factor of pathogens [38], [39]. In contrast, type I LTA from probiotics, especially *Lactobacillus*, serves

beneficial roles in the host immune system by promoting anti-inflammatory responses and even antagonizing various microbe-associated molecular patterns, suggesting its protective role in the host [37], [40], [41].

Previous research has shown that *Lactobacillus* LTAs have anti-biofilm activity against various Gram-positive bacteria [42], [43], [44], [45], [46], [47]. In fact, *Lactobacillus plantarum* LTA (Lp.LTA) prevents *S. aureus* from forming biofilms by increasing the release of AI-2, which in turn suppresses the production of quorum sensing signals and exopolysaccharide [43]. Moreover, Lp.LTA prevents *S. mutans* from forming biofilms by antagonizing its metabolic activity for converting sucrose into EPS [44]. Depending on the *L. plantarum* strain, Lp.LTA can have a different inhibitory effect on the *S. mutans* biofilm [45]. Furthermore, Lp.LTA can inhibit multispecies biofilm of oral microbes [47] and 3-week-old mature biofilm [46]. Although the cell wall structures between Gram-positive and Gram-negative bacteria have significant differences with moieties [48], underlying mechanisms of how *Lactobacillus* LTAs exert their anti-biofilm activity against Gram-negative bacteria are still poorly understood. In addition, it remains unknown whether *Lactobacillus* LTA affects the biofilm of Gram-negative periodontopathogens, such *P. gingivalis*.

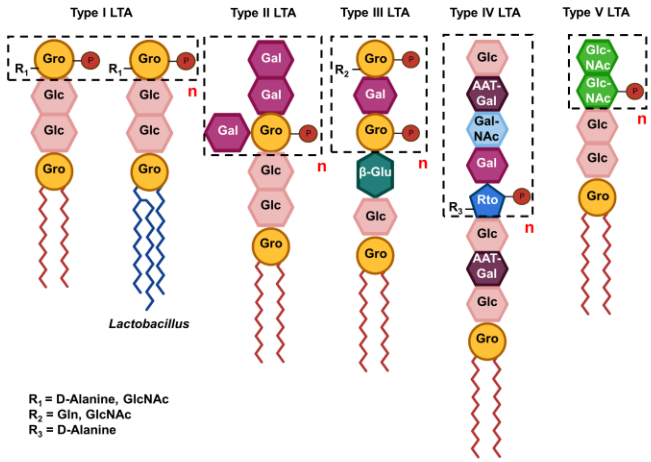

Figure 5. Schematic illustration of LTA structures

LTAs are amphiphilic structures composed of hydrophilic polysaccharides linked to hydrophobic diacyl (red) or triacyl (blue) glycolipids. LTA can be classified into five distinct types as follows: type I LTA (1,3-poly-glycerolphosphate with glycolipid); type II LTA [α-Gal(1–6), α-Gal(1–3), poly-glycerolphosphate with glycolipid]; type III LTA [α-Gal(1–3), poly-glycerolphosphate, β-glucosamine(1–3) with glycolipid]; type IV LTA [2-acetamino-4-amino-2,4,6-trideoxygalactose, N-acetylgalactosamine, poly-ribitol phosphate with glycolipid]; type V LTA (α-D-N-acetylglucosamine repeating units with glycolipid). Structure of type I LTA represents *Staphylococcus aureus* (left) and *Lactobacillus plantarum* (right), type II LTA represents *Lactococcus garvieae*, type III LTA represents *Clostridium innocuum*, type IV LTA represents *Streptococcus pneumoniae*, and type V LTA represents *Clostridium difficile*. R_1, R_2, and R_3 denote backbone substitution. n, repeating unit of each LTA; P, phosphate; Gro, Glycerol; Glc, Glucose; Gal, Galactose; β-Glu, β-Glucan; AAT-Gal, 2-acetamido-4-amino-2,4,6-trideoxy-d-galactose; Gal-NAc, N-acetylgalactosamine; Rto, Ribitol; Glc-NAc, N-acetylglucosamine

Aims of the study

Probiotics, especially *Lactobacillus,* are known to maintain a healthy community of the oral cavity and are emerging as a promising alternative therapy for anti-biofilm agents. However, the use of intact whole cells may lead to adverse effects, such as dysregulated immune systems in individuals, resulting in exaggerated responses to vaccines or allergens. Although the safety of *Lactobacillus* derivatives is under investigation to overcome the limitation of whole cells, the molecular mechanism behind their anti-biofilm activity is still poorly understood. Moreover, Lp.LTA has been shown in previous studies to have anti-biofilm activity against a variety of Gram-positive oral pathogens, and this anti-biofilm activity can vary depending on the strain. However, although the cell wall structures between Gram-positive and Gram-negative bacteria have significant differences with moieties, it is still elusive whether *Lactobacillus* LTA regulates the biofilm formation of Gram-negative periodontopathogen, such as *P. gingivalis*. Therefore, the aims of this study are the following: 1. To investigate the effect of *Lactobacillus* LTAs on *P. gingivalis* biofilm, 2. To elucidate the anti-biofilm mechanisms of *Lactobacillus* LTA against *P. gingivalis* biofilm, 3. To determine the clinical relevance of *Lactobacillus* LTA during bacterial pathogenesis.

Materials and method

Reagents and chemicals

2-mercaptoethanol, ampicillin, avertin, bromophenol blue, calcium chloride, carboxymethylcellulose, chloramphenicol, Coomassie Brilliant Blue G-250, crystal violet, cysteine, DEAE-Sepharose, erythromycin, glycerol, hemin, imidazole, lysozyme, menadione, N-(3-dimethylaminopropyl)-N'-ethylcarbodiimide hydrochloride, N-hydroxysuccinimide beads, N-tosyl-glycyl-L-prolyl-L-lysine 4-nitroanilide acetate salt, Nα-benzoyl-DL-arginine p-nitroanilide hydrochloride, octyl-Sepharose, paraformaldehyde, potassium phosphate, and sodium phosphate were from Sigma-Aldrich (USA). Fetal bovine serum (FBS), penicillin, streptomycin, T4 ligase, and TRIzol were from Thermo Scientifics (USA). Sodium dodecyl sulfate (SDS), sodium chloride, and Tris were from Duchefa Biochemie (Netherlands). Acetic acid, n-butanol, and sodium hydroxide were from Junsei Chemical (Japan). Ethanol and methanol were from Merck (Germany). Isopropyl-β-D-thiogalactopyranoside was obtained from Biosesang (Republic of Korea). Glycine was obtained from Duksan (Republic of Korea). The solution of 100 mM NHS plus 50 mM MES, 5 mM sodium acetate (pH 4.0) were obtained from iClubio (Republic of Korea).

Bacterial strains and culture conditions

For purifying highly-pure and structurally intact LTAs from *Lactobacillus* species such as *L. acidophilus* KACC 12419 (provided by Korean Agricultural Culture Collection, KACC, Republic of Korea), *L. casei* KCTC 3260 (Korean Collection for Type Cultures, KCTC, Republic of Korea), *L. rhamnosus* GG (kindly provided by Kyung Hee

University), *L. plantarum* KCTC10887bp, and *L. reuteri* ATCC 23272 (American Type Culture Collection, ATCC, Manassas, VA), were grown in deMan, Rogosa, and Sharpe (MRS) agar and broth (MB cell, Republic of Korea) for 48 h at 37℃ under aerobic culture condition. *P. gingivalis* ATCC 33277 wild type (WT) and clinical isolates of *P. gingivalis* from patients with aggressive periodontitis (provided by Korean Collection for Oral Microbiology, KCOM, Republic of Korea) were grown on pre-reduced Brain Heart Infusion (Difco, USA) agar plates supplemented with 5 μg/ml hemin, 5 μg/ml menadione, and 5% defibrinated sheep blood (MB cell, Republic of Korea, BHIHM agar with 5% sheep blood) at 37℃ in an anaerobic workstation (Don Whitley, UK) with an atmosphere containing 5% hydrogen, 10% carbon dioxide, and 85% nitrogen. Planktonic cultures of *P. gingivalis* were grown in pre-reduced Brain Heart Infusion broth supplemented with 5 μg/ml hemin and 5 μg/ml menadione (BHIHM). *P. gingivalis* ATCC 33277 of KDP129 (*kgp* deletion) and KDP136 (*kgp, rgpA/B* deletion) were kindly provided by Prof. Young-Jung Jung (Seoul National University). *P. gingivalis*-null mutants were maintained by supplementing BHIHM/ BHIHM agar with 5% sheep blood with 10 μg/ml chloramphenicol (for △*fimA*) or erythromycin (for KDP129 and KDP136). All of the *P. gingivalis* strains were grown at 37℃ under static anaerobic conditions. To check the anti-biofilm activity of Lre.LTA against polymicrobial heterotypic biofilm, *S. gordonii* CH1 and *C. albicans* SC5314 were grown in pre-reduced BHIHM in static anaerobic conditions.

Cell culture and infection conditions

Oral squamous cell carcinoma cell line, YD-38 was maintained at 37℃ in a humidified 95% air and 5% CO_2 environment in 100 mm dish with RPMI-1640 culture medium

(Welgene, Republic of Korea) supplemented with 10% FBS, penicillin, and streptomycin. The cells were treated with the multiplicity of infection (MOI) 100 of live *P. gingivalis* WT, △*fimA*, and KDP136 in the presence or absence of Lre.LTA.

Inorganic phosphate assay

Inorganic phosphate assay, as previously described [38], was used to identify the LTA-containing fractions. In summary, sulfuric acid (Junsei, Tokyo, Japan) and nitric acid (Junsei) were blended with the elutes from the hydrophobic interaction and ion-exchange chromatography, and heated. Following a neutralization step with 3 M sodium hydroxide (Junsei), the mixture was then combined with 100 mM molybdate in 5 M sulfuric acid and 130 mM stannous chloride in glycerol. A microplate reader was used to detect optical density at 600 nm following incubation for 5 min (Molecular Devices, USA). Phosphorus content was determined using potassium phosphate as the reference.

Purification of LTA and generation of Dealanylated and Dealanyl/Deacylated LTA

Pure LTAs from *Lactobacillus* species were extracted as previously described [45]. Briefly, bacterial pellet from each *Lactobacillus* species was harvested and lysed by ultrasonication (Vibracell VCX500) with stirring. Supernatants of each bacterial lysate were mixed with *n*-butanol, and the lower phase, which contained the LTA, was carefully collected and dialyzed by using endotoxin-free distilled water (Daihan Pharm. Co. Ltd) at 4℃ and then lyophilized. Crude extracts of LTAs from each *Lactobacillus* species were further purified by hydrophobic interaction chromatography on octyl-Sepharose and ion-exchange chromatography on DEAE-Sepharose, as previously described [45]. Inorganic phosphate test was used to assess the phosphate content of

LTA. Column fractions containing LTA were gathered, dialyzed, lyophilized, and measured for their dry weight. The presence of potential contaminants, such as endotoxin, protein, and nucleic acid, was then checked in the isolated LTAs. All of the isolated LTAs contained trace quantities of endotoxin, proteins, and nucleic acids, as reported in Table 1. However, since previous studies showed that this levels of contaminants have exceedingly low biological activities [39], [49], the effects of *Lactobacillus* LTAs against *P. gingivalis* biofilm formation were investigated. To generate dealanylated and dealanylated plus deacylated LTA, intact Lre.LTA was treated with 0.1 M Tris-HCl at pH 8.5 for 24 h or 0.5 N NaOH for 2 h, respectively. Each deleted moiety of LTA was dialyzed and further confirmed its deletion by spraying method on the TLC plate as previously described [43].

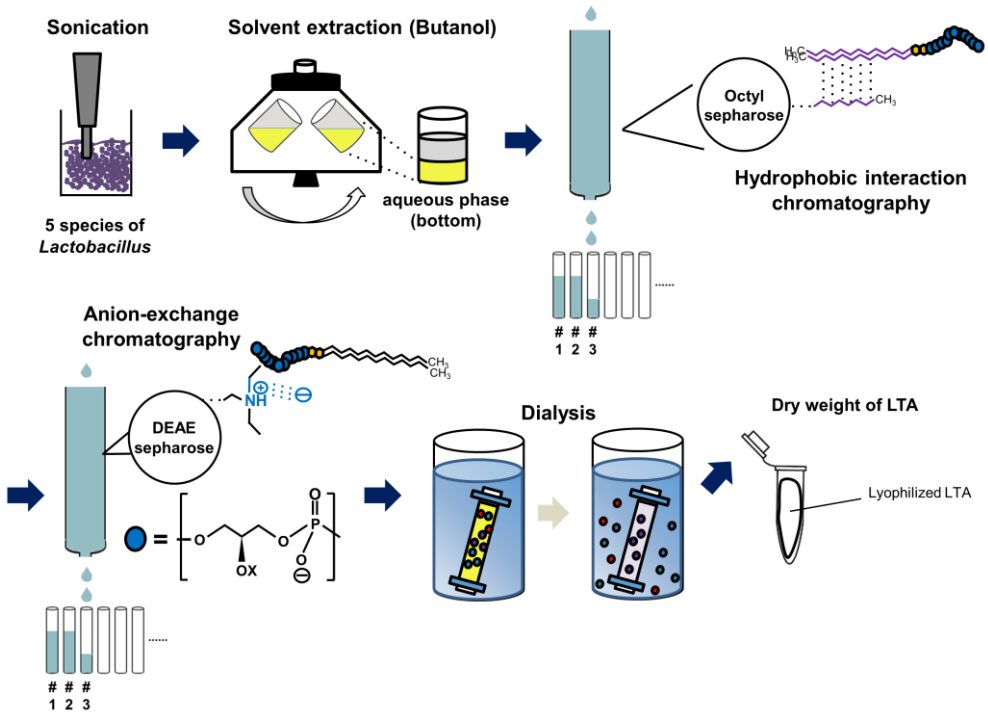

Figure 6. Experimental procedure of *Lactobacillus* LTAs purification

Five species of *Lactobaillus* cultured in flask were harvested by centrifugation. Then, the pellets were sonicated and subsequently mixed with *n*-butanol. Lower phase of aqueous solution containing LTA was dialyzed and then lyophilized. Hydrophobic interaction chromatography followed by ion-exchange chromatography was further conducted to obtain pure LTA. Eluted fraction of LTA was then dialyzed and lyophilized to quantify dry weight of LTA.

TABLE 1 | Analysis of possible impurities in *Lactobacillus* LTA preparations

Lactobacillus LTA	Endotoxin[a] (pg/mg LTA)	Protein[b] (ng/mg LTA)	Nucleic acid[c] (μg/mg LTA)
L. acidophilus	N.D.	N.D.	84.7
L. casei	25	N.D.	44.4
L. rhamnosus	65	N.D.	78.8
L. plantarum	41	N.D.	56.8
L. reuteri	52	N.D.	42.3

[a-c] Endotoxin, protein, and nucleic acid impurity contents were assessed using the Limulus amoebocyte lysate assay, BCA protein assay, and optical density using a spectrophotometer, respectively. N.D.[a], not detected, endotoxin contents below 15 pg/ml of detection limit; N.D.[b], not detected, protein contents below 5 ng/μl of detection limit

Conjugation of FITC with LTA

Fluorescein isothiocyanate (FITC, Invitrogen, USA) and one milligram of Lre.LTA were combined and stirred at room temperature for an hour. The PD-10 desalting column (GE Healthcare, Sweden) was used to remove any unbound FITC following conjugation. FITC-conjugated Lre.LTA (Lre.LTA-FITC) was then dialyzed, lyophilized, and quantified by measuring its phosphate contents.

Cloning, protein Expression, and purification

The primers for amplifying FimA, Glyceraldehyde-3-phosphate dehydrogenase (GAPDH) of *P. gingivalis* were designed according to the sequences of *P. gingivalis* ATCC 33277 (GenBank accession no: AP009380.1) containing restriction sites of BamHI (forward, Enzynomics, Republic of Korea) and AvaI (reverse, Enzynomics, Republic of Korea). Pfu DNA polymerase (Enzynomics, Republic of Korea) was used in PCR to amplify the genomic DNA of *P. gingivalis* under the following conditions: denaturation at 95℃ for 30 s and amplification through 27 cycles of 60℃ for 30 s and 72℃ for 1 min. After electrophoresis, PCR products were extracted from the 1% (w/v) agarose gel using a Power Gel Extraction Kit (Dyne Bio, Republic of Korea). Target genes were cleaved with *BamHI/AvaI*, ligated into a linearized expression vector, pET-21a using T4 ligase, and subjected to transformation. Competent *Escherichia coli* strain DH5α was transformed using a conventional method ($CaCl_2$) to insert plasmids. Transformed bacteria were selected on Luria-Berani (LB) agar plates containing 100 μg/ml of ampicillin. Plasmid containing each target gene was then isolated using the Plasmid Miniprep Kit (Qiagen, Germany), and recombinant clones (*fimA*, *gapdh*) were confirmed by sequencing using T7 primers. For expression, the recombinant plasmids,

pET-21a/*fimA* or *gapdh*, were transformed into competent *E. coli* strain BL21(DE3), selected, and grown in LB medium supplemented with ampicillin (100 µg/ml) at 37℃ with shaking overnight. The overnight cultures were inoculated by 1% (w/v) on the culture flask and grown at 37℃ with shaking until reaching an optical density OD_{600} of 0.5 followed by isopropyl-β-d-thiogalactopyranoside induction (final 1 mM). Culture was further incubated at 37℃ for 4 h 20 min. Bacteria were subsequently centrifuged at 7,000×g, 4℃ for 5 min, and resuspended in lysis buffer [50 mM sodium phosphate, 300 mM NaCl, 100 µg/ml of lysozyme, and protease inhibitor cocktail (Roche, Switzerland)] followed by sonication on ice. Cell homogenate was centrifuged at 12,000×g, 4℃ for 20 min to clarify the cell lysate. The supernatant containing recombinant protein was mixed with Ni^{2+}-NTA agarose beads and inverted gently at 4℃ for an hour. The mixture was packed into chromatography column (Bio-Rad, USA) and washed with wash buffer (50 mM sodium phosphate, 300 mM NaCl, 20 mM imidazole). Recombinant protein was eluted using elution buffers ranging between 100 mM to 250 mM imidazole in lysis buffer. 500 µl of each fraction was collected, and BCA assay (Thermo Scientifics, USA) was conducted to identify the abundance of protein. The fractions containing abundant protein were collected and dialyzed in phosphate-buffered saline at 4℃ with stirring. After dialysis, endotoxin levels were further examined using Limulus amoebocyte lysate assay kit (Lonza, Switzerland), and the absence of endotoxin contaminant was confirmed.

Construction of null mutant strain

Plasmid cloning procedure is identical to "Cloning, protein Expression, and purification" in the materials and method. Deletion of the gene encoding FimA

(PGN_0180) was constructed by replacing it with chloramphenicol acetyltransferase gene (*cat*) using SnapGene software (GSL Biotech, USA). Both upstream and downstream sequences (approximately 1 kbp each) of the *fimA* gene were amplified from genomic DNA of *P. gingivalis* ATCC 33277 strain using primers. Chloramphenicol acetyltransferase gene (*cat*) from pC326 vector was amplified using primers. Both upstream and downstream sequences of the *fimA* gene and chloramphenicol resistance cassette were inserted into the *SalI*/*XbaI*, *XmaI*/*EcoRI*, and *XmaI*/*XbaI* (Enzynomics, Republic of Korea) sites of pUC19 plasmid using T4 ligase, respectively. Electroporation of the *P. gingivalis* ATCC 33277 strain was performed with approximately 1 μg of the conjugated plasmid product containing the *cat* gene. The cells were then plated on BHIHM agar with 5% sheep blood containing chloramphenicol for null mutant selection.

Biofilm assay

Biofilm formation of *P. gingivalis* WT, △*fimA*, KDP129, and KDP136 was determined by crystal violet staining assay as previously described with minor modification [37]. *P. gingivalis* WT, △*fimA*, KDP129, and KDP136 (1×10^9 CFU/ml) were grown in BHIHM broth in a 96-well plate (Eppendorf, Hamburg, Germany) in the presence or absence of LTAs at 37°C for 72 h under anaerobic condition. To evaluate inhibitory activity of Lre.LTA on pre-formed *P. gingivalis* biofilm (WT and △*fimA*), *P. gingivalis* was grown in BHIHM broth in 96-well plate at 37°C for 24 h under anaerobic condition. After the incubation, BHIHM broth in the presence or absence of Lre.LTA was treated and further incubated at 37°C for 72 h under anaerobic condition. For the staining, biofilms were washed with phosphate-buffered saline (PBS) and stained with 0.1% crystal violet

solution (w/v), followed by incubation at RT for 20 min. The stained biofilm was washed with PBS and then dissolved in dissociation buffer [95% ethanol (v/v) and 0.1% acetic acid (v/v) in distilled water] and quantified by optical density at 600 nm (Molecular Devices, USA). To determine anti-biofilm activity of Lre.LTA against *P. gingivalis* colonization in mouse gingival tissues, *P. gingivalis* (1×10^9 CFU/ml) with excised mouse gingival tissues was grown in BHIHM broth in 96-well plate with or without treatment of Lre.LTA at 37ºC for 24 h under anaerobic conditions. Mouse gingival tissues were further washed with PBS and homogenized, followed by serial dilution. Diluted homogenized samples were further spotted on the BHIHM agar with 5% sheep blood and incubated at 37ºC for 7 days under anaerobic conditions. After incubation, total CFU of each group was calculated.

Confocal laser scanning microscopy

Biofilm of *P. gingivalis* WT and △*fimA* was formed on sterile confocal glass-bottom dishes (1×10^9 CFU/ml) in BHIHM broth in the presence or absence of Lre.LTA at 37ºC for 72 h under anaerobic conditions. To evaluate the anti-biofilm activity Lre.LTA against pre-formed *P. gingivalis* biofilm, biofilms were formed for 72 h and were treated with or without Lre.LTA for an additional 24 h under the aforementioned biofilm assay conditions. Samples were then gently rinsed with PBS and stained with SYTO9, SYPRO Ruby, or propidium iodide. Biofilms were observed using a confocal laser scanning microscope after washing with PBS (LSM 800, Zeiss, Oberkochen, Germany). For detecting live *P. gingivalis*, simultaneous dual-channel imaging was employed to show green fluorescence (for SYTO9 at 480/500 nm, Thermo Scientifics, USA) and red fluorescence (for propidium iodide or SYPRO Ruby at 490/635 nm and 450/610 nm,

respectively, Thermo Scientifics, USA). COMSTAT2 software was used to examine Z-stacks of biofilms to determine the total biomass and average thickness of the *P. gingivalis* biofilm. To determine the interaction between Lre.LTA and *P. gingivalis* biofilm, *P. gingivalis* (1×10^9 CFU/ml) biofilm was formed at 37°C for 72 h on confocal dishes in anaerobic conditions and further incubated in the presence or absence of FITC-conjugated Lre.LTA for 6 h. After the incubation, *P. gingivalis* biofilm was stained with DAPI (358/461 nm, Invitrogen, USA) to detect *P. gingivalis* and SYPRO Ruby (450/610 nm) to detect extracellular protein matrix. Localization of Lre.LTA on *P. gingivalis* biofilm was visualized by snapshot, Z-stacks, and snapshot for single-cell ROI was taken using confocal laser scanning microscopy.

Measurement of AI-2 activity

The AI-2 assay was carried out as previously described [43]. In brief, each supernatant from the biofilm formation (72 h) and pre-formed biofilm (additional 24 h) of *P. gingivalis* in the presence or absence of Lre.LTA was centrifuged and harvested by filtering through 0.2 μm pore size filters (Sartorius, Germany). AI-2 reporter strain *Vibrio harveyi* BB170 was cultivated in autoinducer bioassay media (Difco, USA) for an overnight at 30℃, and diluted in new AB medium (1:5,000). Diluted *V. harveyi* BB170 was then combined with *P. gingivalis* supernatants and incubated for 4 h at 30℃ with shaking. Microplate reader (Spark 100M, Switzerland) was used to measure the AI-2 production of *P. gingivalis* biofilm and the AI-2 producing strain *V. harveyi* BB152 was used as positive control.

Gingipain enzymatic activity

Planktonic culture of *P. gingivalis* (5×10^9 CFU/ml) was harvested by centrifugation at 5,000×g for 5 min. After centrifugation, filtered supernatants (for detecting RgpB activity) and the bacterial pellets (for detecting RgpA and Kgp activity) were collected and mixed with reaction buffer (50 mM Tris hydrochloride, pH 7.5; 1 mM $CaCl_2$; 5 mM cysteine). *P. gingivalis* cells (1×10^8 CFU/ml) and supernatants were incubated on an ice-cold 96-well plate with or without Lre.LTA, and a specific substrate for Rgp (500 μM, Nα-benzoyl-DL-arginine p-nitroanilide hydrochloride, BAPNA) or Kgp (500 μM, N-tosyl-glycyl-L-prolyl-L-lysine 4-nitroanilide acetate salt, Z-GPK-pNA) at 37℃ in the dark for 90 min. Substrate hydrolysis was recorded at optical density of 405 nm for 90 min, and activity was expressed by setting the optical density in non-treated group as 100%.

Ni^{2+}-NTA-pull down assay

To verify the interaction between Lre.LTA and *P. gingivalis* protein, a pull down assay was performed. Briefly, Ni^{2+}-NTA agarose beads (Qiagen, Germany) were equilibrated with wash buffer (50 mM sodium phosphate, 300 mM NaCl, and 20 mM imidazole), and immobilized 30 μg of His-tagged recombinant *P. gingivalis* FimA and GAPDH protein. After 1 h incubation and wash for three times, 30 μg of Lre.LTA was added and further incubated at 4℃ for overnight with rotation. Following the incubation, ligand-bound Ni^{2+}-NTA beads were transferred to new 1.5 ml tubes to minimize remaining unbound recombinant proteins or Lre.LTA, and additionally washed five times. Finally, beads were mixed with 2X SDS-sample buffer [100 mM Tris-HCl, 2% SDS, 25% glycerol (v/v), 5% 2-mercaptoethanol (v/v), and 0.01% bromophenol blue (w/v)] and

boiled at 95℃ for 10 min to release the bound proteins and Lre.LTA. The supernatant was then further analyzed using Western blot.

Conjugation of Lre.LTA with NHS-beads

N-hydroxysuccinimide (NHS)-beads (500 mg) were equilibrated with pyrogen-free distilled water and conjugated with or without Lre.LTA (0 or 2.5 mg) with voltex at 4°C for 4 h. NHS or NHS-Lre.LTA conjugated beads were blocked with 0.1 M ethanolamine-HCL (pH 8.0) with voltex at 4°C for 1 h. After blocking, the supernatant was discarded, and beads were washed with pyrogen-free distilled water. Conjugation of Lre.LTA to NHS-beads was checked by Kaiser's test for detecting free amino functional groups [50]. The amount of Lre.LTA in the NHS-beads was calculated by phosphate assay using various concentrations of purified Lre.LTA as a standard.

Identification of Lre.LTA-binding proteins from *P. gingivalis*

P. gingvalis whole cell lysates (1.5 mg) were incubated with 100 mg of blocked NHS-beads at 4℃ for 1 h to eliminate non-specific binding protein. Pre-cleared *P. gingivalis* proteins were further incubated with native beads (100 mg) or Lre.LTA-beads (100 mg) with on a rotation rocker at 4℃ for overnight and washed with PBS. SDS-PAGE was used to separate the bound proteins. The complete bands were trimmed out after the proteins had been stained with Coomassie blue and then subjected to a liquid chromatography hybrid-FT orbitrap mass spectrometer. Mascot Daemon (Matrix Science, London, UK) was used to evaluate the acquired mass and tandem mass spectra using the Uniprot database (taxon ID : *P. gingivalis* ATCC 33277, 431947).

Gel Staining and Western blot

In order to release the bound proteins and Lre.LTA, *P. gingivals* proteins from NHS-Lre.LTA conjugate beads were combined with 2X SDS-sample buffer and heated at 95℃ for 10 min. In a Mini Protean II Dual Slap Cell (BioRad, Germany) chamber, proteins were electrophoresed using 12% polyacrylamide gels for 30 min at 80 V and 120 min at 120 V. The separated proteins were stained with Coomassie G-250 solution [0.1% (w/v) Coomassie Brilliant Blue G-250, 45% (v/v) methanol, and 10% acetic acid (v/v)] for 1 h, and destained with destaining solution [10% (v/v) methanol and 10% acetic acid (v/v)] for overnight. For Western blot anaylsis, samples on 12% or 15% polyacrylamide gels were transferred to polyvinylidene difluoride (PVDF) membrane (Millipore, USA). After blocking with 5% skim milk (Difco, USA) in Tris-buffered saline containing Tween 20 (TBST; 20 mM Tris·HCl, 150 mM NaCl, and 0.05% Tween 20), membranes were probed using mouse monoclonal antibodies for detecting LTA (Hycult, Netherlands), β-actin (Santa Cruz, USA), hexa-histidine (Abcam, UK), and rabbit polyclonal antibody for detecting MCPIP-1 (Abbiotec, USA) (dilution factor 1:1,000). Proteins were detected using horseradish peroxidase conjugated to goat anti-mouse (Jackson ImmunoResearch, USA) or rabbit secondary antibody (SouthernBiotech, USA) (1:3,000) and reacted with the ECL kit (Dyne Bio, Republic of Korea).

Flow cytometry analysis

To determine the interaction between Lre.LTA and *P. gingivalis*, 1×10^8 CFU/ml of *P. gingivalis* was incubated in PBS with Lre.LTA-FITC for 1 h. After washing with PBS, binding of Lre.LTA to *P. gingivalis* was determined by flow cytometry. The mean

fluorescence intensity of Lre.LTA-FITC was analyzed by flow cytometer (FACSverse, BD Biosciences, USA) and FlowJo software (TreeStar, USA).

Surface plasmon resonance analysis

Surface plasmon resonance (SPR) analysis with iMSPR-Pro/A device (iCluebio, Republic of Korea) was used to determine binding kinetics between FimA and Lre.LTA. The mixture of 100 mM NHS plus 50 mM MES (pH 5.0) and 200 mM N-(3-dimethylaminopropyl)-N'-ethylcarbodiimide hydrochloride (1:1, v/v) was used to initially introduce reactive amine groups on the C-Dex100 dextran sensorchip (iCluebio, Republic of Korea). FimA protein (75 μg/ml) was diluted with 5 mM sodium acetate (pH 4.0) and adsorbed on the dextran sensorchip for amine coupling. Active groups were then blocked by 1M ethanolamine (iCluebio, Republic of Korea). After blocking, binding and dissociation were observed by injecting 0–30 μg/ml of Lre.LTA over the FimA surfaces in running buffer (5 mM Hepes, pH 7.4, 75 mM NaCl, 0.0025% tween-20, iCluebio, Republic of Korea) at 25℃ in the flow rate of 10 μg/min. 50 mM glycine in running buffer and further wash steps were added to each concentration of Lre.LTA to regenerate binding. The blank curves from non-treatment of Lre.LTA was subtracted from the data by normalization. After normalization, the association (ka) and dissociation (kd) rate constants were calculated simultaneously by TraceDrawer software version 1.9.2 (Ridgeview Instruments, Sweden). The equilibrium dissociation constants were calculated using these numbers (KD).

RNA isolation

For *P. gingivalis* RNA isolation, biofilm formation of *P. gingivalis* WT in the presence or absence of Lre.LTA as mentioned in biofilm assay was initially incubated at 37°C for 24 h. The biofilm was scraped off and resuspended in PBS. After resuspension, bacterial pellet was harvested by centrifugation at 9,000×g for 3 min. After harvesting samples, total RNA of *P. gingivalis* or YD-38 cells were isolated using a TRIzol extraction method according to the manufacturere's instruction (Thermo Scientific, USA), and *P. gingivalis* was further purified by RNeasy Mini kit (Qiagen, USA) according to the manufacturer's instruction to avoid bacterial DNA contamination.

RNA sequencing and bioinformatics analysis

RNA-Seq was performed to analyze differential gene expression of *P. gingivalis* biofilm in the presence or absence of Lre.LTA. rRNA in total RNA was depleted with NEBNext® rRNA Depletion Kit (New England Biolabs, USA) and followed by library construction using TruSeq Stranded Total RNA Library Prep Gold Kit (Illumina, USA). Transcriptome raw data provided ~ 25 milion reads per sample by Illumnia platform and further checked its quality by the FastQC (https://www.bioinformatics.babraham.ac.uk/projects/fastqc). Trimming was performed to remove low-quality reads from raw data using the Trimmomatic software 0.38 version [51]. Paired-end sequences were mapped to *P. gingivalis* ATCC 33277 available genome (RefSeq assembly accession GCF_000010505.1_ASM1050v1) using Bowtie [52]. Differential gene expression analysis was performed by HTseq version 0.10.0 [53]. Up- or down-regulated gene expression was defined as gene expression that shows at least 1.5-fold difference ($p < 0.05$) to the non-treated group by exactTest using edgeR [54].

Real-time polymerase chain reaction (RT-PCR)

M-MLV Reverse Transcriptase kit (Promega, USA) was used to create cDNA after total RNA from YD-38 cells was extracted using a TRIzol reagent. IL-6, IL-8, and IL-1β mRNA expression levels were assessed by real-time PCR using SYBR Premix Ex TaqTM (Takara Bio Inc., Japan), and GAPDH was utilized as a housekeeping control to normalize each target gene expression. The forward and reverse primer sequences (Bioneer, Seoul, Korea) for the real-time PCR were 5′-TGTGGTTGGGTCAGGGGTGG-3′ and 5′-AGCGCCTTCGGTCCAGTTGC-3′ for IL-6, 5′-GTGCAGTTTTGCCAAGGAGT-3′ and 5′-CTCTGCACCCAGTTTTCCTT-3′ for IL-8, 5′-CAGAAGTACCTGAGCTCGCC-3′ and 5′-AGATTCGTAGCTGGATGCCG-3′ for IL-1β and 5′-AAGGTGAAGGTCGGAGTCAA-3′ and 5′-ATGACAAGCTTCCCGTTCTC-3′ for GAPDH, respectively.

Mouse model of periodontitis

The Institutional Animal Care and Use Committee of Seoul National University approved the study (authorization no. SNU-210118-4-6). The 9 to 10-week-old male C57BL/6 mice (DooYeol Biotech, Republic of Korea) were randomly divided into sham control, ligature, ligature with Lre.LTA, and ligature with infection of *P. gingivalis* WT or null mutants (△*fimA* or KDP136) in the presence or absence of Lre.LTA groups (5 mice in each group). The left maxillary second molar was fastened with a 5-0 silk ligature. Sham group had the ligature immediately removed after 90 min of surgery. After the surgery, 1×10^9 CFU of *P. gingivalis* WT, △*fimA*, or KDP136 with 1.5% carboxymethylcellulose (CMC) were inoculated in the left maxillary molar (three times, 2 days intervals) in the presence or absence of Lre.LTA (50 μg, seven times, every day).

In the control group, mice were treated in the same way with an equal volume of vehicles (1.5% CMC). 7 days after the treatment, mice were euthanized.

Micro-computed tomography

The maxillary molar was micro-computed tomographically scanned (micro-CT; Skyscan1172 scanner, Skyscan, Kontich, Belgium) after fixation in 4% paraformaldehyde. CT-volume software was used to create three-dimensional pictures of the maxillary molar (Skyscan). The average distance from the cementum-enamel junction to the alveolar bone crest (CEJ-ABC) across the four molar sites (M1 to M3) was measured using ImageJ software (National Institutes of Health, USA) to assess the amount of bone loss in the maxillary molar.

Statistical Analysis

Graphed data represents the average of triplicate with error bars displaying the standard deviation. The Student's t-test was used to examine the statistical significance between the indicated treated and non-treated groups. Asterisks (*) denote experimental groups that significantly differ from the control group ($p < 0.05$).

Results

***Lactobacillus* LTAs display structurally different poly-Gro-P depending on their species.**

To evaluate whether *Lactobacillus* LTAs have anti-biofilm activities on biofilm formation of *P. gingivalis*, LTAs from five different species of *Lactobacillus* were purified. Also, since the phosphate contents of column fractions are linearly correlated with their LTA amounts, an inorganic phosphate assay was then carried out for each column fraction from the hydrophobic interaction and ion-exchange chromatography [55]. Phosphate-containing fractions of *L. rhamnosus* (Lr.LTA) and *L. plantarum* (Lp.LTA) revealed comparatively similar fractions ranging from 15 to 21 after purification by hydrophobic interaction chromatography (Figure 7E and 7G, left), while phosphate containing fractions of *L. acidophilus* (La.LTA), *L. casei* (Lc.LTA), and *L. reuteri* (Lre.LTA) (11 to 28) showed similar yet broader range (Figure 7A, 7C, and 7I, left). Following ion-exchange chromatography, the phosphate fraction numbers of Lc.LTA, Lr.LTA, and Lp.LTA (10 to 17) were detected in a comparatively similar range (Figure 7D, 7F, and 7H, right), while ranges of La.LTA (15 to 27) and Lre.LTA (12 to 24) were broader than the other *Lactobacillus* species. However, La.LTA showed the lowest phosphate content among the *Lactobacillus* species, indicating that each *Lactobacillus* species differs in their net charges and degree of hydrophobicity (Figure 7B, 7D, 7F, 7H and 7J, right). After purification and quantification, Western blot was performed to detect *Lactobacillus* LTA using antibody, which recognizes the poly-Gro-P backbone of LTA. Except for *L. acidophilus* LTA, LTA from all *Lactobacillus* species has a poly-Gro-P structure, and silver staining revealed that La.LTA contained a similar

size of LTA with other *Lactobacillus* species, suggesting that La.LTA is not a typical type I LTA (Figure 8A and 8B). Interestingly, inorganic phosphate assay of quantified LTAs showed that Lc.LTA and Lp.LTA had the most abundant phosphate content, while La.LTA appeared to be lower among the *Lactobacillus* species (Figure 8C). This result suggests that each *Lactobacillus* species possess structurally unique LTA in their net charge.

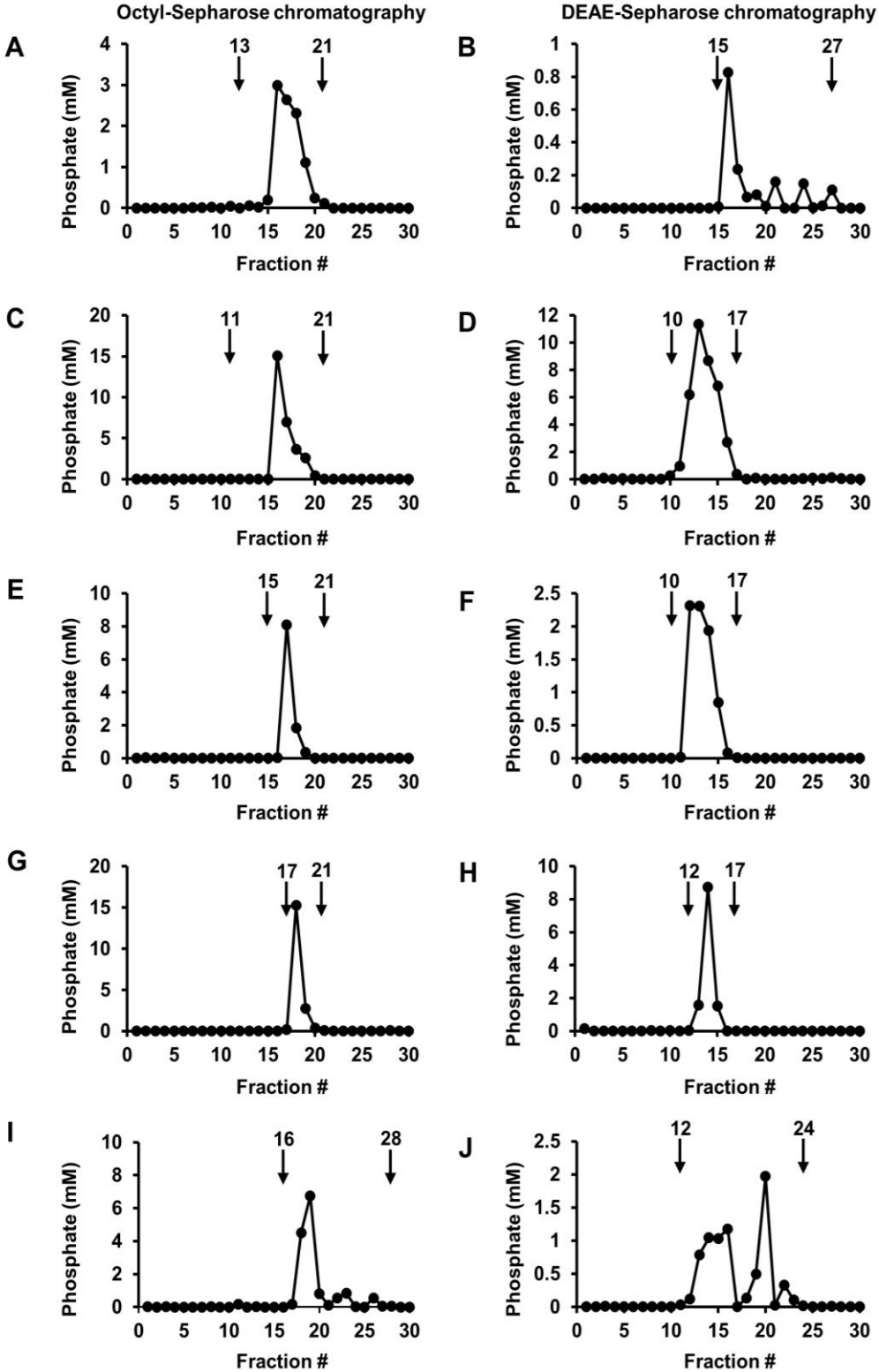
Octyl-Sepharose chromatography
DEAE-Sepharose chromatography
A
B
C
D
E
F
G
H
I
J
Phosphate (mM)
Fraction #
13
21
15
27
11
21
10
17
15
21
10
17
17
21
12
17
16
28
12
24

Figure 7. Elution profiles of LTAs purified from different species of *Lactobacillus*

(A–J) LTAs from several *Lactobacillus* species, including (A-B) *Lactobacillus acidophilus* KACC 12419, (C-D) *Lactobacillus casei* KCTC 3260, (E-F) *Lactobacillus rhamnosus* GG, (G-H) *Lactobacillus plantarum* KCTC10887bp, and (I-J) *Lactobacillus reuteri* ATCC 23272, were purified by sequentially applying butanol extraction, hydrophobic interaction chromatography, and ion-exchange chromatography. Inorganic phosphate assays were then carried out to determine the amount of LTAs in each fraction. Octyl-sepharose, left; DEAE-sepharose, right

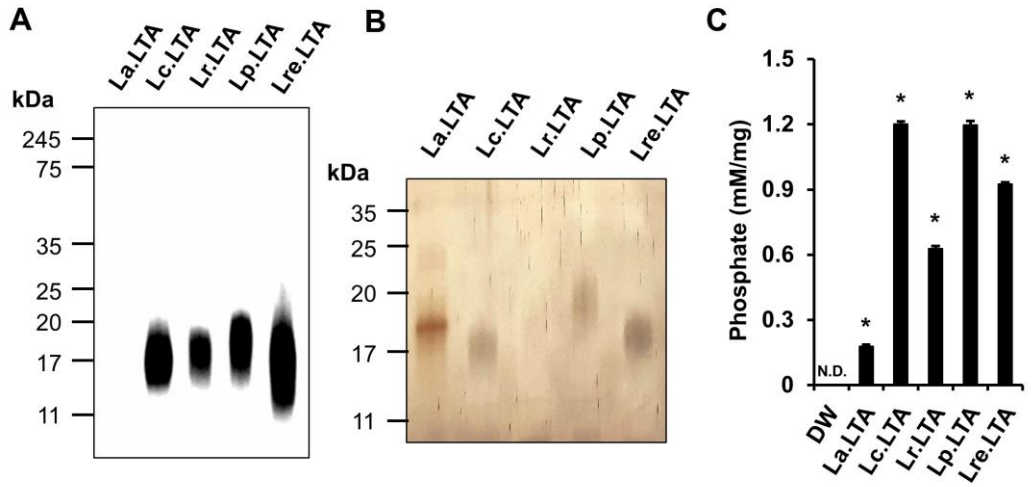

Figure 8. *Lactobacillus* LTAs display structurally different poly-Gro-P depending on their species

After quantification of *Lactobacillus* LTAs, (A) Western blot and (B) silver staining were conducted to detect *Lactobacillus* LTAs. Each of *Lactobacillus* LTA (1 μg) was prepared and separated in 15% SDS-PAGE gel as described in Materials and Method. *Lactobacillus* LTAs were detected by using poly-Gro-P-specific LTA antibody. The position of protein standards presented as kilodaltons (kDa) is indicated on the left. (C) Inorganic phosphate of each *Lactobacillus* LTAs was examined to measure the phosphate contents per 1 mg of each LTA. Asterisk (*) indicates statistical significance at $p < 0.05$ between the control group (DW) and each LTA group. N.D., non-detected

Lre.LTA potently inhibits biofilm formation of *P. gingivalis* compared with other *Lactobacillus* LTAs.

To identify whether *Lactobacillus* LTAs have anti-biofilm activity against *P. gingivalis* biofilm formation *in vitro*, anti-biofilm activity of five species from *Lactobacillus* LTAs was evaluated by crystal violet staining. As shown in Figure 9, Lc.LTA, Lr.LTA, Lp.LTA, and Lre.LTA had a dose-dependent effects on preventing *P. gingivalis* from forming biofilms. In contrast, La.LTA did not affect *P. gingivalis* biofilm formation. Since Lre.LTA displayed the most profound anti-biofilm activity among *Lactobacillus* LTAs, Lre.LTA was chosen for further experiments.

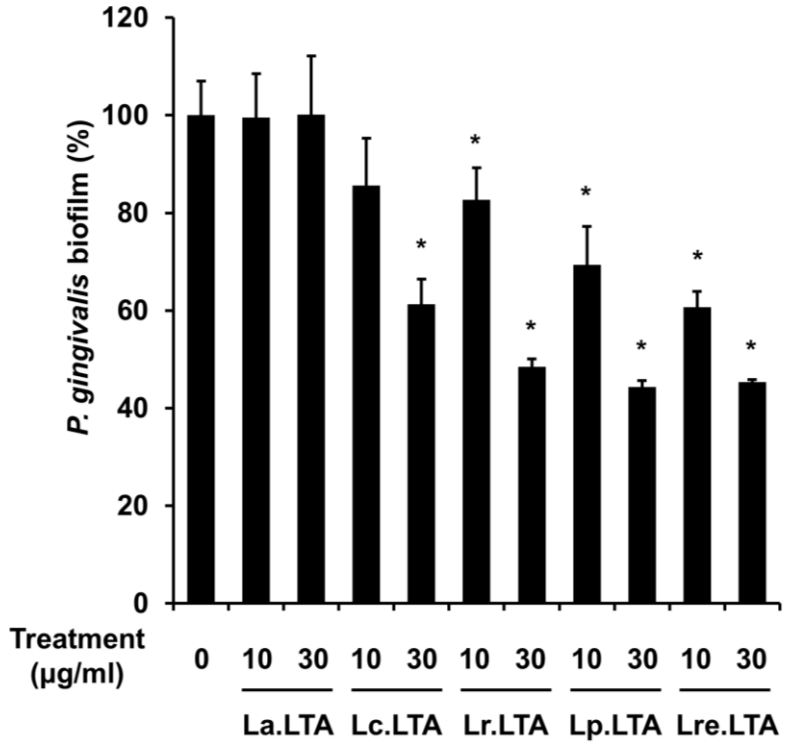

Figure 9. Lre.LTA potently inhibits biofilm formation of *P. gingivalis* compared with other *Lactobacillus* LTAs

P. gingivalis (1×10^9 CFU/ml) was grown on 96-well plates in the absence (non-treatment, vehicle control) or in the presence of LTAs (10 or 30 μg/ml) purified from different species of *Lactobacillus* at 37°C for 72 h in anaerobic conditions. Biofilms were evaluated by crystal violet assay as described in Materials and Method. Biofilm biomass in crystal violet assay was presented as a percentage of the biofilm ± standard deviation of triplicates, considering the optical density in non-treated group as 100%. Asterisk (*) indicates statistical significance at $p < 0.05$ between the groups. La.LTA, *L. acidophilus* LTA; Lc.LTA, *L. casei* LTA; Lr.LTA, *L. rhamnosus* LTA; Lp.LTA, *L. plantarum* LTA; Lre.LTA, *L. reuteri* LTA

Lre.LTA has anti-biofilm activity in both biofilm formation and pre-formed biofilm of *P. gingivalis* without affecting its growth.

Next, dose-dependent inhibitory effect of Lre.LTA on *P. gingivalis* biofilm formation and pre-formed biofilm was examined. The results showed that Lre.LTA dose-dependently inhibited or disrupted the biofilm formation or pre-formed biofilm of *P. gingivalis* (Figure 10A and 10B). To further evaluate the phase dynamics of anti-biofilm activity by Lre.LTA, *P. gingivalis* biofilm was formed at 3, 6, 12, 24, 48, and 72 h with Lre.LTA. The anti-biofilm activity of Lre.LTA began at 6 h, and its inhibition remained effective up to 72 h (Figure 10C). In order to determine the effective time point of Lre.LTA on pre-formed biofilm of *P. gingivalis*, Lre.LTA was treated to pre-formed *P. gingivalis* biofilm and further incubated for 0, 3, 6, 12, 24, and 48 h. As shown in Figure 10D, Lre.LTA disrupted the pre-formed biofilm of *P. gingivalis* starting at 12 h and remained effective until the experimental hour. To identify whether anti-biofilm activity of Lre.LTA is mediated by growth inhibition, the growth of *P. gingivalis* in the presence or absence of Lre.LTA was examined. The result showed that Lre.LTA did not affect the growth of *P. gingivalis* (Figure 10E). Collectively, these results suggest that Lre.LTA has anti-biofilm activity against *P. gingivalis* biofilm without affecting its growth.

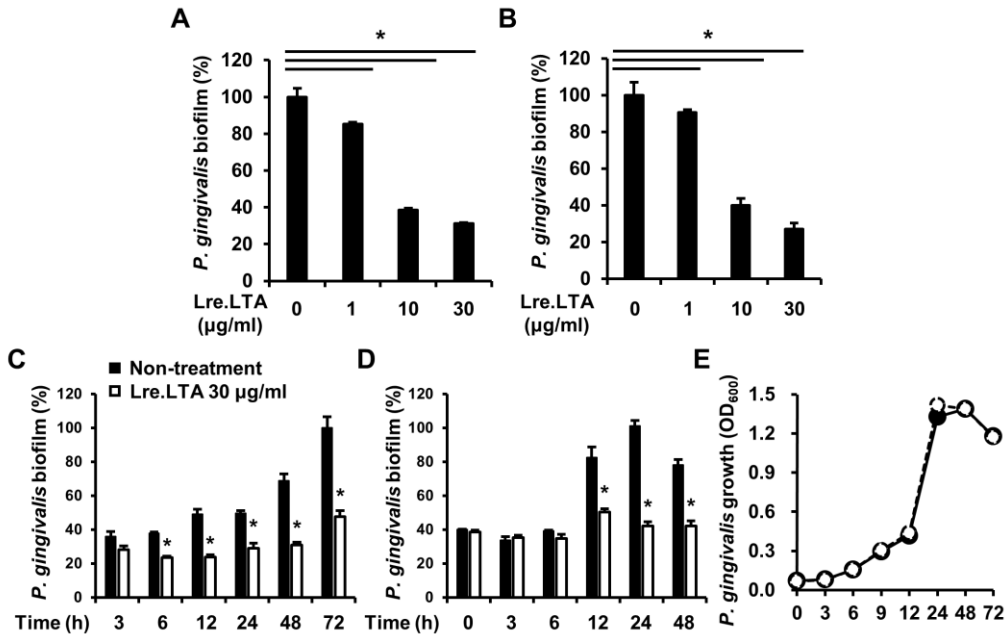

Figure 10. Lre.LTA has anti-biofilm activity in both biofilm formation and pre-formed biofilm of *P. gingivalis* without affecting its growth

(A) *P. gingivalis* (1×10^9 CFU/ml) was grown on 96-well plates in the presence or absence of Lre.LTA (0, 1, 10, or 30 μg/ml) at 37°C for 72 h in anaerobic conditions. (B) Pre-formed biofilm established with *P. gingivalis* (1×10^9 CFU/ml) at 37°C for 72 h in anaerobic conditions on 96-well plates was treated with Lre.LTA (0, 1, 10, or 30 μg/ml) and further incubated for 24 h. (C) *P. gingivalis* (1×10^9 CFU/ml) was grown on 96-well plates at 37℃ in anaerobic conditions for 3, 6, 12, 24, 48, or 72 h in the presence or absence of Lre.LTA (30 μg/ml). (D) Pre-formed biofilm established with *P. gingivalis* (1×10^9 CFU/ml) at 37°C for 72 h in anaerobic conditions on 96-well plates was treated with or without Lre.LTA (0 or 30 μg/ml) and further incubated for 0, 3, 6, 12, 24, or 48 h. (E) *P. gingivalis* was grown for 0, 3, 6, 12, 24, 48, or 72 h in the presence or absence of Lre.LTA (30 μg/ml) under static conditions. Biofilm biomass in crystal violet assay was

presented as a percentage of the biofilm ± standard deviation of triplicates, considering the optical density in non-treated group as 100%. Asterisk (*) indicates statistical significance at $p < 0.05$ between the non-treated and Lre.LTA-treated groups. The growth of *P. gingivalis* was determined by optical density at 600 nm.

Acyl chains are major functional moieties of Lre.LTA responsible for its anti-biofilm activity.

Given that LTA is an amphiphilic molecule composing hydrophilic poly-Gro-P backbone with D-alanine residues and hydrophobic acyl chain of glycolipid (Figure 11A), the functional molecules relevant for Lre.LTA to suppress *P. gingivalis* biofilm formation were identified. D-alanine moieties-deleted Lre.LTA (Deala-Lre.LTA) and both D-alanine and acyl moieties-deleted Lre.LTA (Deala/Deacyl-Lre.LTA) was prepared as described in the Materials and Method, and dealanylation and deacylation of Lre.LTA was further verified by spraying method (Figure 11B). Among the types of Lre.LTA, although the anti-biofilm activity of Deala/Deacyl-Lre.LTA was reduced about 1.5-fold compared to the intact Lre.LTA, the anti-biofilm activity of Deala-Lre.LTA was most effective against *P. gingivalis* biofilm formation (Figure 11C). These results suggest that Lre.LTA having acyl chain moieties is crucial for inhibiting biofilm formation of *P. gingivalis*.

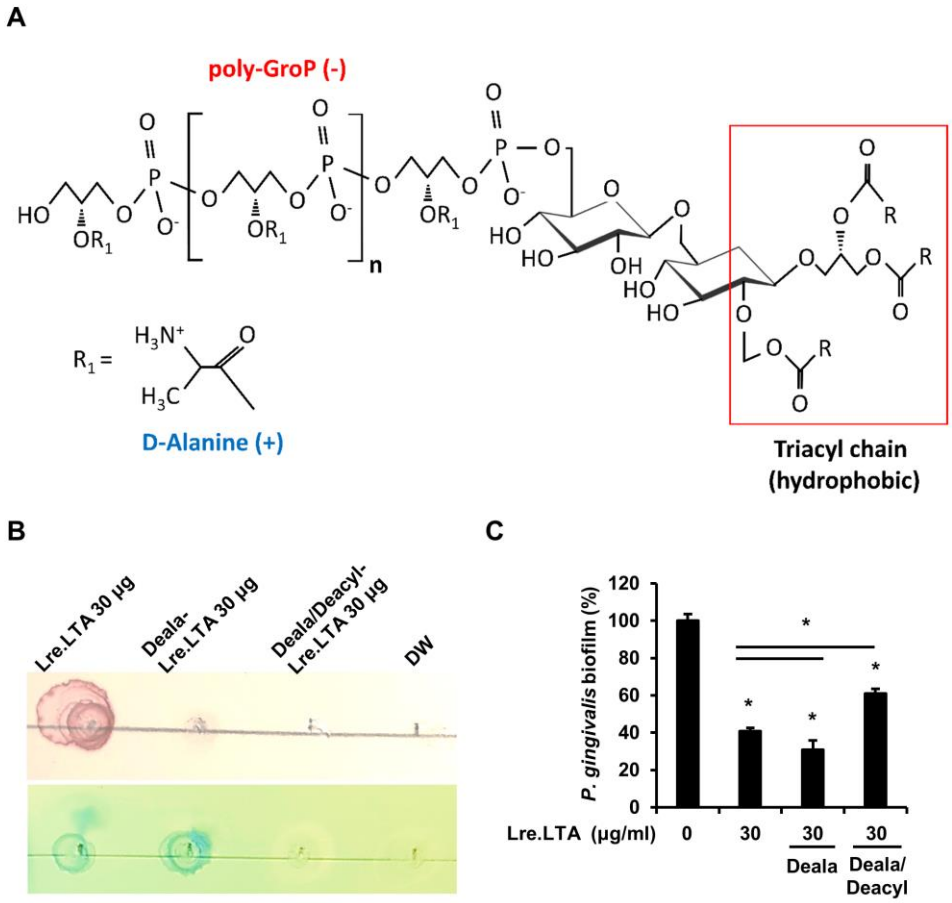

Figure 11. Acyl chains are major functional moieties of Lre.LTA responsible for its anti-biofilm activity

(A) Structure of typical type I LTA from *Lactobacillus* LTA. (B) Dealanylated (Deala) or dealanylated/deacylated (Deala/Deacyl) Lre.LTA was constructed by treatment of Lre.LTA with Tris-HCl or NaOH. Deletion of D-alanine or D-alanine/acyl chain moieties of Lre.LTA was verified by 1% ninhydrin solution or 5% phosphomolybdic acid, respectively. DW, distilled water (C) *P. gingivalis* (1×10^9 CFU/ml) was grown on 96-well plates in the presence or absence of Lre.LTA, Deala-Lre.LTA, or Deala/Deacyl-Lre.LTA (30 μg/ml) at 37°C for 72 h in anaerobic condition. Biofilms were determined

by crystal violet assay as described in Materials and Method. Biofilm biomass in crystal violet assay was presented as a percentage of the biofilm ± standard deviation of triplicates, considering the optical density in non-treated group as 100%. Asterisk (*) indicates statistical significance at $p < 0.05$.

Lre.LTA effectively inhibits the biofilm formation of clinically isolated *P. gingivalis* strains from patients with periodontitis.

To confirm the clinical relevance of these findings, *P. gingivalis* clinical isolates obtained from subgingival dental plaque of patients with periodontitis were grown on 96-well plates in the presence or absence of Lre.LTA. Interestingly, all of the homotypic biofilm formation of *P. gingivalis* clinical isolate was significantly inhibited by Lre.LTA about 30% to 80% (Figure 12A-12F). These results indicate that Lre.LTA inhibits biofilm of *P. gingivalis* clinical isolates, proposing its anti-biofilm potential.

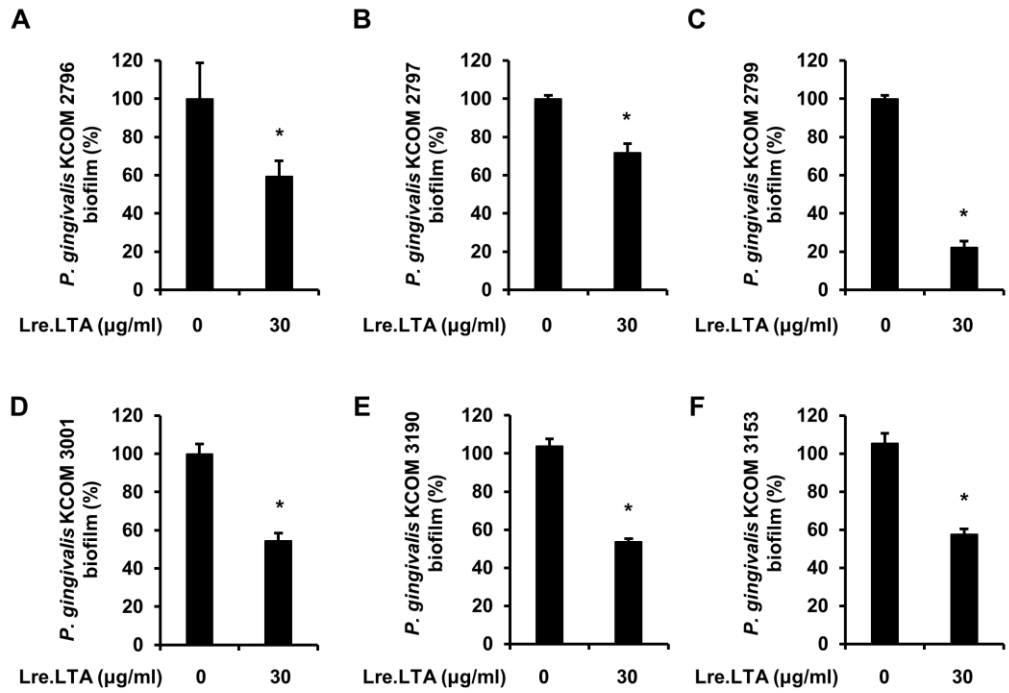

Figure 12. Lre.LTA inhibits the biofilm formation of clinically isolated *P. gingivalis* strains from patients with periodontitis

(A-F) *P. gingivalis* clinical isolates from patients with aggressive periodontitis (1×10^9 CFU/ml) were grown on 96-well plates in the presence or absence of Lre.LTA (30 μg/ml) at 37°C for 72 h in anaerobic conditions. After the incubation, biofilm biomass in crystal violet assay was presented as a percentage of the biofilm ± standard deviation of triplicates, considering the optical density in non-treated group as 100%. Asterisk (*) indicates statistical significance at $p < 0.05$ between the non-treated and Lre.LTA-treated group.

Lre.LTA controls biofilm of polymicrobial community.

P. gingivalis has been reported to interact with various oral bacteria or yeast, such as *F. nucleatum*, *S. gordonii*, and *C. albicans* to give rise to stability and persistence [13]. Especially, *S. gordonii* is well known as an early colonizer and representative accessory pathogen for supporting the accumulation of *P. gingivalis* into heterotypic communities, upregulating its pathogenic potential [11]. Moreover, from subgingival plaque samples, *P. gingivalis* and *S. gordonii* are frequently isolated together [56]. *C. albicans*, a yeast-like fungus, showed a significantly high level of colonization in a periodontal pocket and in patients with chronic periodontitis [57], [58]. Accumulated studies revealed that *C. albicans* forms biofilm, providing a hypoxic environment [59] and protecting *P. gingivalis* via interacting with gingipain and Als3 [60]. To investigate whether Lre.LTA affects the fungal-bacterial polymicrobial biofilm, which can contribute to periodontal disease, polymicrobial biofilm consisting of *S. gordonii*, *P. gingivalis*, and *C. albicans* in the presence or absence of Lre.LTA was confirmed by confocal laser scanning microscopy. Interestingly, Lre.LTA had anti-biofilm activity against polymicrobial biofilm of *S. gordonii*, *C. albicans*, and *P. gingivalis* biofilm formation (Figure 13A) and pre-formed biofilm (Figure 13B). Moreover, the biomass and average thickness of polymicrobial biofilm and extracellular protein matrix (EPM) in biofilm-forming and pre-formed biofilm stages were significantly reduced by Lre.LTA, suggesting Lre.LTA can disperse any stage of polymicrobial biofilm (Figure 13C-13F). Collectively, these data indicate that Lre.LTA controls biofilm of polymicrobial community, suggesting its anti-biofilm potential.

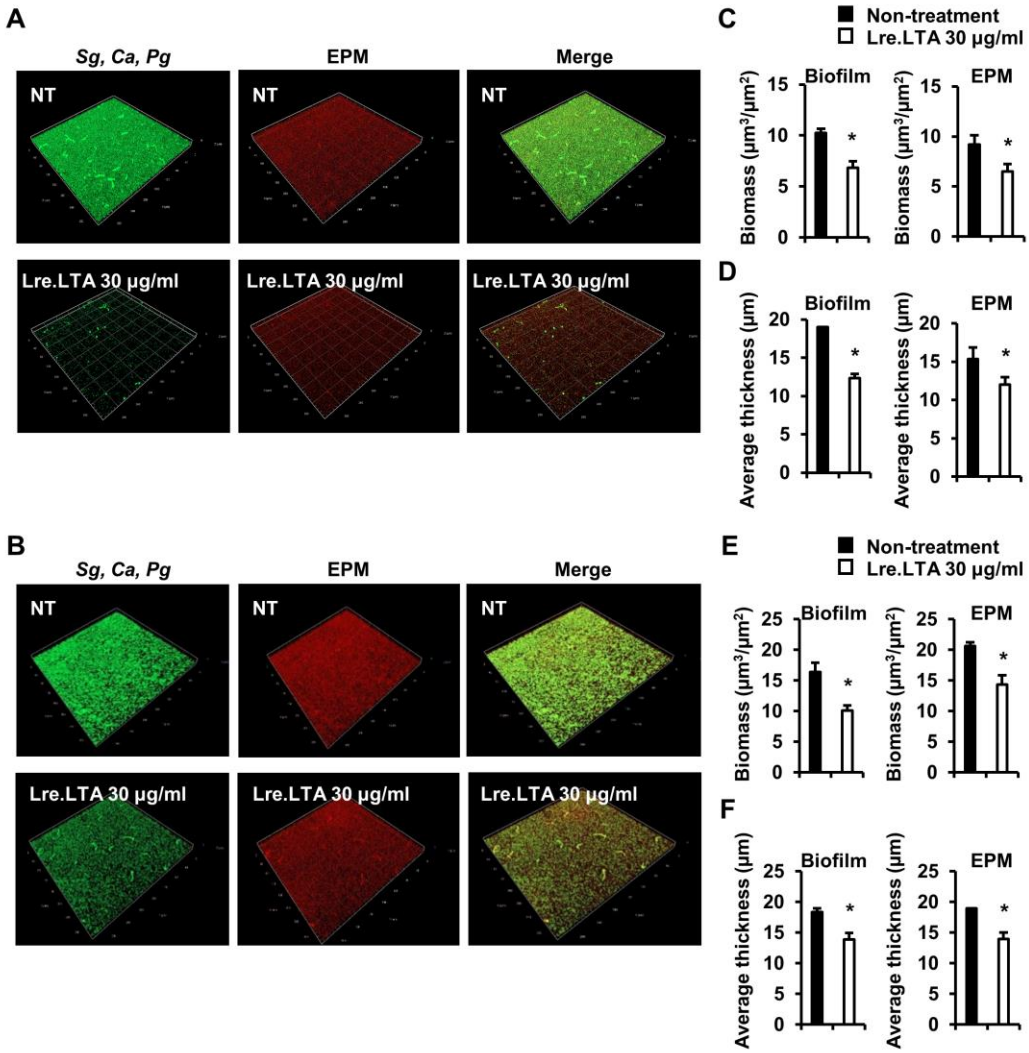

Figure 13. Lre.LTA controls biofilm of polymicrobial community

(A) *S. gordonii*, *C. albicans*, and *P. gingivalis* (1 × 10^9 CFU/ml, respectively) were grown on confocal dishes at 37℃ in anaerobic conditions for 72 h in the presence or absence of Lre.LTA (30 μg/ml). (B) Pre-formed biofilm established with *S. gordonii*, *C. albicans*, and *P. gingivalis* (1 × 10^9 CFU/ml, respectively) were grown on confocal dishes at 37℃ in anaerobic conditions for 72 h in the presence or absence of Lre.LTA (30 μg/ml). (A-B) After the incubation, biofilm was visualized by confocal laser

scanning microscopy by staining with SYTO 9 to detect mixed microbial community and SYPRO Ruby to detect EPM. Three-dimensional Z-stacks in the (A) biofilm formation of mixed microbial community and (B) pre-formed biofilm of mixed microbial community in the presence or absence of Lre.LTA (30 μg/ml) was further examined by confocal laser scanning microscopy. Total biomass and average thickness of polymicrobial species (SYTO 9) and EPM (SYPRO Ruby) during biofilm formation (C and D) and pre-formed biofilm (E and F) were quantified using Comstat2 software. Asterisk (*) indicates statistical significance at $p < 0.05$ between the non-treated and Lre.LTA-treated groups. *Sg, S. gordonii*; *Cg, C. albicans*; *Pg, P. gingivalis*

Lre.LTA disperses extracellular protein matrix of *P. gingivalis* biofilm.

Bacterial biofilm can produce EPS to protect itself from host immune system and antibiotics. Since *P. gingivalis* can produce an EPM [61], the effect of Lre.LTA on EPM of *P. gingivalis* biofilm was identified by confocal laser scanning microscopy. As a result, Lre.LTA dose-dependently dispersed EPM during biofilm formation and pre-formed biofilm while inhibiting *P. gingivalis* biofilm (Figure 14A and 14B). Three-dimensional reconstructions of the Z-stacks also showed that Lre.LTA could inhibit and disperse both *P. gingivalis* biofilm and EPM in biofilm formation and pre-formed biofilm (Figure 14C and 14D). The biomass and average thickness of *P. gingivalis* biofilm and EPM in biofilm-forming and pre-formed biofilm stages were significantly reduced by Lre.LTA, suggesting Lre.LTA can disperse any stage of *P. gingivalis* biofilm and EPM simultaneously (Figure 14E-14H).

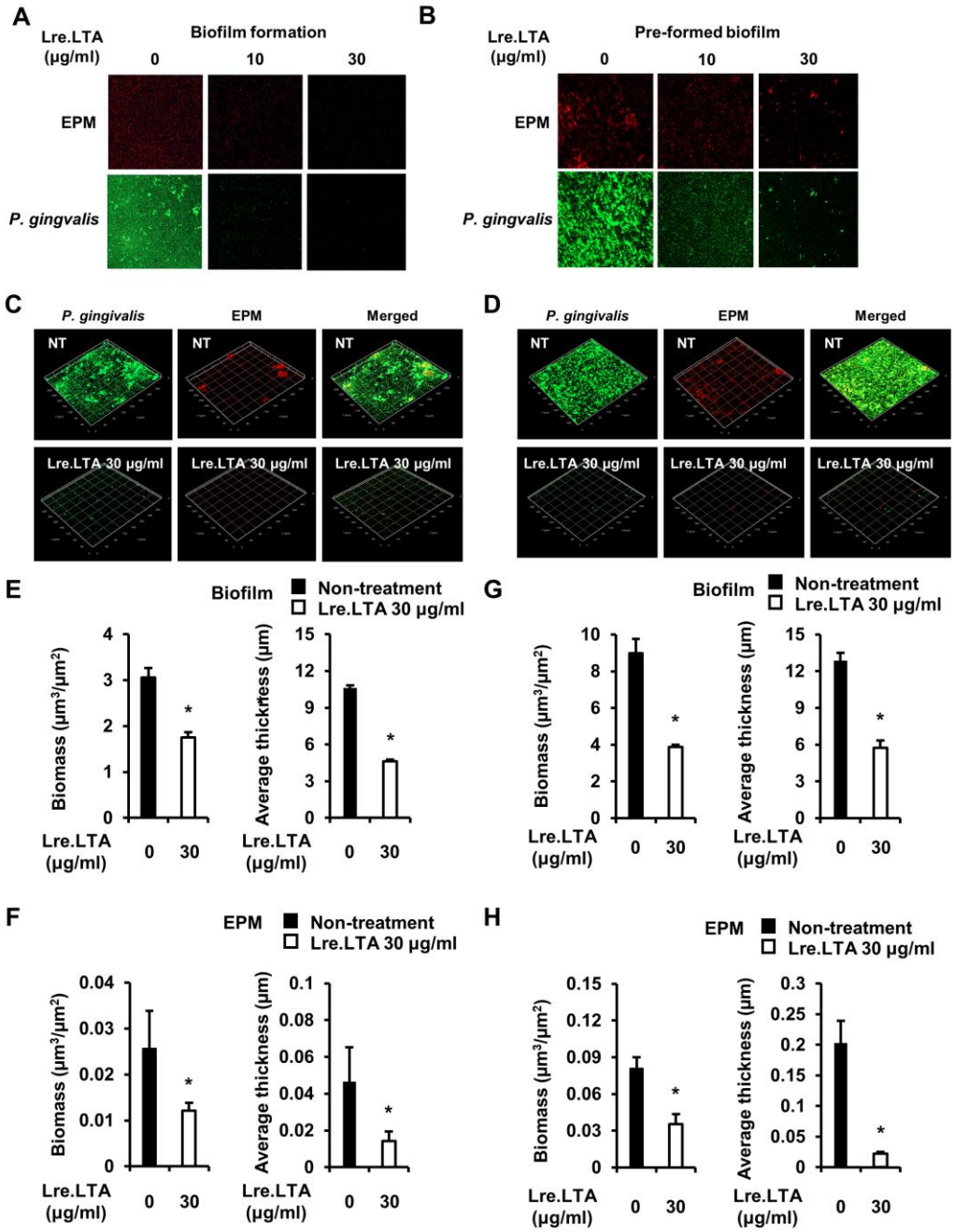

Figure 14. Lre.LTA disperses extracellular protein matrix of *P. gingivalis* biofilm

(A) *P. gingivalis* (1×10^9 CFU/ml) was grown on confocal dishes at 37℃ in anaerobic conditions for 72 h in the presence or absence of Lre.LTA (10 or 30 μg/ml). (B) Pre-

formed biofilm established with *P. gingivalis* (1×10^9 CFU/ml) at 37ºC for 72 h in anaerobic conditions on confocal dishes was treated with Lre.LTA (0, 10, or 30 μg/ml) and further incubated for 24 h. (A and C) biofilm formation of *P. gingivalis* and (B and D) pre-formed biofilm of *P. gingivalis* in the presence or absence of Lre.LTA (0 or 30 μg/ml) was further stained for detecting *P. gingivalis* (SYTO 9) and EPM (SYPRO Ruby) acquired by confocal laser scanning microscopy. Total biomass and average thickness of *P. gingivalis* and EPM during biofilm formation (E and F) and pre-formed biofilm (G and H) were quantified using Comstat2 software. Asterisk (*) indicates statistical significance at $p < 0.05$ between the non-treated (black bar) and Lre.LTA-treated (white bar) groups.

Lre.LTA directly binds with *P. gingivalis* by penetrating extracellular protein matrix.

Since Lre.LTA simultaneously dispersed EPM and *P. gingivalis* biofilm, the anti-biofilm activity of Lre.LTA might be associated with its direct physical interaction with *P. gingivalis*. To test the hypothesis, pre-formed biofilm of *P. gingivalis* was incubated in the presence or absence of Lre.LTA conjugated with FITC for 6 h. After the incubation, *P. gingivalis* and EPM were stained with DAPI, and SYPRO Ruby, respectively. The localization of Lre.LTA-FITC on *P. gingivalis* biofilm was determined by confocal laser scanning microscopy. Confocal microscopic analysis revealed that Lre.LTA colocalized with *P. gingivalis* biofilm and EPM (Figure 15A and 15B). Interestingly, in the region of single-cell interest, Lre-LTA infiltrated the EPM and directly interacted with *P. gingivalis* (Figure 15C). To further evaluate the direct interaction between Lre.LTA and *P. gingivalis*, a planktonic culture of *P. gingivalis* was incubated with or without Lre.LTA-FITC and analyzed with flow cytometry. As shown by increased fluorescent intensity, Lre.LTA could interact with *P. gingivalis* in a dose-dependent manner (Figure 15D). These results suggest that Lre.LTA disperses EPM and *P. gingivalis* biofilm by physical interaction with *P. gingivalis*.

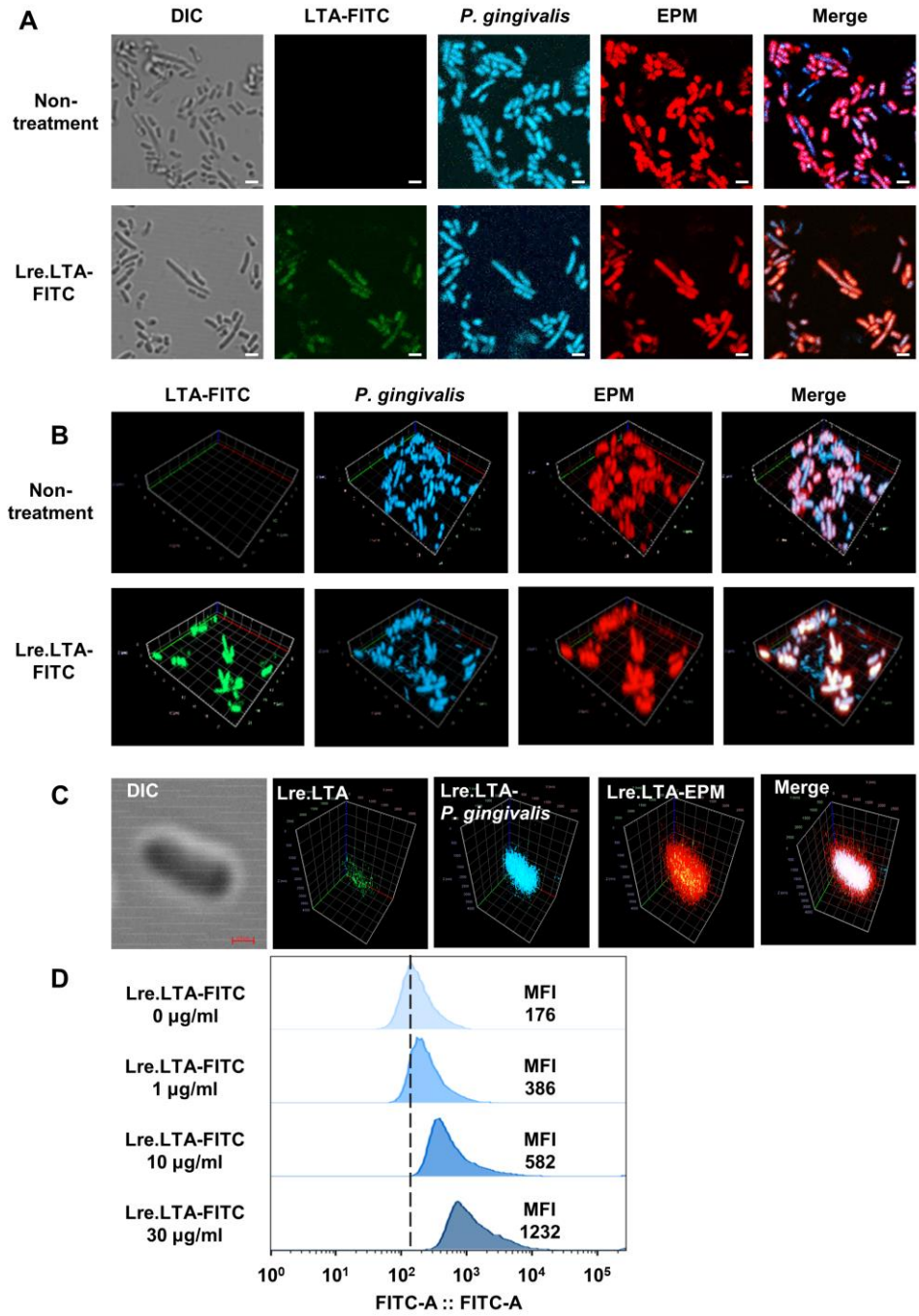

Figure 15. Lre.LTA directly binds with *P. gingivalis* by penetrating extracellular protein matrix

To identify localization of Lre.LTA on *P. gingivalis* biofilm, pre-formed biofilm established with *P. gingivalis* (1×10^9 CFU/ml) at 37°C for 72 h in anaerobic conditions on confocal dishes was treated with or without FITC-conjugated Lre.LTA (0 or 50 μg/ml) and further incubated for 6 h. After incubation, *P. gingivalis* biofilm was stained with DAPI to detect *P. gingivalis* and SYPRO Ruby to detect EPM. Localization of Lre.LTA on *P. gingivalis* biofilm was visualized by (A) snapshot, (B) Z-stacks, and (C) snapshot for single cell regions of interest creation using confocal laser scanning microscopy. The scale bar indicates 2 μm. (D) *P. gingivalis* (1×10^8 CFU/ml) was pre-incubated in the presence or absence of FITC-conjugated Lre.LTA (0, 1, 10, and 30 μg/ml) for 1 h at RT. After incubation, flow cytometry was used to detect the binding of *P. gingivalis* and FITC-conjugated Lre.LTA. The mean fluorescence intensity was analyzed by using FlowJo Software.

Identification of Lre.LTA-binding proteins in *P. gingivalis*.

To identify potential anti-biofilm mechanism of Lre.LTA against *P. gingivalis*, NHS-bead conjugated Lre.LTA from *P. gingivalis* whole cell lysate was precipitated and Lre.LTA binding proteins (Lre.LTA-Bps) were visualized by Coomassie staining to check the protein bands from lysate (Figure 16A). Lre.LTA-Bps in the whole lanes were subsequently identified using liquid chromatography hybrid-FT orbitrap mass spectrometer. A total of 316 proteins were identified in the *P. gingivalis* lysate. Among these proteins, about 73.8%, 21.5%, 1.5%, 1.5%, 0.85%, and 0.85% of proteins were located in unknown, outer membrane, secretion, cytosol, periplasm, and inner membrane, respectively (Figure 16B). Of which, only 30% of proteins were identified as functional proteins (Figure 16C). Based on the percent of molecules in a mixture that adds up to 100 percent, glyceraldehyde-3-phosphate dehydrogenase (GAPDH) in outer membrane, which is known as virulence factor in bacteria [62], was bound to Lre.LTA with the highest amount. Interestingly, major fimbriae (FimA) and arginine gingipain (RgpA) in outer membrane, which are known as critical factors for developing *P. gingivalis* biofilm [20], were predominantly bound to Lre.LTA (Figure 16D), suggesting that Lre.LTA mainly interacts with biofilm-developing factors.

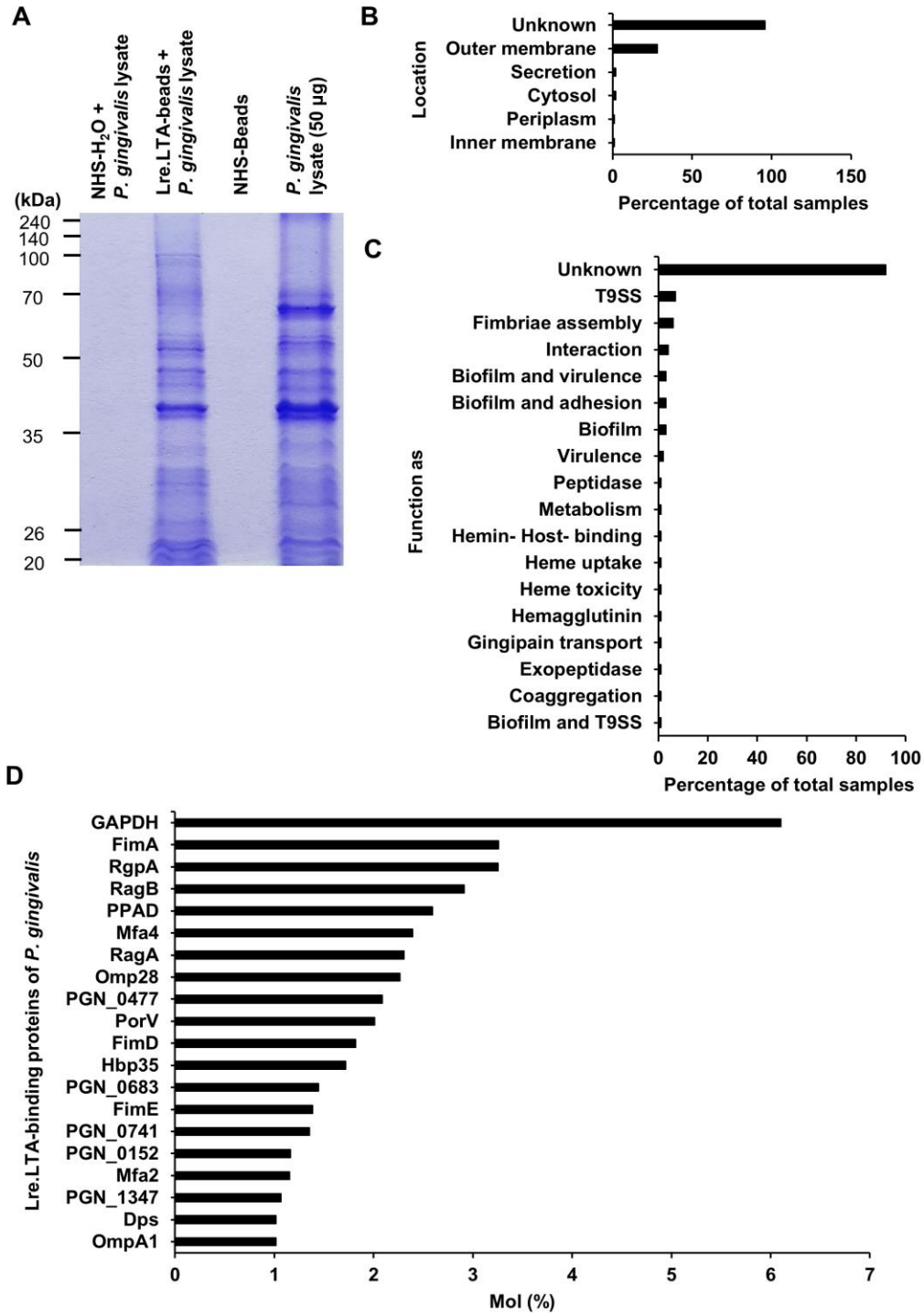

Figure 16. Identification of Lre.LTA-binding proteins in *P. gingivalis*

(A) Ethanolamine-blocked NHS beads (100 mg) conjugated with or without Lre.LTA (0 μg or 500 μg) was incubated with *P. gingivalis* whole cell lysate for overnight at 4°C. After eliminating non-specifically bound lysate from *P. gingivalis*, the bound proteins were separated on 12% SDS-PAGE and stained by Coomassie blue. Ethanolamine-blocked native beads (30 mg) were used as a loading control. High-resolution LTQ-Orbitrap hybrid Fourier transform mass spectrometry was used to further analyze the whole protein bands and (B) location of identified proteins, (C) function of identified proteins, and (D) molecular percentage of NHS-Lre.LTA conjugates in *P. gingivalis* proteins (≥ 0.1% cut-offs) were presented.

Table 2. List of Lre.LTA-binding proteins of *P. gingivalis*

Protein ID	Location	Function as	emPAI	mol%	Reference
Glyceraldehyde-3-phosphate dehydrogenase	OM	Interaction	25.19	6.1025	[63]
Type I fimbrillin, FimA	OM	Biofilm and adhesion	13.45	3.2584	[64]
Gingipain R1, RgpA	OM	Biofilm and virulence	13.43	3.2535	[65]
Receptor antigen B, RagB	OM	Virulence	12.02	2.912	[66]
Peptidylarginine deiminase, PPAD	OM	Biofilm and T9SS	10.7	2.5922	[67]
Fimbrial assembly protein, Mfa4	OM	Biofilm and adhesion	9.87	2.3911	[68]
Receptor antigen A, RagA	OM	Virulence	9.53	2.3087	[66]
Por secretion system protein, PorV	OM	T9SS	8.29	2.0083	[69]
Major fimbrium tip subunit, FimD	OM	Fimbriae assembly	7.51	1.8194	[70]
Hemin binding protein, Hbp35	OM	Hemin- Host- binding	7.09	1.7176	[71]
Minor component, FimE	OM	Fimbriae assembly	5.73	1.3881	[70]
Fimbrial anchor protein, Mfa2	OM	Fimbriae assembly	4.76	1.1532	[70]
Outer membrane protein 41, OmpA1	OM	Biofilm	4.19	1.0151	[72]
DNA starvation/stationary phase protection protein, Dps	Cytosol	Heme toxicity	4.19	1.0151	[73]
Peptidase C25, RgpB	Secretion	Biofilm and virulence	3.48	0.8431	[65]
Lys-specific serine endopeptidase, pepK	Secretion	Peptidase	2.81	0.6808	[69]
Lys-gingipain, Kgp	OM	Biofilm and virulence	2.61	0.6323	[65]
Minor fimbrium subunit, Mfa1	OM	Biofilm and adhesion	2.37	0.5742	[65]
Por secretion system protein, PorZ	OM	T9SS	2.28	0.5524	[69]
Fimbrial assembly protein, FimC	Unknown	Fimbriae assembly	2.23	0.5402	[70]
Transporter,MotA/TolQ/ExbB proton channel family protein	OM	Interaction	1.66	0.4022	[74]
T9SS cargo proteins	Unknown	T9SS	1.63	0.3949	[69]
Por secretion system protein, PorQ	Periplasm	T9SS	1.4	0.3392	[69]
Tip fimbrial protein, Mfa3	OM	Fimbriae assembly	1.34	0.3246	[70]
T9SS cargo proteins	Unknown	T9SS	1.32	0.3198	[69]
Outer membrane protein 40, OmpA2	OM	Biofilm	1.2	0.2907	[72]
TonB-dependent receptor, IhtA	OM	Heme uptake	1.13	0.2738	[75]
Leucine rich repeat-containing domain protein, InlJ	OM	Interaction	1.02	0.2471	[76]
Por secretion system protein, PorP	OM	T9SS	0.82	0.1987	[69]
Dipeptidyl-peptidase, Dpp7	OM	Exopeptidase	0.8	0.1938	[77]
TonB-dependent receptor, PorF	Unknown	T9SS	0.74	0.1793	[69]
VWA domain-containing protein, Mfa5	OM	Fimbriae assembly	0.7	0.1696	[70]
Zn-dependent oligopeptidase (peptidyl-dipeptidase), porT	IM	Gingipain transport	0.62	0.1502	[78]
Universal stress protein, UspA	Unknown	Biofilm	0.53	0.1284	[79]
Hemagglutininprotein, HagA	OM	Hemagglutinin	0.42	0.1017	[80], [81]

* T9SS, Type 9 secretion system; emPAI, exponentially modified protein abundance index; mol%, the portion of molecules in a mixture that sum up to 100%; Om, outer membrane; IM, inner membrane

Lre.LTA interacts with major fimbriae of *P. gingivalis*, FimA.

Since protein expression patterns in whole cell of *P. gingivalis* are quite different, in order to compare the relative binding affinity of Lre.LTA, Lre.LTA was co-precipitated with hexa-histidine tagged recombinant protein of GAPDH or FimA by Ni^{2+}-NTA pull down assay and further identified its protein yield by Western blot. As a result, Lre.LTA was found to interact more strongly with FimA than GAPDH (Figure 17A). Moreover, Figure 17B demonstrates that Lre.LTA dose-dependently bound to FimA with an equilibrium dissociation constant (KD) of 1.22×10^{-7} M. As for the kinetics, the estimated association (k_{on}) and dissociation (k_{off}) constants of Lre.LTA were 8.70×10^{3} $M^{-1}s^{-1}$ and 1.06×10^{-3} s^{-1}, respectively. Collectively, these results suggest that the mechanism for the anti-biofilm activity of Lre.LTA on *P. gingivalis* biofilm might be correlated with physical interaction with major fimbriae, FimA.

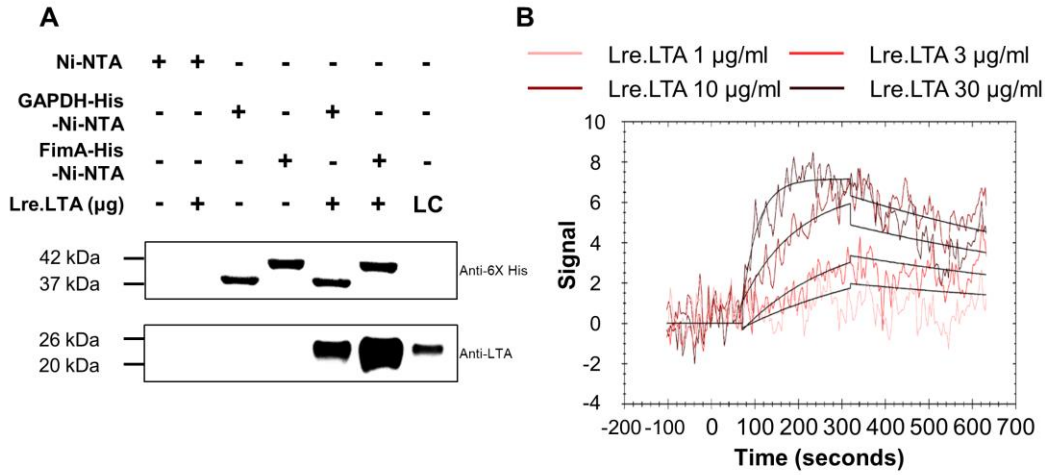

Figure 17. Lre.LTA interacts with major fimbriae of *P. gingivalis*, FimA

(A) Recombinant proteins of *P. gingivalis* FimA or GAPDH (30 μg) conjugated with Ni^{2+}-NTA were incubated in the presence or absence of Lre.LTA (0 μg or 20 μg) for 1 h at 4°C. After Ni^{2+}-NTA pulldown and eliminating non-specifically bound molecules, Western blot was conducted with anti-6X His and anti-LTA antibodies for recombinant proteins and Lre.LTA detection, respectively. LC, loading control (0.1 μg of Lre.LTA) (B) FimA protein (75 μg/ml) was immobilized on the dextran sensorchip. Interaction between FimA and Lre.LTA were observed by injecting 0–30 μg/ml of Lre.LTA over the FimA surfaces in running buffer in the flow rate of 10 μg/min. The blank curves from non-treatment of Lre.LTA was subtracted from the data by normalization.

Lre.LTA inhibits biofilm formation of *P. gingivalis* gingipain-null mutants.

Lre.LTA interacts with arginine gingipain (RgpA), which is involved in the maturation process of major fimbriae, FimA, during biofilm development [65]. To verify whether the function of gingipain in *P. gingivalis* biofilm can be associated with Lre.LTA, biofilm formation of *P. gingivalis* gingipain-null mutant, such as *kgp* (KDP129) and *kgp* with *rgpA/B* null mutant (KDP136), were evaluated by crystal violet assay with or without treatment of Lre.LTA. The data revealed that biofilm formation of *P. gingivalis* KDP129 was inhibited by Lre.LTA (Figure 18A). Moreover, biofilm formation of KDP136 was also inhibited by Lre.LTA (Figure 18B). Compared to the WT, although the function of gingipains is involved in biofilm development of *P. gingivalis* [65], these results suggest that gingipains seem not to be associated with anti-biofilm activity of Lre.LTA.

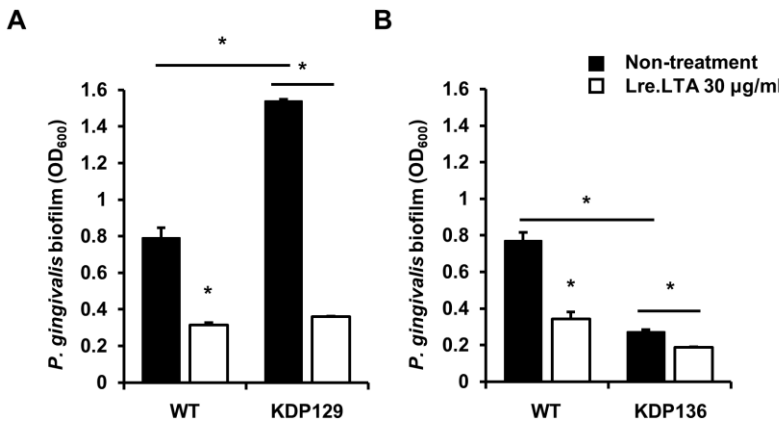

Figure 18. Lre.LTA inhibits biofilm formation of *P. gingivalis* gingipain-null mutants

P. gingivalis WT, (A) KDP129, and (B) KDP136 (1×10^9 CFU/ml, *kgp* null mutant, *kgp* and *rgpA/B* null mutant, respectively) were grown on 96-well plates in the presence or absence of Lre.LTA (30 μg/ml) at 37°C for 72 h in anaerobic conditions. After the incubation, biofilm formations were evaluated by crystal violet staining as described in Materials and Method. Biofilm biomass in crystal violet assay was presented as optical density at 600 nm of the biofilm ± standard deviation of triplicates. Asterisk (*) indicates statistical significance at $p < 0.05$.

Lre.LTA inhibits or disperses biofilm of *P. gingivalis* via interacting with FimA.

Accumulated studies have reported that major fimbriae (FimA) is essential in homotypic biofilm formation of *P. gingivalis* [82]. Since FimA is more potently bound to Lre.LTA than GAPDH with higher affinity, FimA might be associated with Lre.LTA in *P. gingivalis* biofilm inhibition. To validate the hypothesis, *P. gingivalis* FimA-null mutant was generated by homologous recombination and evaluated the anti-biofilm activity of Lre.LTA against *P. gingivalis* FimA-null mutant. As expected, Lre.LTA could not inhibit the biofilm formation and pre-formed biofilm of *P. gingivalis* FimA-null mutant compared to the WT (Figure 19A and 19B). To further evaluate the phase dynamics of anti-biofilm activity by Lre.LTA, biofilm of *P. gingivalis* FimA-null mutant was formed at 3, 6, 12, 24, 48, and 72 h with or without Lre.LTA. The anti-biofilm activity of Lre.LTA abolished at initial time point, and its inhibitory effect remained abolished up to 72 h (Figure 19C). Three-dimensional reconstructions of the Z-stacks also revealed that Lre.LTA could not inhibit and disperse both *P. gingivalis* biofilm formation and pre-formed biofilm (Figure 19D and 19E). Although the biomass and average thickness of *P. gingivalis* biofilm in biofilm-forming and pre-formed biofilm stages were significantly reduced by Lre.LTA treatment, there were no significant differences in the presence or absence of Lre.LTA against biofilm of *P. gingivalis* FimA-null mutant (Figure 19F and 19G). Overall, these data indicate that Lre.LTA inhibits or disperses biofilm of *P. gingivalis* via interacting with major fimbriae, FimA.

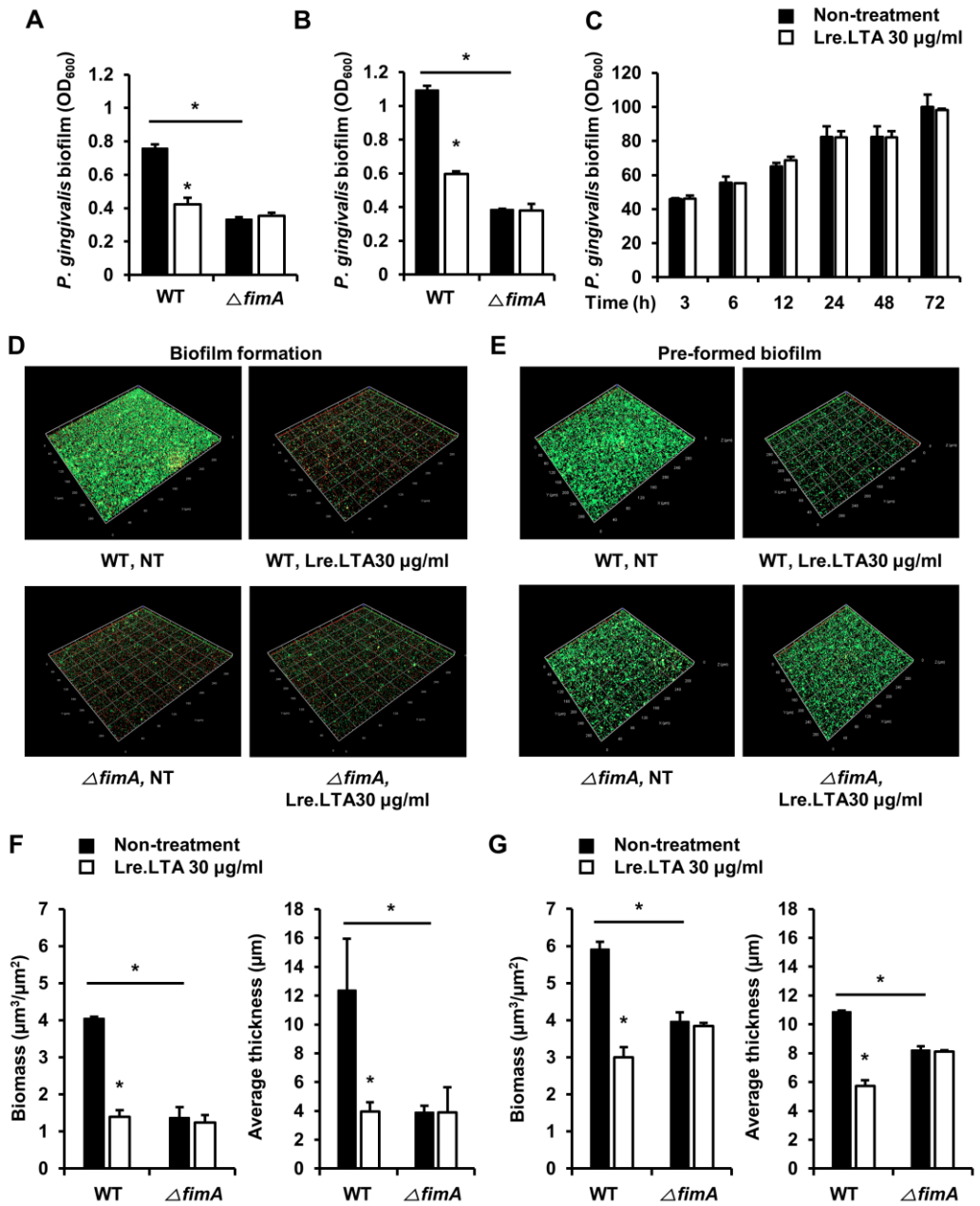

Figure 19. Lre.LTA inhibits or disperses biofilm of *P. gingivalis* via interacting with FimA

(A) *P. gingivalis* △*fimA* (1×10^9 CFU/ml) was grown on 96-well plates in the presence or absence of Lre.LTA (30 μg/ml) at 37°C for 72 h in anaerobic conditions. (B) Pre-

formed biofilm established with *P. gingivalis* △*fimA* (1×10^9 CFU/ml) at 37ºC for 72 h in anaerobic conditions on 96-well plates was treated with or without Lre.LTA (0 or 30 μg/ml) and further incubated for 24 h. (C) *P. gingivalis* △*fimA* (1×10^9 CFU/ml) was grown on 96-well plates at 37℃ in anaerobic conditions for 3, 6, 12, 24, 48, or 72 h in the presence or absence of Lre.LTA (30 μg/ml). (A-C) After the incubation, biofilm biomass was determined by crystal violet staining. (D) *P. gingivalis* △*fimA* (1×10^9 CFU/ml) was grown on confocal dishes at 37℃ in anaerobic conditions for 72 h in the presence or absence of Lre.LTA (30 μg/ml). (E) Pre-formed biofilm established with *P. gingivalis* (1×10^9 CFU/ml) at 37ºC for 72 h in anaerobic conditions on confocal dishes was treated with or without Lre.LTA (0 or 30 μg/ml) and was further incubated for 24 h. After the incubation, *P. gingivalis* biofilm was visualized by confocal laser scanning microscopy by staining with SYTO 9 to detect *P. gingivalis* and propidium iodide to detect dead cells. Three-dimensional Z-stacks in the (D) biofilm formation of *P. gingivalis* △*fimA* and (E) pre-formed biofilm of *P. gingivalis* △*fimA* in the presence or absence of Lre.LTA (30 μg/ml) was further acquired by confocal laser scanning microscopy. Total biomass and average thickness of *P. gingivalis* (SYTO 9) during (F) biofilm formation and (G) pre-formed biofilm were quantified using Comstat2 software. Asterisk (*) indicates statistical significance at $p < 0.05$ between the non-treated and Lre.LTA-treated groups.

Lre.LTA does not affect quorum sensing of *P. gingivalis* biofilm.

Previous studies have demonstrated that *Lactobacillus* LTA inhibits Gram-positive bacterial biofilm by modulating gene expression of biofilm-related operon, which regulates the production of quorum sensing molecules, such as autoinducer-2 (AI-2) [43]. Although quorum sensing system is quite different between Gram-positive and Gram-negative bacteria [83], *P. gingivalis* also utilizes the AI-2 quorum sensing system [20]. Therefore, to determine whether anti-biofilm mechanism of Lre.LTA against *P. gingivalis* biofilm is further correlated with anti-biofilm mechanism of *Lactobacillus* LTA against Gram-positive biofilm, production of AI-2 in the *P. gingivalis* biofilm in the presence or absence of Lre.LTA was then measured by using AI-2 reporter strain, *V. harveyi* BB170. The result from fold changes between non-treatment groups and Lre.LTA-treated groups in the biofilm formation (Figure 20A) and pre-formed biofilm (Figure 20B) of *P. gingivalis* demonstrated that Lre.LTA did not affect the AI-2 production of *P. gingivalis* biofilm. These results suggest that the anti-biofilm activity of Lre.LTA against *P. gingivalis* is not correlated with anti-biofilm mechanism of *Lactobacillus* LTA against Gram-positive bacterial biofilm.

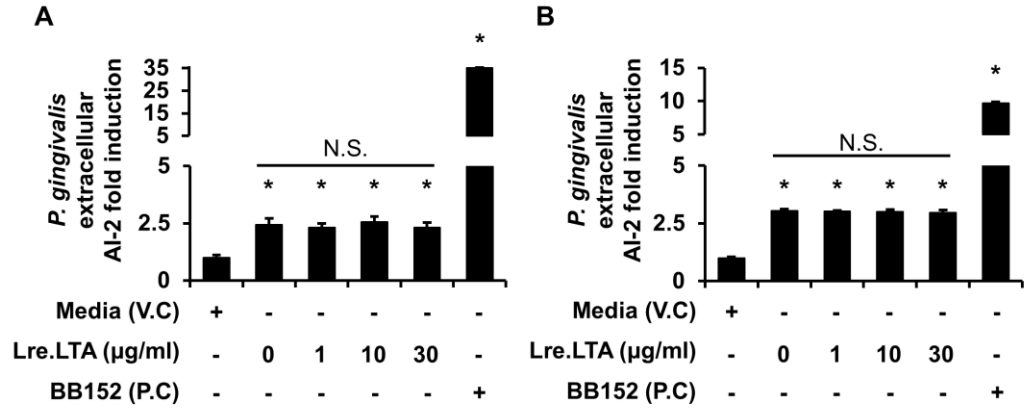

Figure 20. Lre.LTA does not affect quorum sensing of *P. gingivalis* biofilm

The supernatants from (A) biofilm formation of *P. gingivalis* and (B) pre-formed biofilm of *P. gingivalis* for the indicated time period were combined with the AI-2 reporter strain *V. harveyi* BB170 and incubated for 4 h at 30℃ with shaking. *V. harveyi* BB152 and BHIHM medium were used as a positive (P.C) and negative control, respectively. Bioluminescence produced from *V. harveyi* BB170 was measured using a microplate reader. Asterisk (*) indicates statistical significance at $p < 0.05$ between the control group (media, V.C, vehicle control) and Lre.LTA-treated groups. N.S. indicates non-significant between the non-treated group and each Lre.LTA-treated group.

Differential gene expression during *P. gingivalis* biofilm formation: Lre.LTA treated group versus non-treated group.

As shown in the Figure 10C and 19, Lre.LTA inhibits biofilm formation of *P. gingivalis* within 6 h via interaction with FimA. In order to determine whether RNA expression of *P. gingivalis* is further affected during biofilm dispersal by Lre.LTA, RNA sequencing by Illumina platform was carried out. RNA sequencing result revealed that 22,081,862 to 22,680,884 raw reads per each cDNA library were generated, and about 83% of raw reads were successfully aligned to the reference genome of *P. gingivalis* ATCC 33277 (NCBI reference sequence: GCF_000010505.1_ASM1050v1). Following alignment, Lre.LTA-treated group versus non-treated group was analyzed to calculate its fold change of expression. The differentially expressed genes (DEGs) were counted for 22 genes with satisfying $\log_2$ fold change $\geq$ 1.5 and $p < 0.05$. Among them, only 7 genes were up-regulated, and 15 genes were down-regulated by one-way hierarchical clustering heatmap and volcano plot (Figure 21A, 21B, 21C, and Table 3). The result of GO analysis revealed that DEGs were categorized into three major functions, including biological process (23.93%), molecular function (23.1%), and cellular component (2.98%) (Figure 21D). Interestingly, based on the KEGG pathway analysis among the DEGs with satisfying $\log_2$ fold change $\geq$ 1.5 and $p < 0.05$ revealed that metabolic-associated genes, such as *murQ*, PGN_RS05050, and PGN_RS02245 were affected by Lre.LTA (Figure 21B and Table 3). These results suggest that exogenous Lre.LTA affect metabolic-associated genes of *P. gingivalis* during biofilm dispersion.

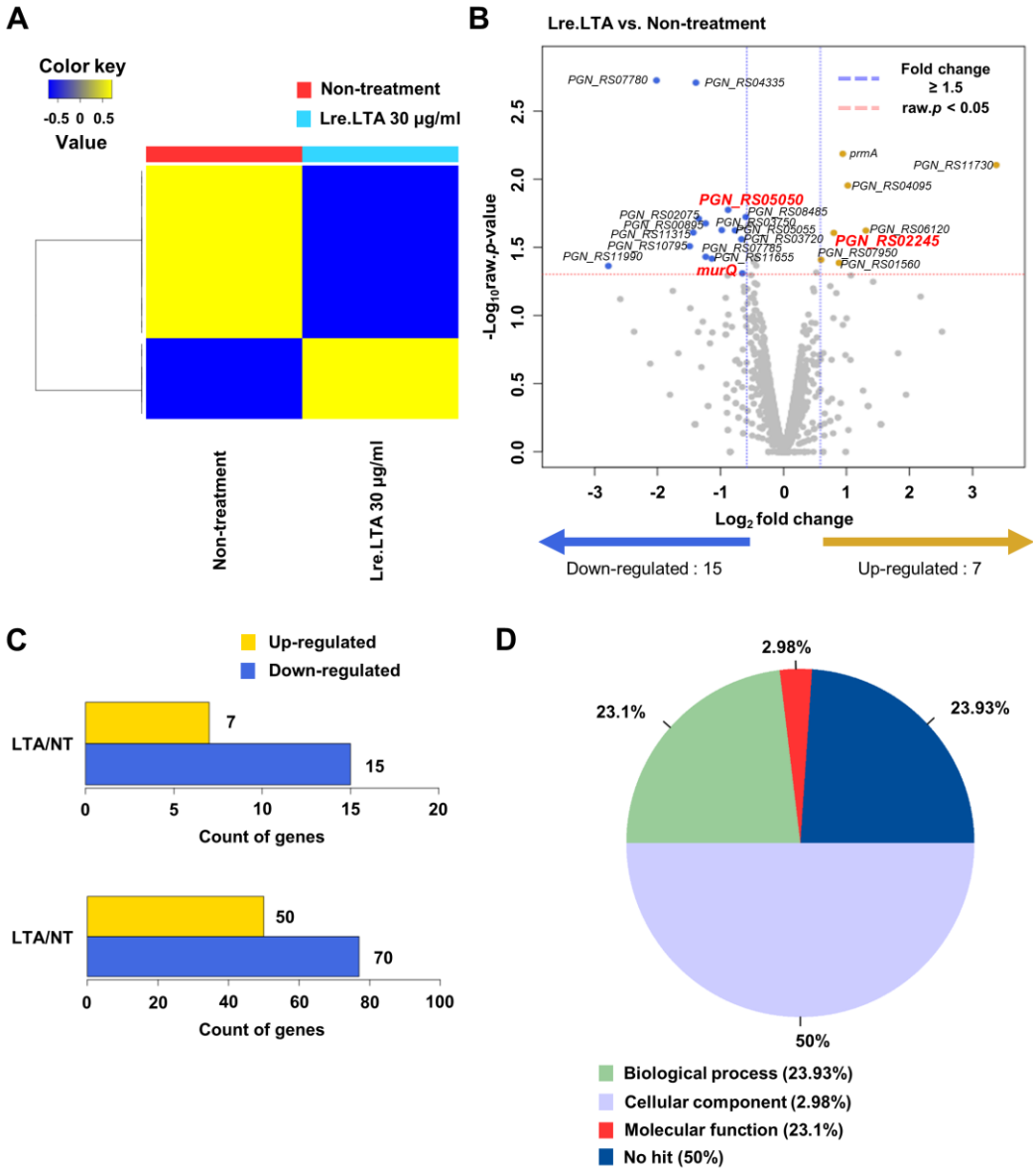

Figure 21. Differential gene expression during *P. gingivalis* biofilm formation: Lre.LTA treated group versus non-treated group

The cDNA libraries were constructed from *P. gingivalis* ATCC 33277 biofilm with or without Lre.LTA (30 μg/ml) for 24 h under anaerobic condition. (A) One-way hierarchical clustering heatmap based on 22 DEGs satisfying with $\log_2$ fold change ≥

1.5 and $p < 0.05$. Yellow and blue based on the color key indicate up- and down-regulated DEGs in the non-treated group compared to Lre.LTA-treated group. (B) Volcano plot between Lre.LTA-treated versus non-treated groups. Genes satisfying with $\log_2$ fold change $\geq$ 1.5 and $p < 0.05$ were represented in blue (left) and dark yellow (right) dots, respectively. (C) Count for up- and down-regulated genes. upper, genes satisfying with $\log_2$ fold change $\geq$ 1.5 and $p < 0.05$; lower, genes satisfying with $\log_2$ fold change $\geq$ 1.5 (D) GO analysis pie chart of 22 DEGs satisfying with $\log_2$ fold change $\geq$ 1.5 and $p < 0.05$.

Table 3. List of DEGs of *P. gingivalis* biofilm compared with Lre.LTA treated vs. non-treated group (log_2 fold change ≥ 1.5 and $p < 0.05$)

Function	Locus_tag	LTA/NT (log_2 Fold change)	LTA/NT (Raw *p* value)	KEGG Pathway
hypothetical protein	PGN_RS11730	10.399506	0.007880255	
IS5/IS1182 family transposase	PGN_RS06120	2.476608	0.023844974	
ABC transporter permease subunit	PGN_RS04095	2.030085	0.011137544	
50S ribosomal protein L11 methyltransferase	PGN_RS03220	1.919976	0.006518794	
hypothetical protein	PGN_RS01560	1.841897	0.041127817	
DUF452 family protein	PGN_RS02245	1.739909	0.024790986	Biotin metabolism
chromate transporter	PGN_RS07950	1.511559	0.039035248	
S41 family peptidase	PGN_RS08485	-1.514908	0.018951449	
N-acetylmuramic acid 6-phosphate etherase	PGN_RS05750	-1.571941	0.049029004	Amino sugar and nucleotide sugar metabolism
U32 family peptidase	PGN_RS03720	-1.587544	0.027586338	
glycosyltransferase	PGN_RS05055	-1.704120	0.023776462	
bifunctional 3-deoxy-7-phosphoheptulonate synthase/chorismate mutase type II	PGN_RS05050	-1.840088	0.0168121	Phenylalanine, tyrosine and tryptophan biosynthesis
DUF2130 domain-containing protein	PGN_RS03750	-1.972853	0.023648425	
DUF1661 domain-containing protein	PGN_RS11655	-2.199353	0.03830181	
cyclodeaminase/cyclohydrolase family protein	PGN_RS07785	-2.353017	0.037097846	
polysaccharide deacetylase family protein	PGN_RS00895	-2.355733	0.021118495	
hypothetical protein	PGN_RS02075	-2.540297	0.019530136	
hypothetical protein	PGN_RS04335	-2.621791	0.001961088	

DUF1661 domain-containing protein	PGN_RS11315	-2.699062	0.024635692
hypothetical protein	PGN_RS10795	-2.806741	0.031052599
OprO/OprP family phosphate-selective porin	PGN_RS07780	-4.045349	0.001887669
DUF1661 domain-containing protein	PGN_RS11990	-6.868434	0.043331447

Table 4. List of DEGs in *P. gingivalis* biofilm compared with Lre.LTA treated vs. non-treated group (log_2 fold change ≥ 1.5)

Function	Locus_tag	LTA/NT (log_2 Fold change)	LTA/NT (Raw *p* value)
hypothetical protein	PGN_RS04045	5.724163	0.131529066
hypothetical protein	PGN_RS11290	4.521867	0.072711657
hypothetical protein	PGN_RS11580	3.854025	0.381172953
hypothetical protein	PGN_RS11515	3.530409	0.189408754
DUF3343 domain-containing protein	PGN_RS08045	2.918957	0.628703772
DUF1661 domain-containing protein	PGN_RS11330	2.918957	0.628703772
hypothetical protein	PGN_RS11695	2.918957	0.628703772
DUF1661 domain-containing protein	PGN_RS11880	2.918957	0.628703772
ISAs1 family transposase	PGN_RS05565	2.682231	0.05653233
hypothetical protein	PGN_RS09770	2.538951	0.461167669
hypothetical protein	PGN_RS10350	2.538951	0.461167669
hypothetical protein	PGN_RS12065	2.538951	0.461167669
IS982 family transposase	PGN_RS02195	2.401888	0.355755161
DUF1661 domain-containing protein	PGN_RS11745	2.100085	0.050868214
IS982 family transposase	PGN_RS05105	2.090181	0.211789173
hypothetical protein	PGN_RS11875	2.043221	0.692095811
IS5 family transposase	PGN_RS09010	2.002556	0.104848706
IS5 family transposase	PGN_RS05165	1.983888	1
DUF1661 domain-containing protein	PGN_RS11000	1.983888	1
IS5 family transposase	PGN_RS07940	1.978977	0.195373271
hypothetical protein	PGN_RS08640	1.924435	0.117166522
T9SS type A sorting domain-containing protein	PGN_RS03870	1.876650	0.439814205
IS982 family transposase	PGN_RS05110	1.820085	0.559727541
IS982 family transposase	PGN_RS11160	1.820085	0.559727541
DUF6122 family protein	PGN_RS11735	1.788584	0.068493817
hypothetical protein	PGN_RS10920	1.732259	0.104469382
DUF1661 domain-containing protein	PGN_RS12050	1.727357	0.731885362
hypothetical protein	PGN_RS04940	1.703231	0.407172821
TonB-dependent receptor	PGN_RS02645	1.697482	0.211409834
Arm DNA-binding domain-containing	PGN_RS02735	1.673182	0.060859682

protein			
nucleotide pyrophosphohydrolase	PGN_RS09195	1.670914	0.593113131
hypothetical protein	PGN_RS12095	1.670914	0.593113131
IS5 family transposase	PGN_RS02875	1.632227	0.430493653
IS982 family transposase	PGN_RS04330	1.573428	0.523804896
hypothetical protein	PGN_RS12070	1.570425	0.620334435
IS4 family transposase	PGN_RS11095	1.564514	0.759851386
precorrin-2 C(20)-methyltransferase	PGN_RS07105	1.551139	0.18848109
hypothetical protein	PGN_RS11565	1.547492	1
DUF1661 domain-containing protein	PGN_RS11805	1.547492	1
hypothetical protein	PGN_RS12040	1.547492	1
hypothetical protein	PGN_RS11365	1.510967	0.19312173
DUF1661 domain-containing protein	PGN_RS11760	1.504183	0.210671486
IS5 family transposase	PGN_RS04650	1.502656	0.349714954
hypothetical protein	PGN_RS11740	-1.504198	0.593113131
relaxase/mobilization nuclease domain-containing protein	PGN_RS04420	-1.505169	0.119867634
DUF721 domain-containing protein	PGN_RS07465	-1.510473	0.102443963
IS30 family transposase	PGN_RS11750	-1.534121	0.064184325
hypothetical protein	PGN_RS06370	-1.536084	0.254665545
hypothetical protein	PGN_RS03355	-1.538794	0.067033425
membrane protein	PGN_RS06980	-1.546058	0.061309969
DUF3276 family protein	PGN_RS03285	-1.551460	0.089995146
IS5 family transposase	PGN_RS00995	-1.557062	0.731885362
hypothetical protein	PGN_RS11915	-1.557062	0.731885362
TonB-dependent receptor	PGN_RS06375	-1.562938	0.177830185
hypothetical protein	PGN_RS05875	-1.568132	0.471999982
aminotransferase class V-fold PLP-dependent enzyme	PGN_RS07130	-1.571921	0.335094005
tRNA (5-methylaminomethyl-2-thiouridine)(34)-methyltransferase MnmD	PGN_RS00900	-1.619402	0.226332622
DUF1661 domain-containing protein	PGN_RS11350	-1.639194	0.559727541
IS30 family transposase	PGN_RS11665	-1.639194	0.559727541
DUF1661 domain-containing protein	PGN_RS10845	-1.648768	0.311691219
malonyl-ACP O-methyltransferase BioC	PGN_RS02250	-1.670585	0.211409834
decaprenyl-phosphate phosphoribosyltransferase	PGN_RS06990	-1.689254	0.439814205

hypothetical protein	PGN_RS10210	-1.689254	0.439814205
hypothetical protein	PGN_RS08650	-1.697538	0.214445823
hypothetical protein	PGN_RS11720	-1.722958	0.352233646
HU family DNA-binding protein	PGN_RS01565	-1.763021	0.121317419
DUF1661 domain-containing protein	PGN_RS10785	-1.798450	1
DUF1661 domain-containing protein	PGN_RS11270	-1.798450	1
hypothetical protein	PGN_RS11690	-1.798450	1
hypothetical protein	PGN_RS11715	-1.798450	1
hypothetical protein	PGN_RS11960	-1.798450	1
histidinol phosphate phosphatase	PGN_RS05720	-1.833862	0.098585319
hypothetical protein	PGN_RS04040	-1.844231	0.692095811
DUF1661 domain-containing protein	PGN_RS11140	-1.844231	0.692095811
GNAT family N-acetyltransferase	PGN_RS08220	-1.847812	0.050964391
DUF1661 domain-containing protein	PGN_RS11175	-1.860681	0.517393651
IS5 family transposase	PGN_RS03075	-1.869149	0.401742164
IS982 family transposase	PGN_RS04120	-1.869149	0.401742164
IS5 family transposase	PGN_RS06660	-1.869149	0.401742164
DUF1661 domain-containing protein	PGN_RS10905	-1.869149	0.401742164
hypothetical protein	PGN_RS10990	-1.869149	0.401742164
DUF1661 domain-containing protein	PGN_RS11970	-1.874310	0.319467384
DUF6078 family protein	PGN_RS04195	-1.885786	0.137985104
hypothetical protein	PGN_RS11820	-1.885786	0.137985104
IS982 family transposase	PGN_RS04505	-1.886594	0.117166522
DUF1905 domain-containing protein	PGN_RS01330	-1.888377	0.074212587
group II intron reverse transcriptase/maturase	PGN_RS02870	-2.187437	0.133183558
DUF1661 domain-containing protein	PGN_RS12010	-2.244421	0.160155559
hypothetical protein	PGN_RS01065	-2.290955	0.461167669
hypothetical protein	PGN_RS11705	-2.290955	0.461167669
hypothetical protein	PGN_RS11800	-2.429477	0.111029597
DUF1661 domain-containing protein	PGN_RS11985	-2.467918	0.239199515
hypothetical protein	PGN_RS09170	-2.559011	0.132070192
hypothetical protein	PGN_RS02635	-2.643448	0.628703772
hypothetical protein	PGN_RS04055	-2.643448	0.628703772
IS5 family transposase	PGN_RS05355	-2.643448	0.628703772
elongation factor P	PGN_RS06720	-2.643448	0.628703772
hypothetical protein	PGN_RS10470	-2.643448	0.628703772

hypothetical protein	PGN_RS02810	-2.788966	0.08848945
DUF1661 domain-containing protein	PGN_RS11400	-3.184402	0.189408754
DUF1661 domain-containing protein	PGN_RS11075	-3.378774	0.066000669
hypothetical protein	PGN_RS12090	-3.488445	0.381172953
IS5/IS1182 family transposase	PGN_RS11780	-4.333442	0.225711524
DUF6261 family protein	PGN_RS02070	-5.178439	0.131529066
IS5 family transposase	PGN_RS06890	-6.023437	0.075793071

Lre.LTA inhibits proteolytic activity of RgpA.

Recent studies revealed that *P. gingivalis* could penetrate the oral epithelium and cytosol of the cell through gingipain [84], [85]. After the invasion, the gingipains, especially RgpA, degrade monocyte chemoattractant protein-induced protein 1 (MCPIP-1), which constitutively expressed by oral epithelium causes a strong anti-inflammatory response for maintaining immune homeostasis. The degradation of MCPIP-1 exacerbates the local pro-inflammatory response and potentiates tissue destruction leading to development of periodontitis [85]. As shown in the Figure 16D and Table 2, since Lre.LTA binds to *P. gingivalis* gingipains, Lre.LTA may counteract and neutralize the RgpA protease activity to protect MCPIP-1 degradation. To validate the hypothesis, gingipain activities were initially assessed according to the percentage rate of enzymatic substrate hydrolysis in the presence of Lre.LTA. Interestingly, only proteolytic activity of RgpA, but not Kgp and secretory RgpB (Figure 22B and 22C), was significantly inhibited by Lre.LTA in a dose-dependent manner (Figure 22A), suggesting a possibility that Lre.LTA may protect the MCPIP-1 degradation by interfering RgpA proteolytic activity.

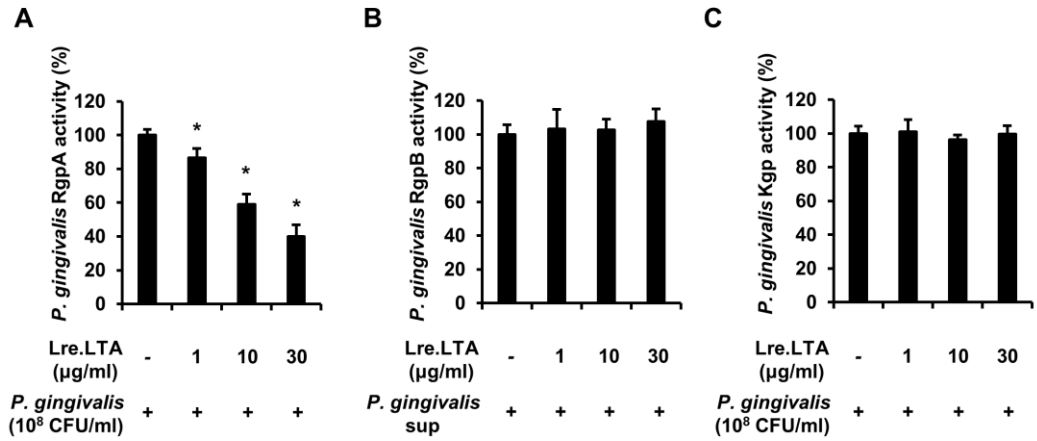

Figure 22. Lre.LTA inhibits proteolytic activity of RgpA

P. gingivalis (5 × 10^9 CFU/ml) was harvested by centrifugation. (A and C) Bacterial pellets (for detecting RgpA and Kgp activity) and (B) filtered supernatants (for detecting RgpB activity) and the were collected and mixed with reaction buffer as described in Materials and Method. *P. gingivalis* cells (1 × 10^8 CFU/ml) and supernatants were incubated on an ice-cold 96-well plate with or without Lre.LTA, and a specific substrate for Rgp (500 μM, Nα-benzoyl-DL-arginine p-nitroanilide hydrochloride, BAPNA) or Kgp (500 μM, N-tosyl-glycyl-L-prolyl-L-lysine 4-nitroanilide acetate salt, Z-GPK-pNA) at 37℃ in the dark for 90 min. (A-C) Substrate hydrolysis was recorded at optical density of 405 nm for 90 min, and activity was expressed by setting the optical density in non-treated group as 100%. Data are presented as means ± standard deviations of assays performed in triplicate. Asterisk (*) indicates statistical significance at $p < 0.05$ between the non-treated and Lre.LTA-treated groups.

Lre.LTA prevents MCPIP-1 degradation by RgpA and attenuates pro-inflammatory cytokines induced by *P. gingivalis*.

Chronic periodontitis is one of the principal causes of the progression of oral squamous cell carcinoma. Since migration and proliferation of epithelium is the hallmark of the periodontitis [86], [87], human oral epithelial squamous cell carcinoma cell line, YD-38 was utilized to verify whether Lre.LTA can protect MCPIP-1 degradation by interfering RgpA. Infection of YD-38 with *P. gingivalis* MOI 100 showed the rapid degradation of MCPIP-1 in 60 minutes. Interestingly, Lre.LTA protected the MCPIP-1 degradation (Figure 23A). Moreover, the RNA expressions of IL-6, IL-8, and IL-1β, which are major pro-inflammatory transcripts regulated by the RNase activity of MCPIP-1, were significantly reduced by Lre.LTA-treated group, these cytokines were not affected by sole treatment of Lre.LTA (Figure 23B).

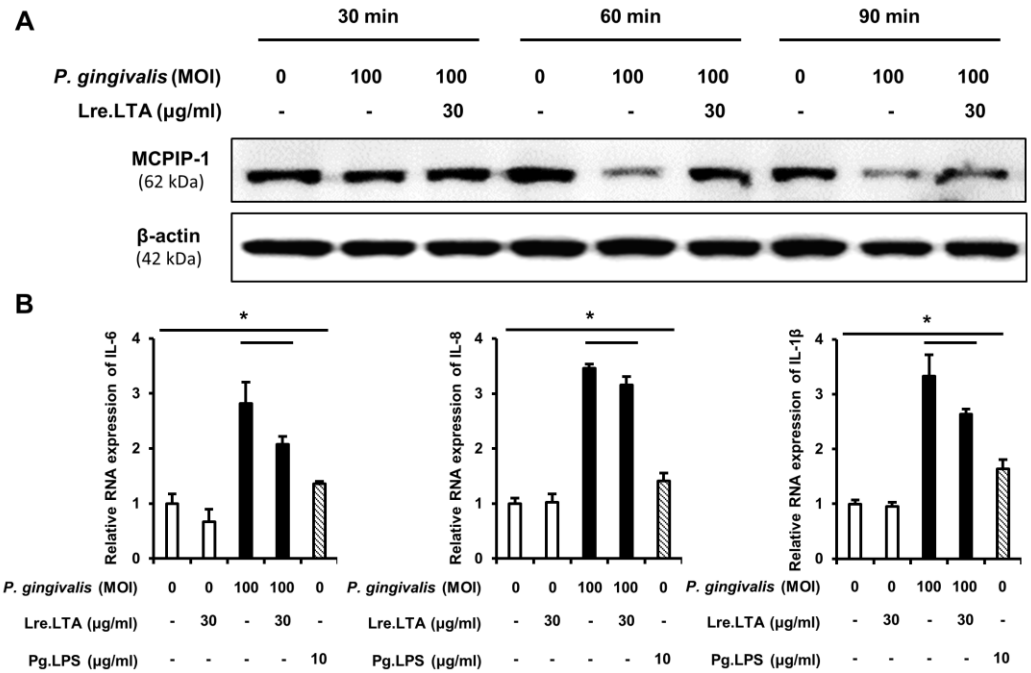

Figure 23. Lre.LTA prevents MCPIP-1 degradation by RgpA and attenuates pro-inflammatory cytokines induced by *P. gingivalis*

YD-38 cells (2×10^6 cells/well) were treated with *P. gingivalis* at the MOI of 0 or 100 in the presence or absence of Lre.LTA (30 μg/ml) (A) at the indicated time points, and (B) for 3 h. At the end of the incubation period, the cells were lysed and subjected to immunoblotting using specific antibodies to MCPIP-1 or β-actin. Quantitative real-time PCR was used to determine gene expression of IL-6, IL-8, and IL-1β. Data are presented as means ± standard deviations of assays performed in triplicate. Asterisk (*) indicates statistical significance at $p < 0.05$.

***P. gingivalis* FimA and RgpA are associated with the degradation of MCPIP-1.**

Previous studies reported that FimA and RgpA could bind to host tissues and cells [88]. To determine the effect of Lre.LTA against *P. gingivalis* FimA and RgpA on MCPIP-1 degradation, YD-38 cells was infected with *P. gingivalis* FimA-null mutant and KDP136 in the presence or absence of Lre.LTA. Notably, compared to WT, while the degradation of MCPIP-1 was alleviated by FimA-null mutant or KDP136 infected group, the effect of Lre.LTA treatment did not illustrate such alleviation, similar to the non-treated group (Figure 24). This result showed that *P. gingivalis* FimA and RgpA are associated with the degradation of MCPIP-1. Collectively, these results indicate that Lre.LTA prevents MCPIP-1 degradation by impeding gingipain activity and can be applied to the treatment of periodontitis.

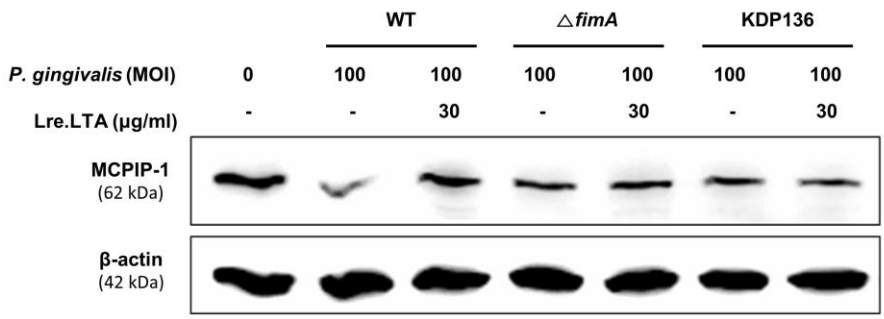

Figure 24. *P. gingivalis* FimA and RgpA are associated with the degradation of MCPIP-1

YD-38 cells (2×10^6 cells/well) were treated with *P. gingivalis* WT, △*fimA*, KDP136 at the MOI of 0 and 100 in the presence or absence of Lre.LTA (30 μg/ml) for 90 min. At the end of the incubation, cells were lysed and subjected to Western blot with anti-MCPIP-1 antibody for detecting MCPIP-1, and anti-β-actin antibody for detecting β-actin.

Lre.LTA ameliorates bone resorption in ligature-induced, *P. gingivalis*-exacerbated periodontitis mouse model.

Previous studies reported that *P. gingivalis* fimbriae and gingipains facilitate its colonization in gingival epithelium, suggesting a possibility that Lre.LTA may initially inhibit colonization of *P. gingivalis* in gingival epithelium [89], [90]. To verify whether Lre.LTA inhibits colonization of *P. gingivalis* in gingival epithelium, excised mouse gingival tissues were incubated with *P. gingivalis* in the presence or absence of Lre.LTA and homogenized to calculate *P. gingivalis* CFU. Interestingly, *P. gingivalis* colonization from mouse gingival tissues was significantly inhibited by Lre.LTA (Figure 25), suggesting that Lre.LTA inhibits *P. gingivalis* colonization in gingival tissue. To further examine whether Lre.LTA could be a therapeutic target for periodontitis, *P. gingivalis*-exacerbated periodontitis mouse model was utilized (Figure 26). The micro-CT analysis showed that the distance between the cemento-enamel junction and the alveolar bone crest (CEJ-ABC) in ligature (Figure 27A) with *P. gingivalis*-infected groups was significantly greater than that of ligature group, suggesting *P. gingivalis*-exacerbated periodontitis was successfully induced (Figure 27B) in mice. Interestingly, the distance of CEJ-ABC of *P. gingivalis* in the presence of Lre.LTA was notably decreased as compared to *P. gingivalis* alone. Moreover, same as Figure 23, compared to WT, while the distance of CEJ-ABC was decreased by FimA-null mutant or KDP136 infected group, Lre.LTA treatment did not show the difference (Figure 27C). This result also proved that *P. gingivalis* FimA and RgpA are associated with the development of periodontitis. Collectively, these results demonstrate that Lre.LTA ameliorates *P. gingivalis*-exacerbated periodontitis model and has a clinical potential for application to periodontitis treatment.

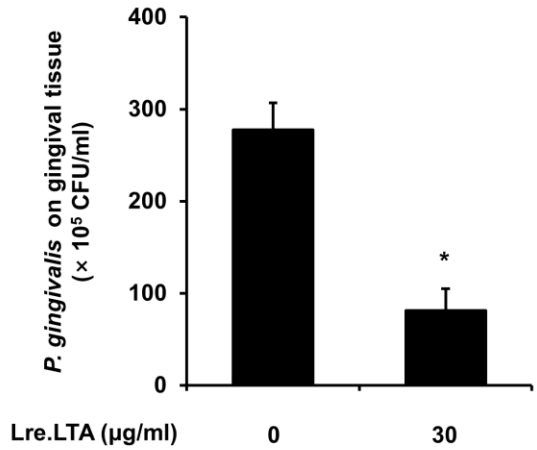

Figure 25. Lre.LTA inhibits *P. gingivalis* colonization in the mouse gingival tissue *ex vivo*

P. gingivalis (1 × 10^9 CFU/ml) with excised mouse gingival tissues was grown in BHIHM broth in 96-well plate with or without treatment of Lre.LTA (0 or 30 μg/ml) at 37°C for 24 h under anaerobic conditions. Mouse gingival tissues were further washed with PBS and homogenized, followed by serial dilution. Diluted homogenized samples were further spotted on the BHIHM agar with 5% sheep blood and incubated at 37°C for 7 days under anaerobic conditions. After incubation, total CFU of each group was calculated. Asterisk (*) indicates statistical significance at $p < 0.05$.

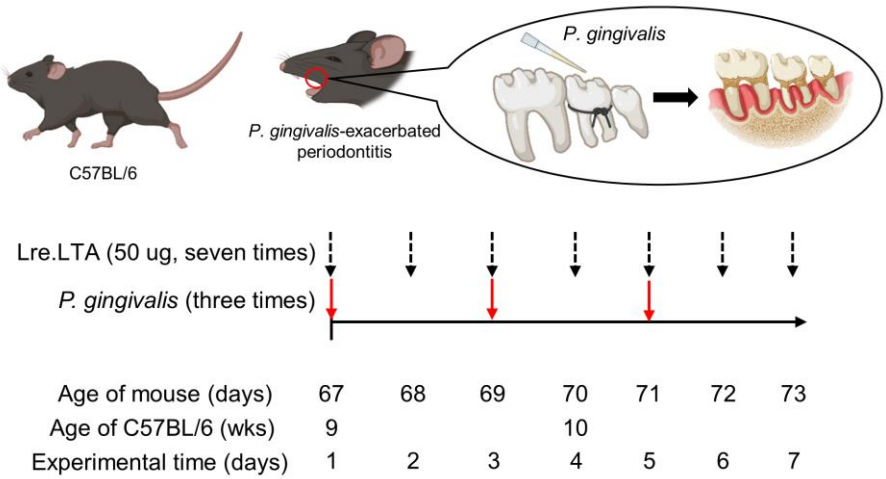

Figure 26. Experimental procedure of ligature-induced, *P. gingivalis*-exacerbated periodontitis mouse model

Mice were randomly divided into sham control, ligature, ligature with Lre.LTA, and ligature with infection of *P. gingivalis* WT or FimA-null mutant, and *kgp* with *rgpA/B* null mutant (KDP136) in the presence of absence of Lre.LTA groups. Second maxillary molar of mice was ligated with 5-0 silk. Sham surgery group had the ligature and was immediately removed after 90 minutes of surgery. After surgery, 1×10^9 CFU of *P. gingivalis* WT, △*fimA*, or KDP136 in 20 μl of PBS with 1.5% CMC was applied to mouse maxillary molars (three times, 2 days apart) in the presence or absence of Lre.LTA (50 μg, seven times, every day). On the last day of experiment, maxilla specimens were collected.

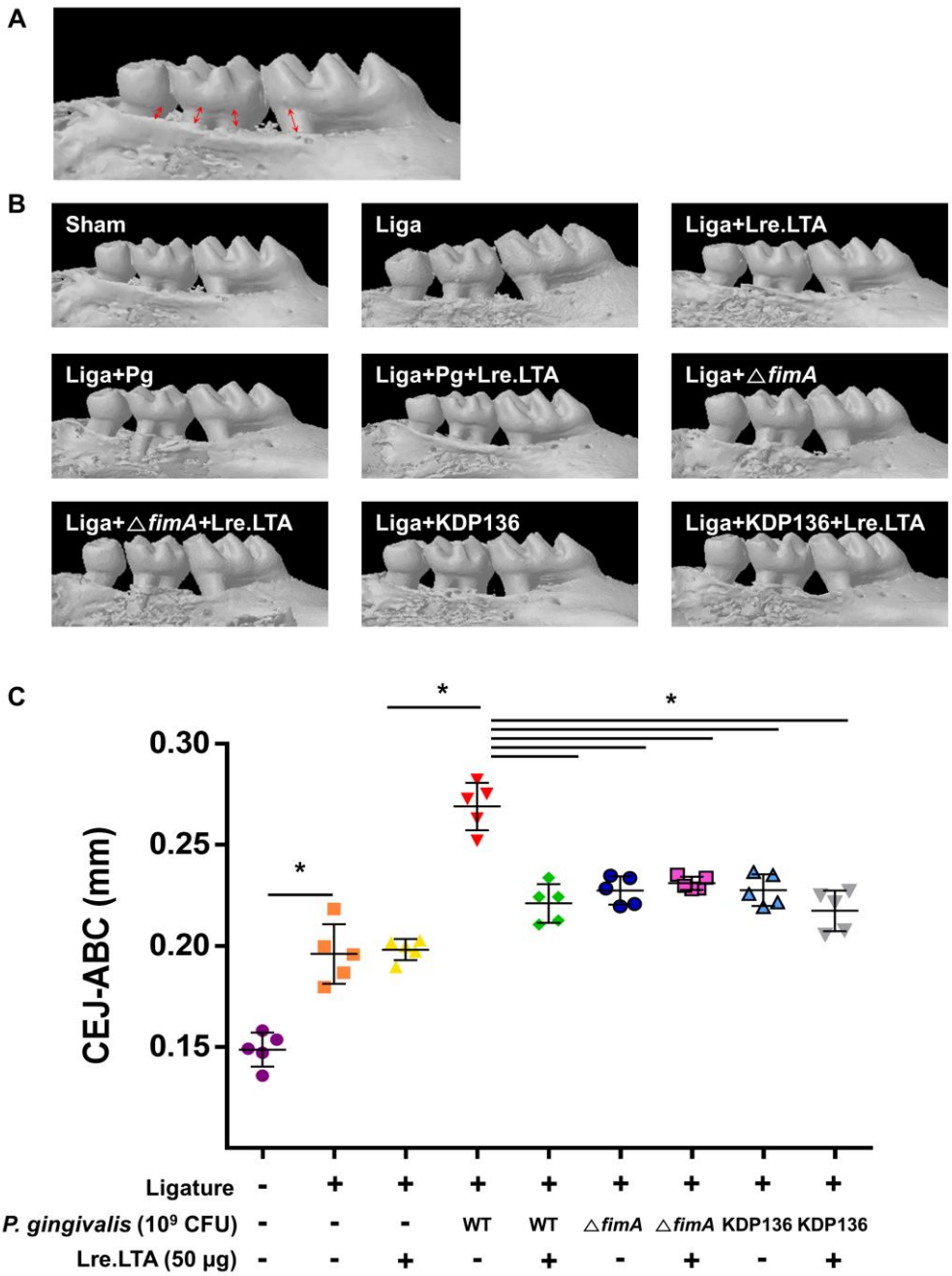

Figure 27. Lre.LTA ameliorates bone resorption in ligature-induced, *P. gingivalis*-exacerbated periodontitis mouse model

Male C57BL/6 mice aged 9 to 10 weeks were randomly separated into groups that sham

control, ligature, ligature with Lre.LTA, and ligature with infection of *P. gingivalis* WT or null mutants in the presence or absence of Lre.LTA groups (N=5, respectively). To induce periodontitis, the second molar on the left side of the mouth was fastened with a 5-0 silk ligature. Sham group had the ligature immediately removed after 90 min of surgery. *P. gingivalis* WT, △*fimA*, or KDP136 (1×10^9 CFU) with 1.5% carboxymethylcellulose (CMC) were inoculated in the left maxillary molar (three times, 2 days intervals) in the presence or absence of Lre.LTA (50 μg, seven times, every day). In the control group, mice were treated in the same way with an equal volume of vehicles (1.5% CMC). 7 days after the treatment, mice were euthanized. Left maxillary molars of mice were scanned by micro-CT and analyzed using CT-volume software. (A) Graphical depiction of the CEJ-ABC distance measurement. Four locations on the first tooth to the third molar were used to gauge distance from the CEJ-ABC. (B) Representative 3D reconstruction images of maxillary molars in each group by CT analyzer show bone loss at day 7 post-ligature placement compared to a sham control group. (C) Total bone loss was measured by average of the CEJ-ABC distances across the four molar sites (M1 to M3) using ImageJ software. Asterisk (*) indicates statistical significance at $p < 0.05$ between the non-treated and Lre.LTA-treated group.

Discussion

LTA from *Lactobacillus* is an amphipathic molecule that has been studied as an anti-biofilm agent against monotypic biofilm of Gram-positive bacteria such as *S. gordonii*, *S. mutans*, *S. aureus*, *E. faecalis*, or oral multispecies biofilm [42], [44], [45], [46], [47]. However, a fundamental understanding whether LTA regulates the bacterial biofilm, especially in Gram-negative bacteria, is generally unknown. In this study, the effect of *Lactobacillus* LTAs on *P. gingivalis* biofilm, which can induce periodontitis was identified. The findings of the current study demonstrated that among the *Lactobacillus* LTAs, Lre.LTA has the most potent inhibitory effect against *P. gingivalis* and polymicrobial biofilm with clinical relevance. In the previous studies, compared to sole treatment of Lp.LTA, the anti-biofilm activity of Lp.LTA in combination with antibiotics or disinfectants against various Gram-positive bacterial biofilm was additively enhanced, suggesting that combination treatment may lower dosages of antibiotics and disinfectants [43], [47]. Since *Lactobacillus* LTAs are also expected to have an additive effect with antibiotics or disinfectants for suppressing *P. gingivalis* biofilm, combination treatment options could lessen the spread of antibiotic-resistant bacteria. Moreover, through screening of *P. gingivalis* proteins target for Lre.LTA, major fimbriae (FimA) and gingipain (RgpA) are major targets of Lre.LTA for inhibiting biofilm and immunomodulatory effect. Overall, this study sheds light on the mechanism how probiotics cell wall components influences oral health.

Glycerol phosphate and acyl chain moieties of Lre.LTA are crucial for inhibiting *P. gingivalis* biofilm. The crystal violet assay using deleted Lre.LTA revealed that Deala-

Lre.LTA displayed more potent anti-biofilm activity than intact Lre.LTA. This is supposedly due to the ratio of D-alanine and poly-Gro-P is vital in inhibiting *P. gingivalis* biofilm. In the present study, Lc.LTA and Lp.LTA had the most abundant phosphate content, while Lre.LTA and Lr.LTA had intermediate phosphate content among *Lactobacillus* LTAs. Nevertheless, anti-biofilm activity was most profoundly demonstrated by Lre.LTA and Lp.LTA, thus illustrating that the quantity of phosphate does not directly corroborate to biofilm inhibition. According to previous reports, the induction of NF-$_{K}$B and pro-inflammatory cytokine such as TNF-α can be varied depending on the phosphate contents in each LTA-purified fraction [91], [92]. Interestingly, compared to the fraction with high phosphate content, the fraction with low phosphate content more potently increased NF-$_{K}$B and TNF-α. Although it has not yet been studied how poly-Gro-P and lipid chain length, or alanine ratio of LTA can be varied depending on each fraction, as in the case of the immune response, the regulatory effect against biofilm can also be varied depending on each fraction. Moreover, previous study showed that among the *L. plantarum* strains, Lp.LTA with broader phosphate fraction, more effectively inhibits Gram-positive bacterial biofilm [45]. Although direct relevance cannot be drawn, Lre.LTA has the broadest range of phosphate fraction numbers compared to other *Lactobacillus* LTAs in the Octyl- and DEAE-Sepharose chromatography, suggesting Lre.LTA has diverse length of acyl chain and poly-Gro-P. Therefore, *Lactobacillus* LTA with diverse length of acyl chain and poly-Gro-P might possess advantages in anti-biofilm activity. However, Further research is required to pinpoint the precise structure of *Lactobacillus* LTA that inhibits *P. gingivalis* biofilm formation.

EPM is one of the components of EPS that contributes to bacterial lifestyle and virulence. Compared to planktonic bacteria, biofilm in EPS displays specific survival advantages such as resistance to antibiotics, immune evasion, and horizontal gene transfer. Therefore, strategies for penetrating EPS and inhibiting biofilm of microbial communities are essential to overcome antibiotic resistance. The present study demonstrated that Lre.LTA penetrates EPM, and directly interacts with *P. gingivalis* leading to inhibition or dispersion of EPM in *P. gingivalis* biofilm. This process suggests that Lre.LTA may not interact with EPM in *P. gingivalis*, but whether additional chemical mechanisms are involved in this process remain unclear. Generally, Gram-negative bacteria mainly produce viscous anionic EPS, while Gram-positive bacteria produce cationic EPS due to wall teichoic acids [93]. Moreover, *P. gingivalis* produces anionic-LPS, a phosphorylated branched mannan, as an EPS source [93], [94], [95]. Predictably, since Lre.LTA purified in this study has broad poly-Gro-P with anionic moieties, Lre.LTA may penetrate EPM and interact with *P. gingivalis*. Furthermore, a previous study reported that zwitterionic lipids can preclude strong ionic interaction and may support the penetration of EPS [96]. As Lre.LTA is a zwitterionic lipid polymer, Lre.LTA may penetrate the EPM of *P. gingivalis*. However, these possibilities also remain to be investigated.

In Gram-positive bacteria, *Lactobacillus* LTA, such as Lp.LTA can inhibit the *S. aureus* biofilm formation by enhancing autoinducer-2 quorum sensing molecule, which down-regulates intracellular adhesion gene, *ica*, required for production of exopolysaccharide [43]. Moreover, a pre-coated plate with Lp.LTA efficiently prevented the surface adhesion of *S. mutans* [44]. Although little is known about how *Lactobacillus* LTA

affects Gram-positive bacteria, these findings imply that *Lactobacillus* LTA may function as a quorum sensing or anti-adhesion molecule to control Gram-positive bacterial biofilm. However, the anti-biofilm activity of Lre.LTA against Gram-negative bacteria, *P. gingivalis*, can be mediated by physical interaction of its major fimbriae without affecting quorum sensing molecule. Moreover, the result of RNA sequencing revealed that Lre.LTA affects metabolism-associated genes of *P. gingivalis* and did not affect the expression of quorum sensing- and adhesion-associated genes during its biofilm dispersion. These results suggest a possibility that the anti-biofilm mechanism of *Lactobacillus* LTA against Gram-positive and Gram-negative bacterial biofilm is quite different. However, additional studies are required to determine whether Gram-positive and Gram-negative bacteria share the anti-biofilm mechanisms by *Lactobacillus* LTA.

According to previous reports, *P. gingivalis* FimA is a filamentous protein without transmembrane and kinase sequences for signal transduction. FimA is also known to be exposed to the outer membrane through polymerization with FimB assembly protein, which is anchored on the outer membrane [97]. Taken together, although FimA is not involved in the signal transduction of *P. gingivalis*, FimA can interact with various host tissues and microbes, indicating that FimA may indirectly modulate the signaling cascade of *P. gingivalis* upon attachment. Transcriptome profiling demonstrated that Lre.LTA modulates metabolism-associated gene expression of *P. gingivalis* during biofilm dispersion. Especially among the 22 DEGs, the analysis of KEGG pathway revealed that biotin metabolism (PGN_RS02245), amino sugar and nucleotide sugar metabolism (PGN_RS05750, *murQ*), and phenylalanine, tyrosine, and tryptophan biosynthesis (PGN_RS05050) of *P. gingivalis* were affected by Lre.LTA. Accumulated

studies reported that gene expression of amino sugar and tryptophan biosynthesis was significantly increased during biofilm development [98], [99], [100], [101], [102]. Contrary to those findings, Lre.LTA inhibited the expression of PGN_RS05750 (*murQ*), and PGN_RS05050, suggesting that Lre.LTA may indirectly induce *P. gingivalis* to transit from the biofilm to the planktonic state during its dispersion. In contrast, Lre.LTA upregulated the gene expression of PGN_RS02245, which is involved in biotin metabolism. Previous studies revealed that biotin metabolism is essential for the bacterial growth [103]. Since bacterial growth rate can be reduced during biofilm development due to nutritional limitations [104], increased biotin metabolism might be associated with the shift from the biofilm to the planktonic state. Transcriptome profiling of the previous study reported that 28 DEGs were identified during biofilm development of *P. gingivalis* ATCC 33277 compared to planktonic state [105], which had a comparable number of DEGs count in the present study. Interestingly, U32 family peptidase, *prtQ* was upregulated during biofilm development, whereas *prtQ* (PGN_RS03720) is significantly downregulated in the present study (Table 3). Collectively, these results raise the possibility that Lre.LTA indirectly regulates metabolism-associated genes during dispersion of *P. gingivalis* biofilm as consequence of interaction between Lre.LTA and FimA.

According to mass spectrometry analysis, Lre.LTA is predominantly bound to various outer membrane proteins. Especially among the functional outer membranes, except for fimbriae, Lre.LTA is bound to RagA, RagB, OmpA1, and OmpA2, which are associated with cell-to-cell adhesion, biofilm, and virulence [66], [72]. RagA and RagB are regarded as virulence factors that are associated with soft tissue destruction and oral

epithelial colonization [66]. Outer membrane protein A, a putative heterotrimer of A1 and A2 subunits, acts as a positive regulator of *P. gingivalis* biofilm formation [72]. Moreover, OmpA1 and A2 are also involved in the adherence and invasion of *P. gingivalis* into oral epithelial cells [72]. These accumulated studies deliver a clinical imperative to employ *Lactobacillus* LTAs to mitigate the overall virulence of *P. gingivalis*.

Major fimbriae (FimA) of *P. gingivalis* is essential in adhering to various oral substrates and host cells [70]. *P. gingivalis* FimA also has a GAPDH binding domain [106] allowing physical attachment to the cell wall of numerous *Streptococcus*, including *S. oralis*, *S. gordonii*, *S. sanguinis*, *S. parasanguinis*, *S. sobrinus*, *S. salivarius*, *S. mutans*, *S. cricetus*, and *S. milleri*, presumably contributing to periodontal pocket colonization [107]. Moreover, minor fimbriae Mfa1 interacts with streptococcal SspA/B surface protein [108], indicating that FimA and Mfa1 may be promising targets for preventing *P. gingivalis* community development. Previous study demonstrated that FimA and Mfa1 interact with toll-like receptor (TLR) 2, leading to induction of multiple pro-inflammatory cytokines. Given that Lre.LTA binds to FimA and Mfa1, Lre.LTA may prevent *P. gingivalis* community development and induction of pro-inflammatory cytokines. In addition, we found that Lre.LTA binds to *P. gingivalis* gingipain and InlJ, which interact with *C. albicans* [60], [76], suggesting that Lre.LTA may alter not only the development of the bacterial community but also the bacterial-fungal connection. The present study demonstrates that Lre.LTA binds to all types of gingipains, a major virulence factor that is involved in numerous disease onsets, such as periodontitis, cardiovascular disease, aspiration pneumonia, Alzheimer’s disease, and diabetes mellitus

[109]. However, among the gingipains, Lre.LTA only inhibits the proteolytic activity of RgpA. Since *Lactobacillus* LTAs are structurally diverse in their net charge and hydrophobicity, further experimentation will be required to identify whether *Lactobacillus* LTAs from different species prevent the proteolytic activity of all types of gingipain.

P. gingivalis FimA and RgpA are associated with the degradation of MCPIP-1, which phenomenon was same as *P. gingivalis*-exacerbated periodontitis model. According to previous studies, FimA is known to play an essential role in attachment to the subgingival pocket, and RgpA has a pivotal role in excessively increasing the host immune response to LPS as well as MCPIP-1 degradation [20], [85], [89]. Therefore, due to functional loss of adhesion or proteolytic activity, these mutants had a reduced MCPIP-1 degradation effect and development of periodontitis in the mouse model compared to the WT. However, in the FimA-null mutant and KDP136 infected group, the effect of Lre.LTA did not show a difference compared to non-treated group. Since previous studies have shown that *P. gingivalis* LPS can solely exacerbate mouse periodontitis model [110], *P. gingivalis* LPS might be involved in MCPIP-1 regulation and the exacerbation of periodontitis. In the previous studies, LPS can induce mucosa-associated lymphoid tissue lymphoma translocation protein 1 (MALT1) expression by triggering TLR4 in macrophage or other cell types [111], [112]. Since MALT1 is the only proven intracellular signaling protein that can degrade MCPIP-1, *P. gingivalis* LPS may affect MCPIP-1 degradation. Second, *P. gingivalis* can upregulate the expression of ZEB2, a transcriptional factor for controlling inflammatory responses in gingival keratinocytes [87]. Previous studies revealed that upregulated ZEB2 significantly

reduced level of MCPIP-1, which led to production of pro-inflammatory cytokines [113], [114]. Overall, these previous studies showed that not only FimA and RgpA, but also LPS could stimulate a pro-inflammatory response in the periodontal tissue and regulate the expression of MCPIP-1. Since the present study showed the possibility that Lre.LTA could not counteract LPS, further studies are needed to screen *Lactobacillus* LTA that can counteract LPS and control its inflammatory responses.

Among the numerous chemicals generated from *Lactobacillus*, LTA is a crucial part of the cell wall that stimulates the host immune system [37]. *Lactobacillus* LTAs have the poly-Gro-P backbone, which is comprised of phosphate and glycerol containing D-alanine, glucose, or galactose residues and coupled with triacylated glycolipid moiety that causes the generation of anti-inflammatory cytokines. However, LTA from *Staphylococcus aureus* has Gro-P backbone with N-acetylglucosamine or D-alanine residues linked with diacylated glycolipid anchor which leads to the production of pro-inflammatory cytokines [37], [115], [116]. The biological features of LTA appear to be highly correlated with their structural diversity. *Lactobacillus* LTAs, including *L. reuteri*, were less immunostimulatory for inducing pro-inflammatory mediators such as IL-6 and tumor necrosis factor-alpha than *Staphylococcus aureus* LTA [39], [117]. Furthermore, *Lactobacillus* LTA appears to possess anti-inflammatory properties. For instance, *L. plantarum* and *L. reuteri* LTA attenuated the pro-inflammatory cytokines such as IL-6 or IL-8 production induced by a pathogen-associated molecular pattern [40], [41], [117]. In this study, Lre.LTA did not induce pro-inflammatory cytokines such as IL-6, IL-8, and IL-1β, suggesting that Lre.LTA is a probiotic effector molecule having an anti-inflammatory effect.

Collectively, the results in the present study demonstrated that among *Lactobacillus* LTAs, especially Lre.LTA inhibits biofilm formation and disperses pre-formed biofilm of *P. gingivalis* via interacting with major fimbriae, FimA, an etiological factor for biofilm formation. Moreover, Lre.LTA can interact with arginine gingipain (RgpA), a major causative cysteine proteinase for degrading anti-inflammatory mediator, MCPIP-1, and inhibit its proteolytic activity, leading to alleviation of periodontitis. These findings provide new insight into how *Lactobacillus* LTA impacts *P. gingivalis* biofilm, virulence, and increase our understanding of communication between Gram-positive and Gram-negative bacteria. Furthermore, based on these molecular background, further study for developing anti-biofilm agents could be useful to maintain a healthy community of the oral cavity with protective effects against periodontal disease.

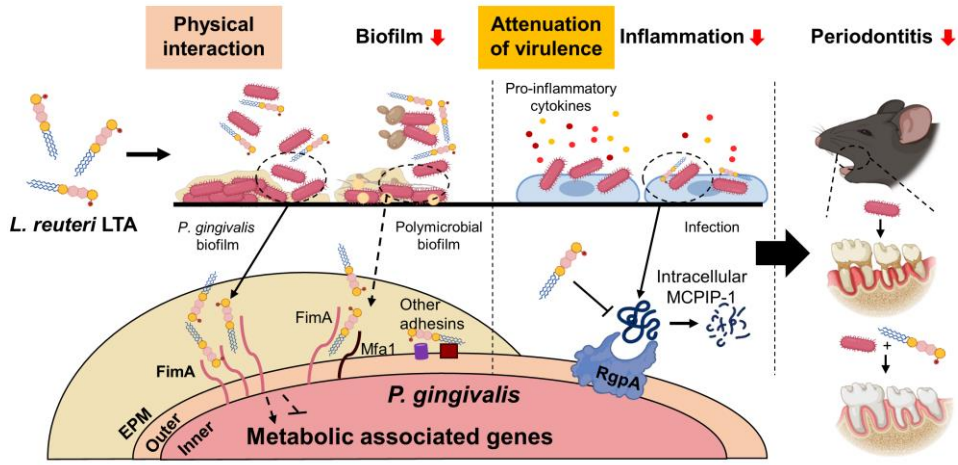

Figure 28. Schematic model for the therapeutic effect of Lre.LTA on the biofilm and pathogenicity of *P. gingivalis*

Lre.LTA disperses biofilm of *P. gingivalis* by physically interacting with major fimbriae, FimA leading to a low-cell density *P. gingivalis* population and regulation of metabolic-associated genes, which are associated with the shift from the biofilm to the planktonic state. Moreover, Lre.LTA interacts with various *P. gingivalis* adhesins and may prevent the development of dysbiotic polymicrobial biofilm. *P. gingivalis* penetrates the gingival surface and initiates the degradation of MCPIP-1 by arginine gingipain (RgpA) leading to development of excessive inflammatory condition. In this context, Lre.LTA can bind to RgpA and inhibit RgpA proteolytic activity for preventing MCPIP-1 degradation and ameliorating inflammatory condition and periodontal diseases.

Conclusion

Since scaling, root planning, antibiotics, and disinfectants struggle to eradicate oral infections by bacterial biofilms, it is necessary to use an efficient alternative technique to prevent oral pathogens from forming biofilms. For this reason, LTAs from different species of *Lactobacillus* were isolated and tested their anti-biofilm activity against *P. gingivalis* biofilm. Although all of the tested *Lactobacillus* LTAs except La.LTA effectively inhibited biofilm formation of *P. gingivalis*, Lre.LTA showed the most effective anti-biofilm activity and was also effective against clinically isolated strains of *P. gingivalis* and heterotypic bacterial-fungal biofilm. Moreover, anti-biofilm activity of Lre.LTA is mediated by interaction with *P. gingivalis* major fimbriae, FimA. Thus, *Lactobacillus* LTAs could be developed as anti-biofilm agents for controlling pathogenic community in the oral cavity. On the other hand, Lre.LTA could interact with arginine gingipain (RgpA) and inhibit its proteolytic activity leading to the inhibition of MCPIP-1 degradation and tissue destruction. These results suggest that Lre.LTA could be developed as a therapeutic agent for maintaining immune homeostasis against oral periodontopathogens. Therefore, controlling *P. gingivalis* biofilm and its virulence by Lre.LTA could be a novel strategy for the application to periodontitis treatment.

References

1. Scharnow AM, Solinski AE, Wuest WM: **Targeting *S. mutans* biofilms: a perspective on preventing dental caries**. *Medchemcomm* 2019, **10**(7):1057-1067.
2. Flemming HC, Wingender J, Szewzyk U, Steinberg P, Rice SA, Kjelleberg S: **Biofilms: an emergent form of bacterial life**. *Nat Rev Microbiol* 2016, **14**(9):563-575.
3. Schulze A, Mitterer F, Pombo JP, Schild S: **Biofilms by bacterial human pathogens: Clinical relevance - development, composition and regulation - therapeutical strategies**. *Microb Cell* 2021, **8**(2):28-56.
4. Deo PN, Deshmukh R: **Oral microbiome: Unveiling the fundamentals**. *J Oral Maxillofac Pathol* 2019, **23**(1):122-128.
5. Lamont RJ, Koo H, Hajishengallis G: **The oral microbiota: dynamic communities and host interactions**. *Nat Rev Microbiol* 2018, **16**(12):745-759.
6. Chen X, Daliri EB, Kim N, Kim JR, Yoo D, Oh DH: **Microbial Etiology and Prevention of Dental Caries: Exploiting Natural Products to Inhibit Cariogenic Biofilms**. *Pathogens* 2020, **9**(7).
7. Nath SG, Raveendran R: **Microbial dysbiosis in periodontitis**. *J Indian Soc Periodontol* 2013, **17**(4):543-545.
8. Usui M, Onizuka S, Sato T, Kokabu S, Ariyoshi W, Nakashima K: **Mechanism of alveolar bone destruction in periodontitis - Periodontal bacteria and inflammation**. *Jpn Dent Sci Rev* 2021, **57**:201-208.
9. Nazir M, Al-Ansari A, Al-Khalifa K, Alhareky M, Gaffar B, Almas K: **Global Prevalence of Periodontal Disease and Lack of Its Surveillance**. *ScientificWorldJournal* 2020, **2020**:2146160.
10. Silva N, Abusleme L, Bravo D, Dutzan N, Garcia-Sesnich J, Vernal R, Hernandez M, Gamonal J: **Host response mechanisms in periodontal diseases**. *J Appl Oral Sci* 2015, **23**(3):329-355.
11. Chawla A, Hirano T, Bainbridge BW, Demuth DR, Xie H, Lamont RJ: **Community signalling between *Streptococcus gordonii* and *Porphyromonas gingivalis* is controlled by the transcriptional regulator CdhR**. *Mol Microbiol* 2010, **78**(6):1510-1522.
12. Li J, Helmerhorst EJ, Leone CW, Troxler RF, Yaskell T, Haffajee AD, Socransky SS, Oppenheim FG: **Identification of early microbial colonizers in human dental biofilm**. *J Appl Microbiol* 2004, **97**(6):1311-1318.
13. Diaz PI, Valm AM: **Microbial Interactions in Oral Communities Mediate Emergent Biofilm Properties**. *J Dent Res* 2020, **99**(1):18-25.
14. Mohanty R, Asopa SJ, Joseph MD, Singh B, Rajguru JP, Saidath K, Sharma U: **Red complex: Polymicrobial conglomerate in oral flora: A review**. *J Family Med Prim Care* 2019, **8**(11):3480-3486.
15. Hajishengallis G: **Periodontitis: from microbial immune subversion to systemic inflammation**. *Nat Rev Immunol* 2015, **15**(1):30-44.
16. Hajishengallis G: **Immunomicrobial pathogenesis of periodontitis: keystones, pathobionts, and host response**. *Trends Immunol* 2014, **35**(1):3-11.
17. Mei F, Xie M, Huang X, Long Y, Lu X, Wang X, Chen L: ***Porphyromonas gingivalis* and Its Systemic Impact: Current Status**. *Pathogens* 2020, **9**(11).
18. Colombo AV, Silva CM, Haffajee A, Colombo APV: **Identification of oral bacteria associated with crevicular epithelial cells from chronic periodontitis lesions**. *J Med Microbiol* 2006, **55**(Pt 5):609-615.
19. How KY, Song KP, Chan KG: ***Porphyromonas gingivalis*: An Overview of Periodontopathic Pathogen below the Gum Line**. *Front Microbiol* 2016, **7**:53.
20. Gerits E, Verstraeten N, Michiels J: **New approaches to combat *Porphyromonas gingivalis***

biofilms. *J Oral Microbiol* 2017, **9**(1):1300366.
21. Mocanu RC, Martu MA, Luchian I, Sufaru IG, Maftei GA, Ioanid N, Martu S, Tatarciuc M: **Microbiologic Profiles of Patients with Dental Prosthetic Treatment and Periodontitis before and after Photoactivation Therapy-Randomized Clinical Trial**. *Microorganisms* 2021, **9**(4).
22. Hill G, Dehn C, Hinze AV, Frentzen M, Meister J: **Indocyanine green-based adjunctive antimicrobial photodynamic therapy for treating chronic periodontitis: A randomized clinical trial**. *Photodiagnosis Photodyn Ther* 2019, **26**:29-35.
23. Van Strydonck DA, Slot DE, Van der Velden U, Van der Weijden F: **Effect of a chlorhexidine mouthrinse on plaque, gingival inflammation and staining in gingivitis patients: a systematic review**. *J Clin Periodontol* 2012, **39**(11):1042-1055.
24. Al-Ahmad A, Ameen H, Pelz K, Karygianni L, Wittmer A, Anderson AC, Spitzmuller B, Hellwig E: **Antibiotic resistance and capacity for biofilm formation of different bacteria isolated from endodontic infections associated with root-filled teeth**. *J Endod* 2014, **40**(2):223-230.
25. Yamaguchi M, Noiri Y, Kuboniwa M, Yamamoto R, Asahi Y, Maezono H, Hayashi M, Ebisu S: ***Porphyromonas gingivalis* biofilms persist after chlorhexidine treatment**. *Eur J Oral Sci* 2013, **121**(3 Pt 1):162-168.
26. Noiri Y, Okami Y, Narimatsu M, Takahashi Y, Kawahara T, Ebisu S: **Effects of chlorhexidine, minocycline, and metronidazole on *Porphyromonas gingivalis* strain 381 in biofilms**. *J Periodontol* 2003, **74**(11):1647-1651.
27. Larsen T: **Susceptibility of *Porphyromonas gingivalis* in biofilms to amoxicillin, doxycycline and metronidazole**. *Oral Microbiol Immunol* 2002, **17**(5):267-271.
28. Ardila CM, Granada MI, Guzman IC: **Antibiotic resistance of subgingival species in chronic periodontitis patients**. *J Periodontal Res* 2010, **45**(4):557-563.
29. van Winkelhoff AJ, Herrera Gonzales D, Winkel EG, Dellemijn-Kippuw N, Vandenbroucke-Grauls CM, Sanz M: **Antimicrobial resistance in the subgingival microflora in patients with adult periodontitis. A comparison between The Netherlands and Spain**. *J Clin Periodontol* 2000, **27**(2):79-86.
30. Nguyen T, Brody H, Radaic A, Kapila Y: **Probiotics for periodontal health-Current molecular findings**. *Periodontol 2000* 2021, **87**(1):254-267.
31. Ishikawa KH, Mita D, Kawamoto D, Nicoli JR, Albuquerque-Souza E, Lorenzetti Simionato MR, Mayer MPA: **Probiotics alter biofilm formation and the transcription of *Porphyromonas gingivalis* virulence-associated genes**. *J Oral Microbiol* 2020, **12**(1):1805553.
32. Kobayashi R, Kobayashi T, Sakai F, Hosoya T, Yamamoto M, Kurita-Ochiai T: **Oral administration of *Lactobacillus gasseri* SBT2055 is effective in preventing *Porphyromonas gingivalis*-accelerated periodontal disease**. *Sci Rep* 2017, **7**(1):545.
33. Giordani B, Parolin C, Vitali B: **Lactobacilli as Anti-biofilm Strategy in Oral Infectious Diseases: A Mini-Review**. *Front Med Technol* 2021, **3**:769172.
34. Zawistowska-Rojek A, Tyski S: **Are Probiotic Really Safe for Humans?** *Pol J Microbiol* 2018, **67**(3):251-258.
35. Baek KT, Bowman L, Millership C, Dupont Sogaard M, Kaever V, Siljamaki P, Savijoki K, Varmanen P, Nyman TA, Grundling A *et al*: **The Cell Wall Polymer Lipoteichoic Acid Becomes Nonessential in *Staphylococcus aureus* Cells Lacking the ClpX Chaperone**. *mBio* 2016, **7**(4).
36. Lebeer S, Claes IJ, Vanderleyden J: **Anti-inflammatory potential of probiotics: lipoteichoic acid makes a difference**. *Trends Microbiol* 2012, **20**(1):5-10.
37. Kang SS, Sim JR, Yun CH, Han SH: **Lipoteichoic acids as a major virulence factor causing inflammatory responses via Toll-like receptor 2**. *Arch Pharm Res* 2016, **39**(11):1519-1529.
38. Han SH, Kim JH, Martin M, Michalek SM, Nahm MH: **Pneumococcal lipoteichoic acid**

(LTA) is not as potent as staphylococcal LTA in stimulating Toll-like receptor 2. *Infect Immun* 2003, **71**(10):5541-5548.
39. Ryu YH, Baik JE, Yang JS, Kang SS, Im J, Yun CH, Kim DW, Lee K, Chung DK, Ju HR *et al*: **Differential immunostimulatory effects of Gram-positive bacteria due to their lipoteichoic acids**. *Int Immunopharmacol* 2009, **9**(1):127-133.
40. Kim KW, Kang SS, Woo SJ, Park OJ, Ahn KB, Song KD, Lee HK, Yun CH, Han SH: **Lipoteichoic Acid of Probiotic *Lactobacillus plantarum* Attenuates Poly I:C-Induced IL-8 Production in Porcine Intestinal Epithelial Cells**. *Front Microbiol* 2017, **8**:1827.
41. Noh SY, Kang SS, Yun CH, Han SH: **Lipoteichoic acid from *Lactobacillus plantarum* inhibits Pam2CSK4-induced IL-8 production in human intestinal epithelial cells**. *Mol Immunol* 2015, **64**(1):183-189.
42. Jung S, Park OJ, Kim AR, Ahn KB, Lee D, Kum KY, Yun CH, Han SH: **Lipoteichoic acids of lactobacilli inhibit *Enterococcus faecalis* biofilm formation and disrupt the preformed biofilm**. *J Microbiol* 2019, **57**(4):310-315.
43. Ahn KB, Baik JE, Yun CH, Han SH: **Lipoteichoic Acid Inhibits *Staphylococcus aureus* Biofilm Formation**. *Front Microbiol* 2018, **9**:327.
44. Ahn KB, Baik JE, Park OJ, Yun CH, Han SH: ***Lactobacillus plantarum* lipoteichoic acid inhibits biofilm formation of *Streptococcus mutans***. *PLoS One* 2018, **13**(2):e0192694.
45. Lee D, Im J, Park DH, Jeong S, Park M, Yoon S, Park J, Han SH: ***Lactobacillus plantarum* Lipoteichoic Acids Possess Strain-Specific Regulatory Effects on the Biofilm Formation of Dental Pathogenic Bacteria**. *Front Microbiol* 2021, **12**:758161.
46. Kim AR, Kang M, Yoo YJ, Yun CH, Perinpanayagam H, Kum KY, Han SH: ***Lactobacillus plantarum* lipoteichoic acid disrupts mature *Enterococcus faecalis* biofilm**. *J Microbiol* 2020, **58**(4):314-319.
47. Kim AR, Ahn KB, Yun CH, Park OJ, Perinpanayagam H, Yoo YJ, Kum KY, Han SH: ***Lactobacillus plantarum* Lipoteichoic Acid Inhibits Oral Multispecies Biofilm**. *J Endod* 2019, **45**(3):310-315.
48. Li J, Koh JJ, Liu S, Lakshminarayanan R, Verma CS, Beuerman RW: **Membrane Active Antimicrobial Peptides: Translating Mechanistic Insights to Design**. *Front Neurosci* 2017, **11**:73.
49. Hong SW, Baik JE, Kang SS, Yun CH, Seo DG, Han SH: **Lipoteichoic acid of *Streptococcus mutans* interacts with Toll-like receptor 2 through the lipid moiety for induction of inflammatory mediators in murine macrophages**. *Mol Immunol* 2014, **57**(2):284-291.
50. Hong SW, Seo DG, Baik JE, Cho K, Yun CH, Han SH: **Differential profiles of salivary proteins with affinity to *Streptococcus mutans* lipoteichoic acid in caries-free and caries-positive human subjects**. *Mol Oral Microbiol* 2014, **29**(5):208-218.
51. Bolger AM, Lohse M, Usadel B: **Trimmomatic: a flexible trimmer for Illumina sequence data**. *Bioinformatics* 2014, **30**(15):2114-2120.
52. Langmead B, Trapnell C, Pop M, Salzberg SL: **Ultrafast and memory-efficient alignment of short DNA sequences to the human genome**. *Genome Biol* 2009, **10**(3):R25.
53. Anders S, Pyl PT, Huber W: **HTSeq--a Python framework to work with high-throughput sequencing data**. *Bioinformatics* 2015, **31**(2):166-169.
54. Robinson MD, McCarthy DJ, Smyth GK: **edgeR: a Bioconductor package for differential expression analysis of digital gene expression data**. *Bioinformatics* 2010, **26**(1):139-140.
55. Morath S, Geyer A, Hartung T: **Structure-function relationship of cytokine induction by lipoteichoic acid from *Staphylococcus aureus***. *J Exp Med* 2001, **193**(3):393-397.
56. Griffen AL, Beall CJ, Campbell JH, Firestone ND, Kumar PS, Yang ZK, Podar M, Leys EJ: **Distinct and complex bacterial profiles in human periodontitis and health revealed by 16S pyrosequencing**. *ISME J* 2012, **6**(6):1176-1185.
57. Urzua B, Hermosilla G, Gamonal J, Morales-Bozo I, Canals M, Barahona S, Coccola C, Cifuentes V: **Yeast diversity in the oral microbiota of subjects with periodontitis:**

***Candida albicans* and *Candida dubliniensis* colonize the periodontal pockets**. *Med Mycol* 2008, **46**(8):783-793.
58. Sardi JC, Duque C, Hofling JF, Goncalves RB: **Genetic and phenotypic evaluation of *Candida albicans* strains isolated from subgingival biofilm of diabetic patients with chronic periodontitis**. *Med Mycol* 2012, **50**(5):467-475.
59. Fox EP, Cowley ES, Nobile CJ, Hartooni N, Newman DK, Johnson AD: **Anaerobic bacteria grow within *Candida albicans* biofilms and induce biofilm formation in suspension cultures**. *Curr Biol* 2014, **24**(20):2411-2416.
60. Bartnicka D, Karkowska-Kuleta J, Zawrotniak M, Satala D, Michalik K, Zielinska G, Bochenska O, Kozik A, Ciaston I, Koziel J *et al*: **Adhesive protein-mediated cross-talk between *Candida albicans* and *Porphyromonas gingivalis* in dual species biofilm protects the anaerobic bacterium in unfavorable oxic environment**. *Sci Rep* 2019, **9**(1):4376.
61. Kim HM, Davey ME: **Synthesis of ppGpp impacts type IX secretion and biofilm matrix formation in *Porphyromonas gingivalis***. *NPJ Biofilms Microbiomes* 2020, **6**(1):5.
62. Whitworth DE, Morgan BH: **Synergism Between Bacterial GAPDH and OMVs: Disparate Mechanisms but Co-Operative Action**. *Front Microbiol* 2015, **6**:1231.
63. Maeda K, Nagata H, Kuboniwa M, Ojima M, Osaki T, Minamino N, Amano A: **Identification and characterization of *Porphyromonas gingivalis* client proteins that bind to *Streptococcus oralis* glyceraldehyde-3-phosphate dehydrogenase**. *Infect Immun* 2013, **81**(3):753-763.
64. Enersen M, Nakano K, Amano A: ***Porphyromonas gingivalis* fimbriae**. *J Oral Microbiol* 2013, **5**.
65. Kuboniwa M, Amano A, Hashino E, Yamamoto Y, Inaba H, Hamada N, Nakayama K, Tribble GD, Lamont RJ, Shizukuishi S: **Distinct roles of long/short fimbriae and gingipains in homotypic biofilm development by *Porphyromonas gingivalis***. *BMC Microbiol* 2009, **9**:105.
66. Potempa J, Madej M, Scott DA: **The RagA and RagB proteins of *Porphyromonas gingivalis***. *Mol Oral Microbiol* 2021, **36**(4):225-232.
67. Vermilyea DM, Ottenberg GK, Davey ME: **Citrullination mediated by PPAD constrains biofilm formation in *P. gingivalis* strain 381**. *NPJ Biofilms Microbiomes* 2019, **5**(1):7.
68. Ikai R, Hasegawa Y, Izumigawa M, Nagano K, Yoshida Y, Kitai N, Lamont RJ, Yoshimura F, Murakami Y: **Mfa4, an Accessory Protein of Mfa1 Fimbriae, Modulates Fimbrial Biogenesis, Cell Auto-Aggregation, and Biofilm Formation in *Porphyromonas gingivalis***. *PLoS One* 2015, **10**(10):e0139454.
69. Nakayama K: ***Porphyromonas gingivalis* and related bacteria: from colonial pigmentation to the type IX secretion system and gliding motility**. *J Periodontal Res* 2015, **50**(1):1-8.
70. Hasegawa Y, Nagano K: ***Porphyromonas gingivalis* FimA and Mfa1 fimbriae: Current insights on localization, function, biogenesis, and genotype**. *Jpn Dent Sci Rev* 2021, **57**:190-200.
71. Hiratsuka K, Hayakawa M, Kiyama-Kishikawa M, Sasaki Y, Hirai T, Abiko Y: **Role of the hemin-binding protein 35 (HBP35) of *Porphyromonas gingivalis* in coaggregation**. *Microb Pathog* 2008, **44**(4):320-328.
72. Naylor KL, Widziolek M, Hunt S, Conolly M, Hicks M, Stafford P, Potempa J, Murdoch C, Douglas CW, Stafford GP: **Role of OmpA2 surface regions of *Porphyromonas gingivalis* in host-pathogen interactions with oral epithelial cells**. *Microbiologyopen* 2017, **6**(1).
73. Smalley JW, Olczak T: **Heme acquisition mechanisms of *Porphyromonas gingivalis* - strategies used in a polymicrobial community in a heme-limited host environment**. *Mol Oral Microbiol* 2017, **32**(1):1-23.
74. Ho MH, Lamont RJ, Xie H: **Identification of *Streptococcus cristatus* peptides that repress expression of virulence genes in *Porphyromonas gingivalis***. *Sci Rep* 2017, **7**(1):1413.
75. Yukitake H, Naito M, Sato K, Shoji M, Ohara N, Yoshimura M, Sakai E, Nakayama K:

Effects of non-iron metalloporphyrins on growth and gene expression of *Porphyromonas gingivalis*. *Microbiol Immunol* 2011, **55**(3):141-153.
76. Sztukowska MN, Dutton LC, Delaney C, Ramsdale M, Ramage G, Jenkinson HF, Nobbs AH, Lamont RJ: **Community Development between *Porphyromonas gingivalis* and *Candida albicans* Mediated by InlJ and Als3**. *mBio* 2018, **9**(2).
77. Nishimata H, Ohara-Nemoto Y, Baba TT, Hoshino T, Fujiwara T, Shimoyama Y, Kimura S, Nemoto TK: **Identification of Dipeptidyl-Peptidase (DPP)5 and DPP7 in *Porphyromonas endodontalis*, Distinct from Those in *Porphyromonas gingivalis***. *PLoS One* 2014, **9**(12):e114221.
78. Sato K, Sakai E, Veith PD, Shoji M, Kikuchi Y, Yukitake H, Ohara N, Naito M, Okamoto K, Reynolds EC *et al*: **Identification of a new membrane-associated protein that influences transport/maturation of gingipains and adhesins of *Porphyromonas gingivalis***. *J Biol Chem* 2005, **280**(10):8668-8677.
79. Chen W, Honma K, Sharma A, Kuramitsu HK: **A universal stress protein of *Porphyromonas gingivalis* is involved in stress responses and biofilm formation**. *FEMS Microbiol Lett* 2006, **264**(1):15-21.
80. Dashper SG, Mitchell HL, Seers CA, Gladman SL, Seemann T, Bulach DM, Chandry PS, Cross KJ, Cleal SM, Reynolds EC: ***Porphyromonas gingivalis* Uses Specific Domain Rearrangements and Allelic Exchange to Generate Diversity in Surface Virulence Factors**. *Front Microbiol* 2017, **8**:48.
81. Tezuka A, Hamajima S, Hatta H, Abiko Y: **Inhibition of *Porphyromonas gingivalis* hemagglutinating activity by IgY against a truncated HagA**. *J Oral Sci* 2006, **48**(4):227-232.
82. Kuboniwa M, Amano A, Inaba H, Hashino E, Shizukuishi S: **Homotypic biofilm structure of *Porphyromonas gingivalis* is affected by FimA type variations**. *Oral Microbiol Immunol* 2009, **24**(3):260-263.
83. Zhou L, Zhang Y, Ge Y, Zhu X, Pan J: **Regulatory Mechanisms and Promising Applications of Quorum Sensing-Inhibiting Agents in Control of Bacterial Biofilm Formation**. *Front Microbiol* 2020, **11**:589640.
84. Takeuchi H, Sasaki N, Yamaga S, Kuboniwa M, Matsusaki M, Amano A: ***Porphyromonas gingivalis* induces penetration of lipopolysaccharide and peptidoglycan through the gingival epithelium via degradation of junctional adhesion molecule 1**. *PLoS Pathog* 2019, **15**(11):e1008124.
85. Gasiorek A, Dobosz E, Potempa B, Ciaston I, Wilamowski M, Oruba Z, Lamont RJ, Jura J, Potempa J, Koziel J: **Subversion of Lipopolysaccharide Signaling in Gingival Keratinocytes via MCPIP-1 Degradation as a Novel Pathogenic Strategy of Inflammophilic Pathobionts**. *mBio* 2021, **12**(3):e0050221.
86. Elebyary O, Barbour A, Fine N, Tenenbaum HC, Glogauer M: **The Crossroads of Periodontitis and Oral Squamous Cell Carcinoma: Immune Implications and Tumor Promoting Capacities**. *Front Oral Health* 2020, **1**:584705.
87. Ohshima J, Wang Q, Fitzsimonds ZR, Miller DP, Sztukowska MN, Jung YJ, Hayashi M, Whiteley M, Lamont RJ: ***Streptococcus gordonii* programs epithelial cells to resist ZEB2 induction by *Porphyromonas gingivalis***. *Proc Natl Acad Sci U S A* 2019, **116**(17):8544-8553.
88. Aleksijevic LH, Aleksijevic M, Skrlec I, Sram M, Sram M, Talapko J: ***Porphyromonas gingivalis* Virulence Factors and Clinical Significance in Periodontal Disease and Coronary Artery Diseases**. *Pathogens* 2022, **11**(10).
89. Alaei SR, Park JH, Walker SG, Thanassi DG: **Peptide-Based Inhibitors of Fimbrial Biogenesis in *Porphyromonas gingivalis***. *Infect Immun* 2019, **87**(3).
90. Andrian E, Grenier D, Rouabhia M: ***Porphyromonas gingivalis*-epithelial cell interactions in periodontitis**. *J Dent Res* 2006, **85**(5):392-403.
91. Morath S, Geyer A, Spreitzer I, Hermann C, Hartung T: **Structural decomposition and**

heterogeneity of commercial lipoteichoic Acid preparations. *Infect Immun* 2002, **70**(2):938-944.
92. Hashimoto M, Tawaratsumida K, Kariya H, Kiyohara A, Suda Y, Krikae F, Kirikae T, Gotz F: **Not lipoteichoic acid but lipoproteins appear to be the dominant immunobiologically active compounds in *Staphylococcus aureus***. *J Immunol* 2006, **177**(5):3162-3169.
93. Wang Y: **Liposome as a delivery system for the treatment of biofilm-mediated infections**. *J Appl Microbiol* 2021, **131**(6):2626-2639.
94. Rangarajan M, Aduse-Opoku J, Hashim A, Paramonov N, Curtis MA: **Characterization of the alpha- and beta-mannosidases of *Porphyromonas gingivalis***. *J Bacteriol* 2013, **195**(23):5297-5307.
95. Madej M, Nowakowska Z, Ksiazek M, Lasica AM, Mizgalska D, Nowak M, Jacula A, Bzowska M, Scavenius C, Enghild JJ *et al*: **PorZ, an Essential Component of the Type IX Secretion System of *Porphyromonas gingivalis*, Delivers Anionic Lipopolysaccharide to the PorU Sortase for Transpeptidase Processing of T9SS Cargo Proteins**. *mBio* 2021, **12**(1).
96. Meers P, Neville M, Malinin V, Scotto AW, Sardaryan G, Kurumunda R, Mackinson C, James G, Fisher S, Perkins WR: **Biofilm penetration, triggered release and in vivo activity of inhaled liposomal amikacin in chronic *Pseudomonas aeruginosa* lung infections**. *J Antimicrob Chemother* 2008, **61**(4):859-868.
97. Kloppsteck P, Hall M, Hasegawa Y, Persson K: **Structure of the fimbrial protein Mfa4 from *Porphyromonas gingivalis* in its precursor form: implications for a donor-strand complementation mechanism**. *Sci Rep* 2016, **6**:22945.
98. de Souza AA, Takita MA, Coletta-Filho HD, Caldana C, Yanai GM, Muto NH, de Oliveira RC, Nunes LR, Machado MA: **Gene expression profile of the plant pathogen Xylella fastidiosa during biofilm formation in vitro**. *FEMS Microbiol Lett* 2004, **237**(2):341-353.
99. Hamilton S, Bongaerts RJ, Mulholland F, Cochrane B, Porter J, Lucchini S, Lappin-Scott HM, Hinton JC: **The transcriptional programme of *Salmonella enterica* serovar Typhimurium reveals a key role for tryptophan metabolism in biofilms**. *BMC Genomics* 2009, **10**:599.
100. Kawada-Matsuo M, Mazda Y, Oogai Y, Kajiya M, Kawai T, Yamada S, Miyawaki S, Oho T, Komatsuzawa H: **GlmS and NagB regulate amino sugar metabolism in opposing directions and affect *Streptococcus mutans* virulence**. *PLoS One* 2012, **7**(3):e33382.
101. Poquet I, Saujet L, Canette A, Monot M, Mihajlovic J, Ghigo JM, Soutourina O, Briandet R, Martin-Verstraete I, Dupuy B: ***Clostridium difficile* Biofilm: Remodeling Metabolism and Cell Surface to Build a Sparse and Heterogeneously Aggregated Architecture**. *Front Microbiol* 2018, **9**:2084.
102. Rahman MA, Amirkhani A, Chowdhury D, Mempin M, Molloy MP, Deva AK, Vickery K, Hu H: **Proteome of *Staphylococcus aureus* Biofilm Changes Significantly with Aging**. *Int J Mol Sci* 2022, **23**(12).
103. Belda E, Voland L, Tremaroli V, Falony G, Adriouch S, Assmann KE, Prifti E, Aron-Wisnewsky J, Debedat J, Le Roy T *et al*: **Impairment of gut microbial biotin metabolism and host biotin status in severe obesity: effect of biotin and prebiotic supplementation on improved metabolism**. *Gut* 2022, **71**(12):2463-2480.
104. Rabin N, Zheng Y, Opoku-Temeng C, Du Y, Bonsu E, Sintim HO: **Biofilm formation mechanisms and targets for developing antibiofilm agents**. *Future Med Chem* 2015, **7**(4):493-512.
105. Sanchez MC, Romero-Lastra P, Ribeiro-Vidal H, Llama-Palacios A, Figuero E, Herrera D, Sanz M: **Comparative gene expression analysis of planktonic *Porphyromonas gingivalis* ATCC 33277 in the presence of a growing biofilm versus planktonic cells**. *BMC Microbiol* 2019, **19**(1):58.
106. Sojar HT, Genco RJ: **Identification of glyceraldehyde-3-phosphate dehydrogenase of epithelial cells as a second molecule that binds to *Porphyromonas gingivalis* fimbriae**.

FEMS Immunol Med Microbiol 2005, **45**(1):25-30.
107. Maeda K, Nagata H, Nonaka A, Kataoka K, Tanaka M, Shizukuishi S: **Oral streptococcal glyceraldehyde-3-phosphate dehydrogenase mediates interaction with *Porphyromonas gingivalis* fimbriae**. *Microbes Infect* 2004, **6**(13):1163-1170.
108. Lamont RJ, Hajishengallis G: **Polymicrobial synergy and dysbiosis in inflammatory disease**. *Trends Mol Med* 2015, **21**(3):172-183.
109. Chow YC, Yam HC, Gunasekaran B, Lai WY, Wo WY, Agarwal T, Ong YY, Cheong SL, Tan SA: **Implications of *Porphyromonas gingivalis* peptidyl arginine deiminase and gingipain R in human health and diseases**. *Front Cell Infect Microbiol* 2022, **12**:987683.
110. Zhang X, Zhang X, Qiu C, Shen H, Zhang H, He Z, Song Z, Zhou W: **The imbalance of Th17/Treg via STAT3 activation modulates cognitive impairment in P. gingivalis LPS-induced periodontitis mice**. *J Leukoc Biol* 2021, **110**(3):511-524.
111. Monajemi M, Pang YCF, Bjornson S, Menzies SC, van Rooijen N, Sly LM: **Malt1 blocks IL-1beta production by macrophages in vitro and limits dextran sodium sulfate-induced intestinal inflammation in vivo**. *J Leukoc Biol* 2018, **104**(3):557-572.
112. Gu H, Zheng S, Han G, Yang H, Deng Z, Liu Z, He F: **Porcine Reproductive and Respiratory Syndrome Virus Adapts Antiviral Innate Immunity via Manipulating MALT1**. *mBio* 2022, **13**(3):e0066422.
113. Marona P, Gorka J, Mazurek Z, Wilk W, Rys J, Majka M, Jura J, Miekus K: **MCPIP1 Downregulation in Clear Cell Renal Cell Carcinoma Promotes Vascularization and Metastatic Progression**. *Cancer Res* 2017, **77**(18):4905-4920.
114. Kwapisz O, Gorka J, Korlatowicz A, Kotlinowski J, Waligorska A, Marona P, Pydyn N, Dobrucki JW, Jura J, Miekus K: **Fatty Acids and a High-Fat Diet Induce Epithelial-Mesenchymal Transition by Activating TGFbeta and beta-Catenin in Liver Cells**. *Int J Mol Sci* 2021, **22**(3).
115. Shiraishi T, Yokota S, Morita N, Fukiya S, Tomita S, Tanaka N, Okada S, Yokota A: **Characterization of a Lactobacillus gasseri JCM 1131T lipoteichoic acid with a novel glycolipid anchor structure**. *Appl Environ Microbiol* 2013, **79**(10):3315-3318.
116. Jang KS, Baik JE, Han SH, Chung DK, Kim BG: **Multi-spectrometric analyses of lipoteichoic acids isolated from Lactobacillus plantarum**. *Biochem Biophys Res Commun* 2011, **407**(4):823-830.
117. Lu Q, Guo Y, Yang G, Cui L, Wu Z, Zeng X, Pan D, Cai Z: **Structure and Anti-Inflammation Potential of Lipoteichoic Acids Isolated from Lactobacillus Strains**. *Foods* 2022, **11**(11).

국문초록

유산균 유래 리포테이코익산의 바이오필름 제어기전과 치주염 치료 효과

이 동 욱
서울대학교 대학원 치의과학과 면역 및 분자미생물학 전공
(지도교수: 한 승 현, 이학박사)

1. 목 적

바이오필름은 세균이 무기 혹은 유기 표면에 부착하여 생성된 집락체로서 항생제등의 다양한 약물에 대한 내성을 제공하는 것이 특징이다. 이를 제어하기 위한 다양한 연구들 사이에서 최근 프로바이오틱스 중 특히 *Lactobacillus*를 구강 바이오필름 제어소제로 개발하기 위한 연구들이 진행되고 있다. 하지만, 생균 또는 사균의 형태로 프로바이오틱스를 사용할 시, 면역기능의 손상과 같은 부작용이 있는 것으로 보고되고 있어 사용상의 안전성 문제가 제기되고 있다. 이러한 이유로 해당 부작용을 최소화하기 위해 바이오필름 제어능을 보유한 *Lactobacillus* 유래물질 분리 및 효능평가 연구들이 진행되고 있으나, 현재까지 이들에 의한 바이오필름 제어관련 분자적 메커니즘은 명확히 규명되어 있지 않은 상태이다. 다른 한편으로 이전 연구를 통해 *L. plantarum*의 세포벽 구성 성분 중 하나인 리포테이코익산이 다양한 그람 양성 구강유해균의 바이오필름을 제어할 수 있음을 규명하였으며, 바이오필름 제어능은 *L. plantarum* 아종에 따라 다를 수 있음을 확인하였다. 그러나 *Porphyromonas gingivalis*를 포함한 그람 음성 구강유해균의 바이오필름 형성에 대한 *Lactobacillus* 리포테이코익산의 효과는 현재까지 검증된 바 없다. 따라서 본 연구에서는 *P. gingivalis* 바이오필름에 대한 종별 유래 *Lactobacillus* 리포테이코익산의 효과를 확인하고 이에 관련된 분자적 메커니즘을 규명하고, 나아가 병인학적 기전에 대한 리포테이코익산의 생물학적 의의를 규명하고자 한다.

2. 방 법

*P. gingivalis*의 바이오필름 조절에 대한 *Lactobacillus* 종별 리포테이코익산의 역할을 규명하기 위해 부탄올을 사용하여 리포테이코익산을 1차 분리를 수행하고 소수성 상호작용 및 이온화성 크로마토그래피를 이용해 리포테이코익산을 최종 정제하였다. 리포테이코익산 중 효과가 *P. gingivalis* 바이오필름에 가장 좋았던 *L. reuteri* 리포테이코익산을 추후 실험에 활용하였으며, *P. gingivalis* 바이오필름 조절에 대한 리포테이코익산의 메커니즘을 확인하기 위해 야생형 *P. gingivalis* 및 섬모단백질, 진지페인 돌연변이를 사용하였고 추가적으로 실제 환자에서 분리한 *P. gingivalis* 균주들이 사용되었다. *P. gingivalis* 바이오필름을 저해하는 리포테이코익산의 중요인자를 확인하기 위해, Tris-HCl을 이용하여 리포테이코익산의 D-알라닌 성분을 제거하였으며, NaOH를 이용하여 리포테이코익산의 D-알라닌과 지질을 제거하였다. *P. gingivalis*의 바이오필름은 크리스탈 바이올렛 기법 및 공초점 현미경 분석을 통해 양적 확인하였다. 리포테이코익산과 상호작용하는 *P. gingivalis*의 단백질을 규명하기 위해 NHS에 리포테이코익산을 교차결합시킨 후 *P. gingivalis* 용균액과 혼합하여 전기영동을 수행하였다. Coomassie를 이용하여 겔을 염색시킨 후 나타난 밴드를 잘라내어 액체성 크로마토그래피 분석을 통해 단백질을 규명하였다. 이후 *P. gingivalis*에 대한 리포테이코익산의 상호작용, 숙주 감염, 유전자 발현과 같은 조절 메커니즘은 공초점 현미경 분석, 유세포분석, 세포배양, 웨스턴 블롯, 실시간 유전자 PCR, RNA 유전체 분석, AI-2 분석, 기질-가수분해 분석, Ni^{2+}-NTA 침전기법이 사용되었다. 마지막으로 리포테이코익산이 치주염에 대한 치료제로서의 개발 가능성을 확인하기 위해, 마우스 치아 결찰에 *P. gingivalis* 감염으로 악화된 치주염 모델을 유발한 다음, 마이크로 X선 촬영을 통해 효과를 확인하였다.

3. 결 과

크리스탈 바이올렛 기법을 통해 *Lactobacillus* 종별 리포테이코익산 중 *L. reuteri*의 리포테이코익산이 *P. gingivalis* 바이오필름 형성에서 가장 효과가 좋았음을 확인하였으며, 추후 실험은 모두 *L. reuteri*의 리포테이코익산을 활용하여 메커니즘을 확인하였다. 리포테이코익산 기능기 제거 실험을 통해 리포테이코익산에서 다중글리세롤인산기 및 지질 구성성분이 *P. gingivalis*

바이오필름을 저해할 수 있는 주요 작용기임을 확인하였다. 추가적으로 리포테이코익산이 실제 치주염 환자에서 분리한 *P. gingivalis*의 바이오필름을 저해할 뿐만 아니라, 다종간 바이오필름 또한 저해할 수 있음을 확인하였다. 공초점 현미경 분석을 통해 리포테이코익산의 바이오필름 저해능력은 *P. gingivalis*와의 직접적인 상호작용에 의해 일어나는 것을 확인하였으며, 흥미롭게도 *P. gingivalis*의 표면 단백질 중 바이오필름 형성을 관장하는 것으로 알려져 있는 섬모 단백질인 FimA와 진지페인인 RgpA에 결합하는 것을 질량분석법을 통해 확인하였다. 이들 중 섬모 단백질이 결여되었을 때, 리포테이코익산에 대한 항바이오필름 효과가 나타나지 않았으며, 해당 결과는 결국 리포테이코익산이 섬모 단백질인 FimA와 상호작용하는 것을 통해 *P. gingivalis*의 바이오필름이 저해된다는 것을 보여주었다. 또한, RNA 유전체 분석을 통해 FimA에 의해 바이오필름이 저해된 이후 물질대사와 연관된 유전자의 발현이 변화되는 것을 확인하였다. 더 나아가, 리포테이코익산이 RgpA의 단백질 가수분해적 기능을 억제할 수 있는 것을 확인하였으며, 해당 단백질은 monocyte chemoattractant protein-induced protein 1 (MCPIP-1)을 분해하는 것을 통해 치주염을 유발하는 것이 기존에 보고 되어있다. 웨스턴 블롯 및 실시간 유전자 PCR을 통해 리포테이코익산이 진지페인에 의한 MCPIP-1의 분해를 억제하는 것을 확인하였으며, 이를 통해 염증성 사이토카인이 완화됨을 확인하였다. 이와 동일하게, 리포테이코익산이 치주염 또한 완화시키는 것을 마우스 실험을 통해 증명하였다.

4. 결 론

본 연구에서 바이오필름 형성과정 또는 이미 형성된 *P. gingivalis* 바이오필름의 표면에 리포테이코익산이 작용하여 바이오필름을 저해하고 *P. gingivalis*의 병원성 또한 저해할 수 있음을 확인할 수 있었다. 해당 결과를 통해 리포테이코익산이 병원성 박테리아 공동체를 제어하고, 구강 병원성 균들에게서 면역 항상성을 유지할 수 있는 하나의 구강 치료제로서 개발될 수 있는 가능성을 제시하였다. 덧붙여, 이러한 리포테이코익산의 바이오필름 및 병원성 제어능력은 치주염 치료의 새로운 전략이 될 수 있다는 것을 보여주었다.

주요어 : *Lactobacillus*, 리포테이코익산, *Porphyromonas gingivalis*, 치주염, 항바이오필름제